Title
Engineering Biomaterials to Direct Stem Cell Fate

Author
Conway, Anthony Baer

Publication Date
2013

Peer reviewed|Thesis/dissertation

Engineering Biomaterials to Direct Stem Cell Fate

by

Anthony Baer Conway

A dissertation submitted in partial satisfaction of the

requirements for the degree of

Doctor of Philosophy

in

Chemical Engineering

in the

Graduate Division

of the

University of California, Berkeley

Committee in charge:

Professor David V. Schaffer, Chair
Professor Danielle Tullman-Ercek
Professor Kevin E. Healy

Spring 2013

Abstract

Engineering Biomaterials to Direct Stem Cell Fate

by

Anthony Baer Conway

Doctor of Philosophy in Chemical Engineering

University of California, Berkeley

Professor David V. Schaffer, Chair

The native microenvironment in which a cell resides greatly affects its function. The biochemical signals presented to the cell, the three-dimensional (3D) spatial organization or manner in which they are presented, and even the mechanical properties of the surrounding tissue all play an integral role in regulating its innate function. For example, neural stem cells (NSCs) – cells that are able to continuously replicate without losing their intrinsic properties (self-renew) as well as differentiate into all mature neural cell types (multipotent) – and pluripotent cells in the blastocyst – which gives rise to human embryonic stem cells (hESCs) in culture – naturally reside within a local microenvironment that carefully regulates their proliferation and subsequent differentiation. However, in general, numerous downstream applications involving stem cells require cell isolation and extensive culture outside the body, and when these cells are extracted from their natural environments, it is exceedingly difficult to control their behavior. To be able to expand these stem cells and their progeny one needs to understand and emulate their natural environments, or niches.

Within the stem cell niche, numerous cellular signaling systems involve the presentation of multivalent ligands, which upon binding to their cognate receptor induce a process of receptor clustering that is apparently critical for signal transduction. In our investigation of factors that naturally form higher-order signaling complexes, we discovered that the transmembrane protein ephrin-B2 significantly enhances neuronal differentiation of NSCs upon ligand multimerization. By inducing signaling through its receptor EphB4, ephrin-B2 upregulates transcription factors which have been identified as contributors to neuronal differentiation. Through *in vivo* immunostaining and short hairpin RNA (shRNA) interference, we have also identified astrocytes as the endogenous source of ephrin-B2 in the adult rat brain. These findings indicate the first example of an Eph-family protein in regulating stem cell lineage commitment in the adult nervous system and the first example of a cell membrane-bound factor that contributes to adult hippocampal neurogenesis through multivalent signaling.

Multivalent binding of ligands can often initiate cellular signal transduction, either secreted or cell-surface tethered, to target cell receptors, leading to receptor clustering. Since multivalent ligands can be significantly more potent than corresponding monovalent interaction, engineering synthetic multivalent ligands to organize receptors into nanoscale clusters is an attractive approach to elicit desired downstream cellular responses. We create for the first time

multivalent ligands that influence stem cell fate, both *in vitro* and *in vivo*. The ectodomain of ephrin-B2, normally an integral membrane protein ligand, was conjugated to a soluble biopolymer to yield multivalent conjugates that potently induced signaling within and neuronal differentiation of neural stem cells, in culture and within the brain. Furthermore, synthetic multivalent conjugates of ephrin-B1 strongly enhanced human embryonic and induced pluripotent stem cell differentiation into functional dopaminergic neurons. Multivalent bioconjugates thus represent a powerful tool for controlling stem cell fate *in vitro* and *in vivo*.

Currently, the technological capacity to restore neuronal function in degenerating or injured regions of the adult brain is severely limited. Only in two regions of the adult mammalian brain – the subventricular zone (SVZ) and hippocampus – are NSCs capable of continuously generating new neurons, enabled by a complex repertoire of factors that precisely regulate the activation, proliferation, differentiation, and integration of the newborn cells. A growing number of studies also report low level neurogenesis in regions of the adult brain outside these established neurogenic niches – potentially via NSC recruitment or activation of local, quiescent NSCs – under perturbations such as ischemia, cell death, or viral gene delivery of proneural growth factors. We have explored whether implantation of engineered biomaterials can stimulate neurogenesis in normally quiescent regions of the brain. Specifically, recombinant versions of factors found within the NSC microenvironment, Sonic hedgehog and ephrin-B2, were conjugated to long polymers, thereby creating highly bioactive, multivalent ligands that begin to emulate components of the neurogenic niche. In this engineered biomaterial microenvironment, new neuron formation was observed in normally non-neurogenic regions of the brain, the striatum and cortex, and combining these multivalent biomaterials with SDF-1α increased neuronal commitment of newly divided cells 7- to 8-fold in these regions. Additionally, the decreased hippocampal neurogenesis of geriatric rodents was partially rescued toward levels of young animals. We thus demonstrate for the first time *de novo* neurogenesis in both the cortex and striatum of adult rodents stimulated solely by delivery of synthetic biomaterial forms of proteins naturally found within adult neurogenic niches, offering the potential to replace neurons lost in neurodegenerative disease or injury as an alternative to cell implantation.

TABLE OF CONTENTS

LIST OF TABLES AND FIGURES

ACKNOWLEDGEMENTS

There are many people I'd like to thank for their contributions to this work. Firstly, my advisor Dave Schaffer has been an excellent mentor during my time at Berkeley. He has helped me develop into the scientist I am today and has provided helpful guidance and advice during my thesis work. I would also like to thank my other dissertation committee members, Danielle Tullman-Ercek and Kevin Healy, for their helpful discussions and feedback during both my qualifying exam preparation as well as in preparing this manuscript.

For funding, I am thankful to the University of California, the National Institutes of Health, and the California Institute for Regenerative Medicine.

I owe much appreciation to all members of the Schaffer lab that I have come in contact during my thesis work. For their help training me on many of the techniques in the lab I'd like to thank both Joe Peltier and Lauren Little for being so patient and supportive during my first year. Randy Ashton was also very helpful in his ability and willingness to teach me many of the protocols I used throughout my time at Berkeley. I greatly enjoyed Jamie Bergen's presence in the lab as she was an incredibly capable and efficient scientist that was able to lighten any mood with her unique sense of humor. I owe many thanks to Dan Stone for his advice both in and out of the lab regarding molecular biology techniques and career advice. Stephanie Willerth was also very supportive and helpful while in the lab. During their time at Berkeley and even as professors in Seoul and Santa Clara, Kwang-il Lim and Prashanth Asuri have been extraordinarily kind and accommodating with regards to career advice, lab techniques, and just as overall outstanding human beings. The other members of the "old" side of lab – Ashley Fritz, John Weinstein, Jonathan Foley, Melissa Kotterman, and Noem Ramey – have kept me sane during those hectic days and long nights in lab. There are not enough nice things to say about Noem, but suffice it to say I could not have gotten through graduate school so smoothly without her help both in and out of lab.

Outside of lab there were many other individuals who made my time in graduate school an absolute pleasure, despite the numerous difficulties which invariably arose. I'd first like to thank my parents and younger brother Michael for being so supportive and encouraging, both in my academic career and life in general. Melissa Kotterman I feel deserves another mention as even though she was incredibly helpful and supportive in lab, she also was (and is) a great friend that I am forever grateful I've met. Nick Young and John Alper, fellow classmates at Berkeley, have provided me with an alternative view of graduate school outside of my own lab as well as acted as great friends with a similar passion for craft beer.

Lastly, I'd like to thank Sophia Skowronski who I met while here at Berkeley. Her love and support have enriched my life in many ways, and the last few years at graduate school would not have been as fulfilling without her.

CHAPTER 1

INTRODUCTION

Stem Cells

Stem cells – unique cell types defined by their potential for indefinite self-renewal, or ability to proliferate in an undifferentiated state without losing intrinsic properties, as well as capacity to differentiate into one more specialized cell types – were first discovered in mouse bone marrow over 50 years ago [1,2]. These cells were discovered to be multipotent, in that they were capable of only generating one or more specialized mature cell type, whereas another class of stem cell known as pluripotent stem cells can give rise to any cell type of the adult organism (**Fig. 1**). It was not until more than 30 years after the discovery of hematopoietic stem cells within the bone marrow that the pluripotent stem cells which form the human – human embryonic stem cells (hESCs) – were discovered and isolated [3]. Furthermore, it was recently discovered that mature cell types can be reverted into induced pluripotent stem cells (iPSCs) using a specific cocktail of factors, which can then be differentiated into any mature cell type.

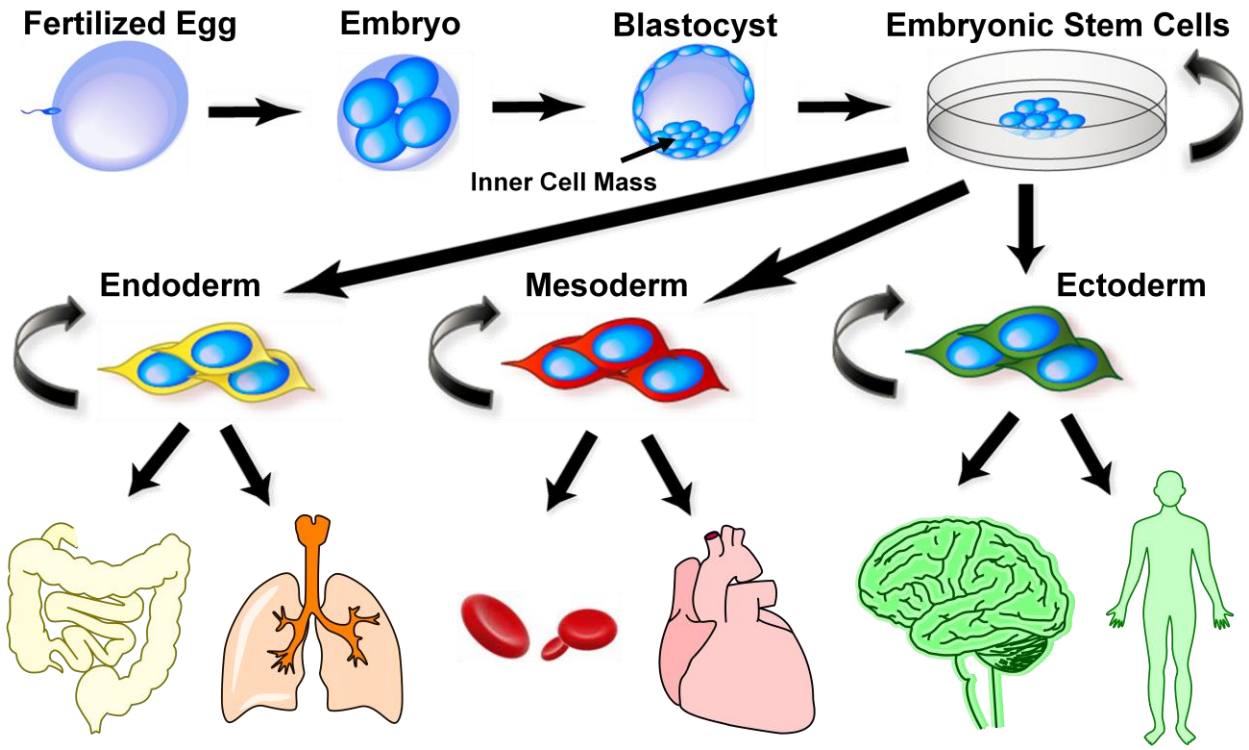

Figure 1: Pluripotency of embryonic stem cells (ESCs). After a specific number of days post-fertilization of the egg, the blastocyst forms which consists of the inner cell mass and the trophectoderm. ESCs are isolated from the inner cell mass and cultured, which can continuously self-renew for a theoretically infinite number of generations or can be differentiated into cell types of the three germ layers which form the adult organism.

Both pluripotent embryonic stem cells and multipotent stem cells found within the adult organism have clinical potential for generating therapeutically relevant cell types to treat human

disease. Neural stem cells (NSCs) isolated from the adult brain or differentiated from hESCs, for instance, can be differentiated into neurons, astrocytes, or oligodendrocytes to treat patients with degenerated neurons as a result of neurodegenerative disease or traumatic injury (**Fig. 2**). Understanding the process of how NSCs become specific mature cell types, however, is necessary before any successful therapies can be developed and implemented in the clinic.

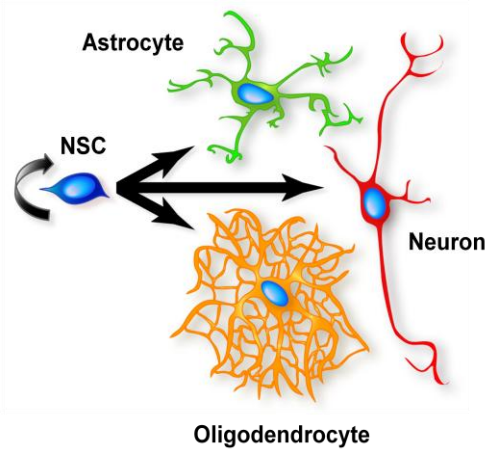

Figure 2: Multipotent differentiation of adult neural stem cells (NSCs). NSCs present postnatally within the adult brain have the potential to continuously self-renew by dividing without losing their intrinsic properties, as well as differentiate into the three major cellular lineages of the brain: astrocytes, neurons, and oligodendrocytes.

Adult Neurogenesis

Adult neurogenesis, or the creation of new neurons in the adult brain (**Fig. 3**), has been observed in a number of mammalian species, including humans [4,5,6,7,8], and this process is believed to contribute to the synaptic plasticity necessary for learning and memory acquisition throughout a lifetime [6,9,10,11,12,13]. In the mammalian brain, neurogenesis persists throughout adulthood in both the subgranular zone (SGZ) of the hippocampal dentate gyrus (DG) [4,12,14,15] and the subventricular zone (SVZ) of the lateral ventricles [8,16]. The absence of newly formed neurons in the adult CNS outside of these regions in both rodents [17,18] and in humans [18,19] suggests that this process is tightly regulated and that specific factors in the SGZ and SVZ niches are permissive towards neurogenesis. Moreover, the observation that aberrant neurogenesis occurs in patients with neurological pathologies that disrupt the natural chemistry of the brain, e.g. depression [20], epilepsy [21], and neurodegenerative diseases [22,23], further supports the notion that a delicate equilibrium of cues exists within the adult neurogenic niche that regulates cell proliferation and differentiation [13]. Although adult neurogenesis is known to contribute to learning and memory behaviors and may be beneficially employed to treat brain injury [23,24,25], the precise nature of the intrinsic cues that regulate this process still remains unclear. Further exploration of the interplay between factors present in the hippocampal niche contributing to neurogenesis is necessary to more completely understand this process and thus enable synthetic engineering of the neural stem cell microenvironment.

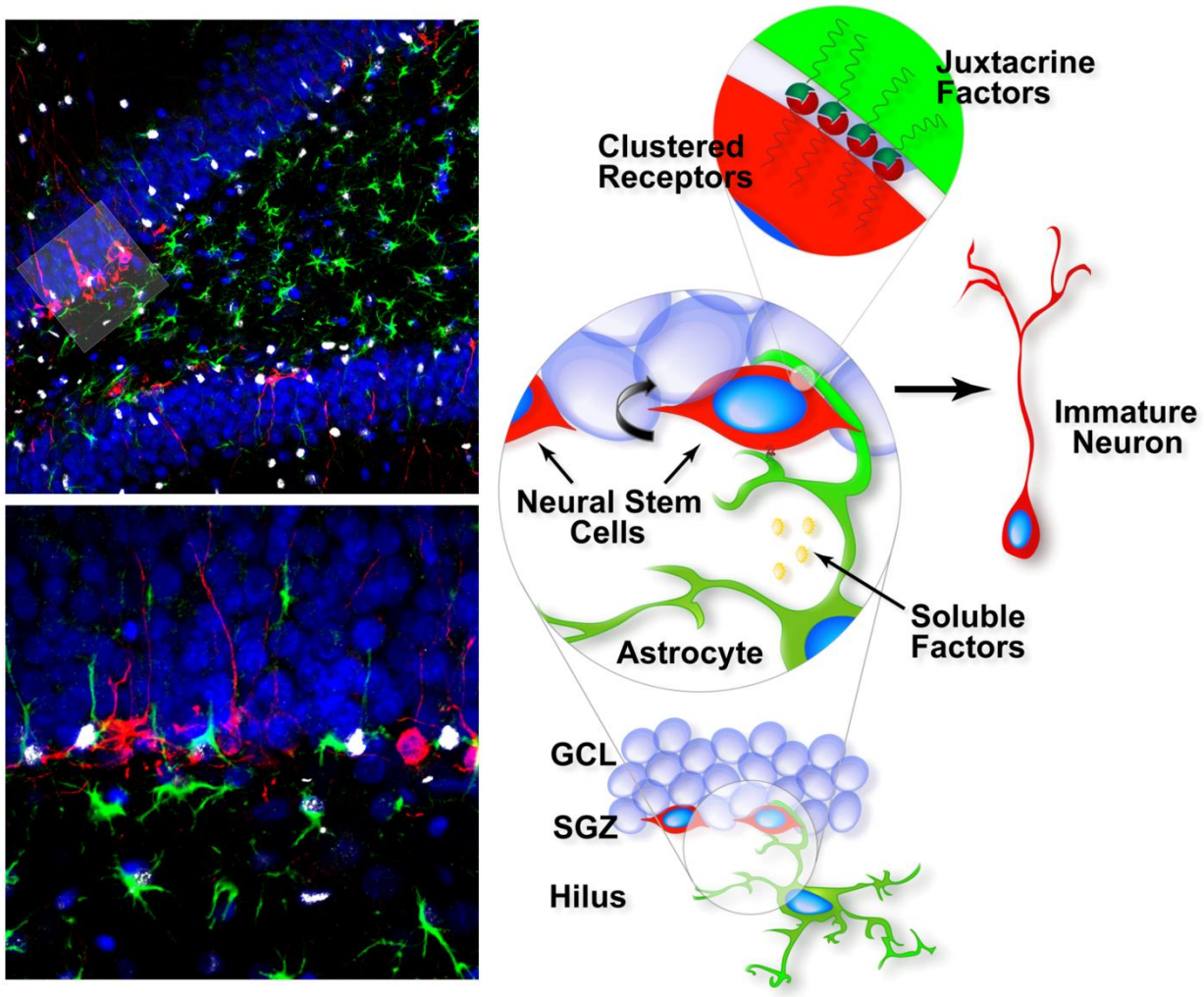

Figure 3: The adult hippocampal NSC niche. Confocal images (left) of the adult hippocampal dentate gyrus at low (top) and high (bottom) magnification. $Sox2^{+}$ (white) cells indicate NSCs and immature neural cell types, which are in close proximity to astrocytes (green) in the hilus which present either cell membrane-bound factors (juxtacrine) or freely soluble factors (paracrine) to NSCs to induce their differentiation or proliferation via NSC receptor activation. All cell nuclei are shown in blue. NSCs are found within the subgranular zone (SGZ) and differentiate into immature neurons (red) before maturing and migrating into the granular cell layer (GCL); however they can self-renew or differentiate into glial lineages as well. These processes are carefully regulated by factors within the stem cell microenvironment.

Biophysical Regulation within the Stem Cell Niche

Stem cells reside within most tissues throughout the lifetimes of mammalian organisms. To maintain their capacities for division and differentiation – and thereby build, maintain, and regenerate organ structure and function – these cells require extensive and precise regulation, and a critical facet of this control is the local environment or niche surrounding the cell. It is well known that soluble biochemical signals play important roles within such niches, and a number of biophysical aspects of the microenvironment – including mechanical cues and spatiotemporally varying biochemical signals – have also been increasingly recognized to contribute to the repertoire of stimuli that regulate various stem cells in various tissues of both vertebrates and

invertebrates. For example, biochemical factors immobilized to the extracellular matrix or the surface of neighboring cells can be spatially organized in their placement (**Fig. 4**). Furthermore, the extracellular matrix provides mechanical support and regulatory information, such as its elastic modulus and interfacial topography, which modulate key aspects of stem cell behavior. Numerous examples of each of these modes of regulation indicate that biophysical aspects of the niche must be appreciated and studied in conjunction with its biochemical properties.

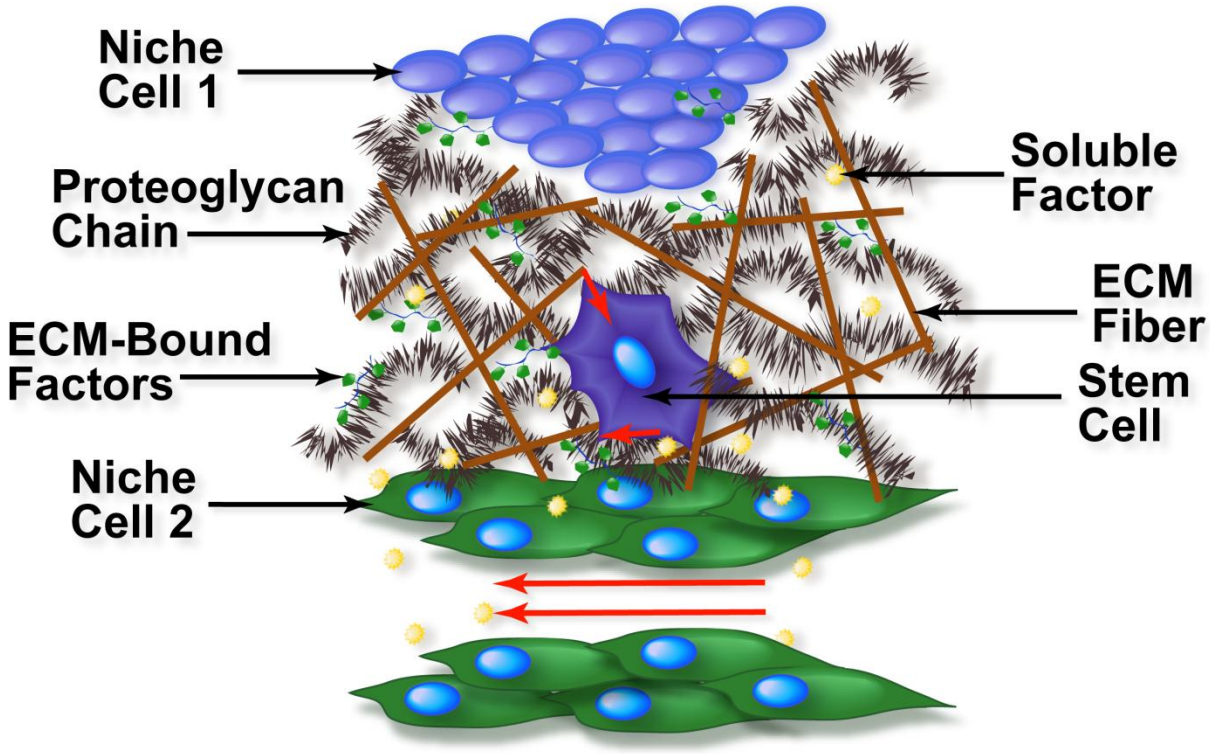

Figure 4: Mechanical and biophysical interactions in the stem cell niche. The native microenvironment, or niche, in which a stem cell resides can be highly complex, consisting of various cell types, ECM molecules, and growth factors (yellow). Proteoglycans and ECM proteins bind and immobilize otherwise soluble growth factors, providing functional sites for cell binding as well as mechanical stability of the space surrounding a stem cell in its niche. ECM fibers, as well as neighboring niche cells, provide mechanical support and stimuli (short red arrows) to influence stem cell fate. The degree of "crosslinking" of the various ECM molecules also affects the pore size in the niche, dictating the rate of diffusion of soluble factors as well as the ability of niche cells to infiltrate nearby space. Finally, flow through local vasculature (long red arrows) mechanically shears endothelial and other cells (green), which may in turn affect nearby stem cells.

The concept that the behavior of a stem cell can be modulated by factors in its immediate vicinity arose several decades ago in studies of spleen-colony forming cells, which were later appreciated to be hematopoietic stem and progenitor cells (HSPCs) [26]. It was hypothesized that these HSPCs and their progeny were distinct cell populations that possessed an "age-structure," such that once the progeny left their stem cell niche during developmental "aging", their stem-like qualities were lost, and entry into a new niche promoted differentiation into a more mature, lineage-committed cell type. Subsequent work with *Drosophila* germ stem cells [27], as well as other systems, demonstrated that the niche is a region that regulates stem cell fate decisions by presenting that cell with specific repertoires of soluble and immobilized

extracellular factors. It is increasingly being appreciated that many of these signals are biophysical in nature, particularly biochemical factors that are spatiotemporally modulated, mechanical cues, and electrostatic cues. Over the past several years, numerous examples have emerged in which the first two of these properties in particular have been demonstrated to play key regulatory roles.

Many factors that are often thought of as soluble are known to harbor matrix-binding domains that immobilize them to the solid phase of tissue. For example, fibroblast growth factors (FGFs), platelet-derived growth factors (PDGFs), transforming growth factors (TGFs), vascular endothelial growth factors (VEGFs), Hedgehogs, and numerous cytokines contain heparin-binding domains [28,29,30,31]. Immobilization of such factors to the extracellular matrix (ECM) often modulates their activity by promoting sustained signaling via inhibiting receptor-mediated endocytosis [32], increasing their local concentration and establishing concentration gradients emanating from the source [33], and otherwise modulating the spatial organization of factors in a manner that affects signaling. As an example, compared to soluble VEGF, VEGF bound to collagen preferentially activates VEGFR2, associates with β1 integrins, and promotes the association of all of these molecules into focal adhesions [34]. There are also strong examples of synthetic systems that harness these phenomena, the first of which involved tethering epidermal growth factor (EGF) to immobilized poly(ethylene oxide) (PEO) to prolong growth factor signaling in rat hepatocyte cultures [35]. A subsequent study showed that immobilization of Sonic hedgehog (Shh) onto interpenetrating polymer network (IPN) surfaces, along with the integrin engaging peptide RGD, induced potent osteoblastic differentiation of bone marrow-derived mesenchymal stem cells (MSCs), whereas soluble Shh enhanced proliferation [36]. As another example, crosslinking heparin-binding peptides to fibrin gels along with neurotrophic factor 3 (NT-3) and PDGF resulted in neuronal and oligodendrocytic differentiation of mouse neural stem cells (NSCs) with inhibition of astrocytic differentiation [37]. Finally, immobilization of leukemia inhibitory factor (LIF) to a synthetic polymer surface supported mouse embryonic stem cell (mESC) pluripotency for up to two weeks in the absence of soluble LIF, indicating the advantage of substrate functionalization in lowering cell culture reagent costs as well as facilitating future multifactorial cell fate screening experiments [38].

Multivalency

Immobilization of cues to the solid phase — i.e. the extracellular matrix (ECM) and/or the surface of adjacent cells — also offers the opportunity to modulate the nanoscale organization in which these factors are presented. Growing evidence has indicated that multivalency, or ligands that display multiple copies of recognition elements to bind multiple receptors simultaneously (**Fig. 5**), can exert potent effects on cell behavior [39,40,41,42]. For example, seminal work using a synthetic system to present clusters of ECM-derived adhesion ligands showed that the spatial organization of ECM cues can also impact cell responses. Specifically, on surfaces functionalized with the integrin adhesion ligand YGRGD in various states of valency, fibroblast attachment did not vary as a function of ligand valency, yet substrates bearing highly clustered or multivalent, peptides required significantly lower ligand densities to induce cell spreading and migration [43]. In recent work that explored the behavior of MSCs in a 3D hydrogel functionalized with RGD peptides, using a fluorescence resonance energy transfer technique investigators found that the cells apparently reorganized the peptides into clusters upon integrin binding [44].

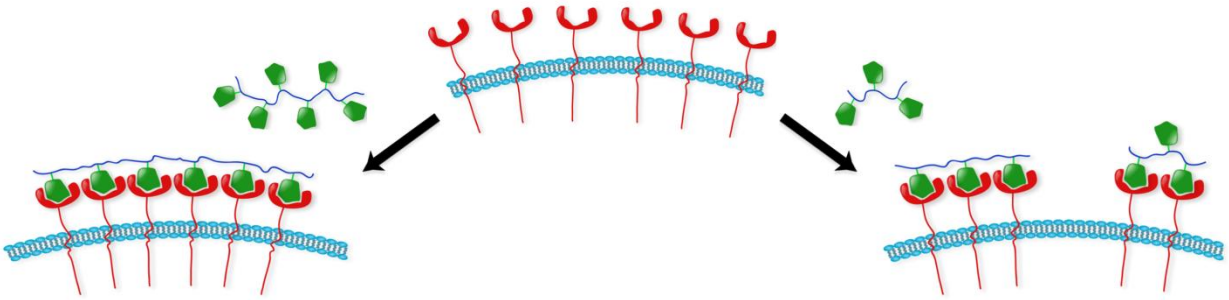

Figure 5: Schematic of molecules of differing valencies inducing differential receptor clustering on the cell membrane. Unassociated receptors on the cell membrane are induced to cluster by binding with multivalent ligands which is both thermodynamically and biochemically favorable. The extent of receptor clustering is dependent on the ligand valency of the multivalent molecule.

The role of ligand clustering also extends to growth factors and morphogens, which are present throughout various tissues, including the adult hippocampus (**Fig. 3**). The morphogen Hedgehog (Hh) and its family member Shh, best known for their role in tissue patterning during development, have been shown to require nanoscale clustering to achieve long-range paracrine signaling [45]. Additionally, the growth factor TGF-β is able to induce distinct differential signaling by activating either a homomeric or heteromeric form of its receptor, which needs to be dimerized or tetramerized before signaling can occur [46]. Furthermore, cell membrane-bound ligands, e.g. Delta/Jagged that activate the Notch receptor and ephrins that activate corresponding Eph receptors, often require oligomerization to transduce biochemical signaling cascades [47,48]. The creation of synthetically clustered, or multivalent, ligands offers a useful tool to study basic biological aspects of receptor clustering as well as a reagent to better control stem cell self-renewal or differentiation. For example, Shh has been chemically conjugated to the long polymer chain hyaluronic acid (HA) at varying stoichiometric ratios to produce a range of multivalent forms of Shh, and higher valency Shh bioconjugates exerted progressively higher potencies in inducing the osteogenic differentiation of a primary fibroblast line with MSC characteristics [49].

Such multivalent ligand-receptor interactions are sometimes required for downstream signaling initiation [50], and the degree of multivalency may dictate the potency of numerous elicited responses [51]. Therefore, the generation of multivalent versions of synthetic or recombinant forms of these ligands may aid in both basic investigation of signaling mechanisms and the development of high potency signaling molecules for therapeutic application.

The current established method for oligomerizing proteins involves antibody-induced clustering (**Fig. 6**); however, this method is not well controlled, resulting in a range of oligomer sizes which can undergo dissociation [50]. Here, we describe a protocol for synthesizing multivalent ligands in a modular fashion via chemical conjugation of recombinant protein to long HA polymer chains. We have successfully utilized this technique to develop multivalent Sonic hedgehog (Shh) and demonstrate that higher valency Shh increases potency [49]. HA polymers are flexible, allowing for rotation of bound ligands, and by varying the conjugation ratio of protein to HA a range of valencies can be achieved. These multivalent ligands can be employed to activate pathways that benefit from receptor clustering, study the basic role of ligand/ receptor clustering in signaling, and generate potent signaling agonists for therapeutic application. This concept has recently been extended to create highly active and multivalent versions of ligands

that are naturally integral membrane proteins, known as ephrins (Conway *et al.*, manuscript submitted).

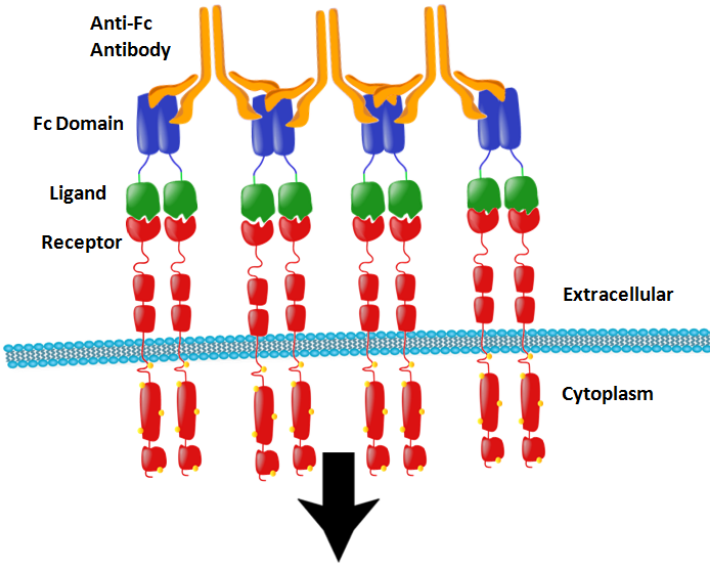

Figure 6: Schematic of antibody-induced ligand clustering of recombinant ligands and cell membrane-bound receptors. Recombinant proteins containing an IgG Fc region fused to the receptor-binding domain of a ligand is clustered by incubating with antibodies which recognize and bind the Fc domain. Adding into cultures of cells subsequently clusters cell membrane-bound receptors, initiating intracellular downstream signaling.

Ephrins

Ephrins are a diverse class of cell membrane-bound proteins that interact with transmembrane Eph receptors on neighboring cells to initiate signaling in both the sending and receiving cells, termed bidirectional signaling (**Fig. 7**). Interestingly, both ephrins and their Eph receptors require the formation of higher-order complexes (tetrameric or more) to induce intracellular signaling [52]. Eph/ephrin signaling is known to influence the spatial organization of cells by regulating cell migration [53], attraction and repulsion forces between contacting cells [54], and the formation and guidance of cellular protrusions [48]. Ephrins are also known to have an active role in formation of neuronal circuitry, including synapse formation and axon guidance [55]. The role of ephrins and their receptors in mesodermal [56,57] and endodermal [58] stem cell proliferation and maturation is well established; however, little is known about their role in regulating stem cell differentiation, or fate choices in general, and in the developing and adult central nervous system (CNS). Here, we present a novel role for Eph/ephrin signaling in regulating stem cell lineage commitment in the adult brain.

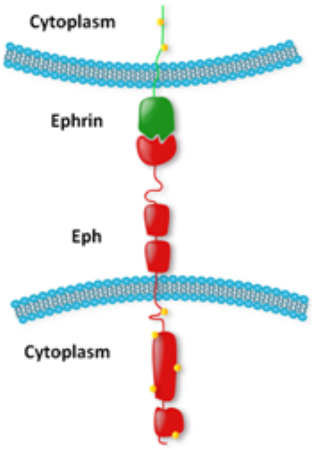

Figure 7: Eph-ephrin binding. Cell membrane bound ephrin ligands bind cell membrane bound Eph receptors. An EphB receptor is pictured above, whereas EphA receptors do not possess a cytoplasmic domain.

Understanding the properties and effects of each complex component of a local stem cell microenvironment is an essential step toward understanding the stem cell itself. In particular, the ability of a stem cell to respond to spatiotemporally varying biochemical cues and distinct mechanical and physical stimuli within its surroundings is being increasingly recognized and will continue to be elucidated in the years to come. The effect of substrate stiffness on stem cell fate has been becoming more appreciated in recent years, and other facets of the niche's solid phase – including spatial organization in the presentation of biochemical information, electrostatics [59], and biomolecular transport [60] – will increasingly be investigated. While technological limitations in the ability control, quantify, and image these properties currently exist, advances in super-resolution microscopy may be combined with stem cell research to enable considerable progress [61].

Furthermore, an appreciation of these interactive processes in natural tissue may greatly aid the development of stem cell therapies to treat numerous human diseases. For example, this basic knowledge may enable therapeutic modulation of endogenous stem cells via altering the niche, as well as offer opportunities to create more effective large scale culture systems and bioreactors to expand and differentiate stem cells. Furthermore, the creation of in vitro cell and tissue equivalents of therapeutically relevant organs, enabled by the technological advances and optimized model culture systems, will enable both basic and therapeutic investigations of human disease biology. Therefore, as is evidenced by an increasing number of important studies, a blend of biology, chemistry, physics, and engineering can empower progress in both basic and translational directions.

References

1. Till JE, Mc CE. (1961) A direct measurement of the radiation sensitivity of normal mouse bone marrow cells. *Radiat Res* 14:213-222.
2. Becker AJ, Mc CE, Till JE. (1963) Cytological demonstration of the clonal nature of spleen colonies derived from transplanted mouse marrow cells. *Nature* 197:452-454.

3. Thomson JA, Itskovitz-Eldor J, Shapiro SS, Waknitz MA, Swiergiel JJ, Marshall VS, Jones JM. (1998) Embryonic stem cell lines derived from human blastocysts. *Science* 282:1145-1147.
4. Eriksson PS, Perfilieva E, Bjork-Eriksson T, Alborn AM, Nordborg C, Peterson DA, Gage FH. (1998) Neurogenesis in the adult human hippocampus. *Nat Med* 4:1313-1317.
5. Clelland CD, Choi M, Romberg C, Clemenson GD, Jr., Fragniere A, Tyers P, Jessberger S, Saksida LM, Barker RA, Gage FH, Bussey TJ. (2009) A functional role for adult hippocampal neurogenesis in spatial pattern separation. *Science* 325:210-213.
6. Snyder JS, Hong NS, McDonald RJ, Wojtowicz JM. (2005) A role for adult neurogenesis in spatial long-term memory. *Neuroscience* 130:843-852.
7. Zhao C, Deng W, Gage FH. (2008) Mechanisms and functional implications of adult neurogenesis. *Cell* 132:645-660.
8. Curtis MA, Kam M, Nannmark U, Anderson MF, Axell MZ, Wikkelso C, Holtas S, van Roon-Mom WM, Bjork-Eriksson T, Nordborg C, Frisen J, Dragunow M, Faull RL, Eriksson PS. (2007) Human neuroblasts migrate to the olfactory bulb via a lateral ventricular extension. *Science* 315:1243-1249.
9. Alvarez-Buylla A, Kirn JR, Nottebohm F. (1990) Birth of projection neurons in adult avian brain may be related to perceptual or motor learning. *Science* 249:1444-1446.
10. Kirn J, O'Loughlin B, Kasparian S, Nottebohm F. (1994) Cell death and neuronal recruitment in the high vocal center of adult male canaries are temporally related to changes in song. *Proc Natl Acad Sci U S A* 91:7844-7848.
11. Schmidt-Hieber C, Jonas P, Bischofberger J. (2004) Enhanced synaptic plasticity in newly generated granule cells of the adult hippocampus. *Nature* 429:184-187.
12. van Praag H, Schinder AF, Christie BR, Toni N, Palmer TD, Gage FH. (2002) Functional neurogenesis in the adult hippocampus. *Nature* 415:1030-1034.
13. Suh H, Deng W, Gage FH. (2009) Signaling in Adult Neurogenesis. *Annu Rev Cell Dev Biol*.
14. Altman J, Das GD. (1965) Autoradiographic and histological evidence of postnatal hippocampal neurogenesis in rats. *J Comp Neurol* 124:319-335.
15. Kempermann G, Kuhn HG, Gage FH. (1997) More hippocampal neurons in adult mice living in an enriched environment. *Nature* 386:493-495.
16. Goldman SA, Nottebohm F. (1983) Neuronal production, migration, and differentiation in a vocal control nucleus of the adult female canary brain. *Proc Natl Acad Sci U S A* 80:2390-2394.
17. Shihabuddin LS, Horner PJ, Ray J, Gage FH. (2000) Adult spinal cord stem cells generate neurons after transplantation in the adult dentate gyrus. *J Neurosci* 20:8727-8735.
18. Manganas LN, Zhang X, Li Y, Hazel RD, Smith SD, Wagshul ME, Henn F, Benveniste H, Djuric PM, Enikolopov G, Maletic-Savatic M. (2007) Magnetic resonance spectroscopy identifies neural progenitor cells in the live human brain. *Science* 318:980-985.
19. Spalding KL, Bhardwaj RD, Buchholz BA, Druid H, Frisen J. (2005) Retrospective birth dating of cells in humans. *Cell* 122:133-143.
20. Gould E, Cameron HA, Daniels DC, Woolley CS, McEwen BS. (1992) Adrenal hormones suppress cell division in the adult rat dentate gyrus. *J Neurosci* 12:3642-3650.

21. Jessberger S, Zhao C, Toni N, Clemenson GD, Jr., Li Y, Gage FH. (2007) Seizure-associated, aberrant neurogenesis in adult rats characterized with retrovirus-mediated cell labeling. *J Neurosci* 27:9400-9407.
22. Winner B, Rockenstein E, Lie DC, Aigner R, Mante M, Bogdahn U, Couillard-Despres S, Masliah E, Winkler J. (2008) Mutant alpha-synuclein exacerbates age-related decrease of neurogenesis. *Neurobiol Aging* 29:913-925.
23. Tattersfield AS, Croon RJ, Liu YW, Kells AP, Faull RL, Connor B. (2004) Neurogenesis in the striatum of the quinolinic acid lesion model of Huntington's disease. *Neuroscience* 127:319-332.
24. Arvidsson A, Collin T, Kirik D, Kokaia Z, Lindvall O. (2002) Neuronal replacement from endogenous precursors in the adult brain after stroke. *Nat Med* 8:963-970.
25. Gage FH, Coates PW, Palmer TD, Kuhn HG, Fisher LJ, Suhonen JO, Peterson DA, Suhr ST, Ray J. (1995) Survival and differentiation of adult neuronal progenitor cells transplanted to the adult brain. *Proc Natl Acad Sci U S A* 92:11879-11883.
26. Schofield R. (1978) The relationship between the spleen colony-forming cell and the haemopoietic stem cell. *Blood Cells* 4:7-25.
27. Xie T, Spradling AC. (2000) A niche maintaining germ line stem cells in the Drosophila ovary. *Science* 290:328-330.
28. Ye S, Luo Y, Lu W, Jones RB, Linhardt RJ, Capila I, Toida T, Kan M, Pelletier H, McKeehan WL. (2001) Structural basis for interaction of FGF-1, FGF-2, and FGF-7 with different heparan sulfate motifs. *Biochemistry* 40:14429-14439.
29. Khachigian LM, Chesterman CN. (1992) Platelet-derived growth factor and alternative splicing: a review. *Pathology* 24:280-290.
30. Hasan M, Najjam S, Gordon MY, Gibbs RV, Rider CC. (1999) IL-12 is a heparin-binding cytokine. *J Immunol* 162:1064-1070.
31. Chang SC, Mulloy B, Magee AI, Couchman JR. (2011) Two distinct sites in sonic Hedgehog combine for heparan sulfate interactions and cell signaling functions. *J Biol Chem* 286:44391-44402.
32. Tayalia P, Mooney DJ. (2009) Controlled growth factor delivery for tissue engineering. *Adv Mater* 21:3269-3285.
33. Saha K, Schaffer DV. (2006) Signal dynamics in Sonic hedgehog tissue patterning. *Development* 133:889-900.
34. Chen TT, Luque A, Lee S, Anderson SM, Segura T, Iruela-Arispe ML. (2010) Anchorage of VEGF to the extracellular matrix conveys differential signaling responses to endothelial cells. *J Cell Biol* 188:595-609.
35. Kuhl PR, Griffith-Cima LG. (1996) Tethered epidermal growth factor as a paradigm for growth factor-induced stimulation from the solid phase. *Nat Med* 2:1022-1027.
36. Ho JE, Chung EH, Wall S, Schaffer DV, Healy KE. (2007) Immobilized sonic hedgehog N-terminal signaling domain enhances differentiation of bone marrow-derived mesenchymal stem cells. *J Biomed Mater Res A* 83:1200-1208.
37. Willerth SM, Rader A, Sakiyama-Elbert SE. (2008) The effect of controlled growth factor delivery on embryonic stem cell differentiation inside fibrin scaffolds. *Stem Cell Res* 1:205-218.
38. Alberti K, Davey RE, Onishi K, George S, Salchert K, Seib FP, Bornhauser M, Pompe T, Nagy A, Werner C, Zandstra PW. (2008) Functional immobilization of signaling proteins enables control of stem cell fate. *Nat Methods* 5:645-650.

39. Mammen M, Choi S.-K. & Whitesides, G.M. (1998) Polyvalent Interactions in Biological Systems: Implications for Design and Use of Multivalent Ligands and Inhibitors. *Angew. Chem. Int. Ed.* 37: 2754-2794.
40. Kiessling LL, Gestwicki JE, Strong LE. (2000) Synthetic multivalent ligands in the exploration of cell-surface interactions. *Curr Opin Chem Biol* 4:696-703.
41. Gestwicki JE, Strong LE, Kiessling LL. (2000) Tuning chemotactic responses with synthetic multivalent ligands. *Chem Biol* 7:583-591.
42. Jones DS, Coutts SM, Gamino CA, Iverson GM, Linnik MD, Randow ME, Ton-Nu HT, Victoria EJ. (1999) Multivalent thioether-peptide conjugates: B cell tolerance of an anti-peptide immune response. *Bioconjug Chem* 10:480-488.
43. Maheshwari G, Brown G, Lauffenburger DA, Wells A, Griffith LG. (2000) Cell adhesion and motility depend on nanoscale RGD clustering. *J Cell Sci* 113 (Pt 10):1677-1686.
44. Huebsch N, Arany PR, Mao AS, Shvartsman D, Ali OA, Bencherif SA, Rivera-Feliciano J, Mooney DJ. (2010) Harnessing traction-mediated manipulation of the cell/matrix interface to control stem-cell fate. *Nat Mater* 9:518-526.
45. Vyas N, Goswami D, Manonmani A, Sharma P, Ranganath HA, VijayRaghavan K, Shashidhara LS, Sowdhamini R, Mayor S. (2008) Nanoscale organization of hedgehog is essential for long-range signaling. *Cell* 133:1214-1227.
46. Dore JJ, Jr., Edens M, Garamszegi N, Leof EB. (1998) Heteromeric and homomeric transforming growth factor-beta receptors show distinct signaling and endocytic responses in epithelial cells. *J Biol Chem* 273:31770-31777.
47. Artavanis-Tsakonas S, Rand MD, Lake RJ. (1999) Notch signaling: cell fate control and signal integration in development. *Science* 284:770-776.
48. Pasquale EB. (2005) Eph receptor signalling casts a wide net on cell behaviour. *Nat Rev Mol Cell Biol* 6:462-475.
49. Wall ST, Saha K, Ashton RS, Kam KR, Schaffer DV, Healy KE. (2008) Multivalency of Sonic hedgehog conjugated to linear polymer chains modulates protein potency. *Bioconjug Chem* 19:806-812.
50. Davis S, Gale NW, Aldrich TH, Maisonpierre PC, Lhotak V, Pawson T, Goldfarb M, Yancopoulos GD. (1994) Ligands for EPH-related receptor tyrosine kinases that require membrane attachment or clustering for activity. *Science* 266:816-819.
51. Arlaud GJ, Colomb MG, Gagnon J. (1987) A Functional-Model of the Human C1 Complex - Emergence of a Functional-Model. *Immunol Today* 8:106-111.
52. Stein E, Lane AA, Cerretti DP, Schoecklmann HO, Schroff AD, Van Etten RL, Daniel TO. (1998) Eph receptors discriminate specific ligand oligomers to determine alternative signaling complexes, attachment, and assembly responses. *Genes Dev* 12:667-678.
53. Foster KE, Gordon J, Cardenas K, Veiga-Fernandes H, Makinen T, Grigorieva E, Wilkinson DG, Blackburn CC, Richie E, Manley NR, Adams RH, Kioussis D, Coles MC. (2010) EphB-ephrin-B2 interactions are required for thymus migration during organogenesis. *Proc Natl Acad Sci U S A* 107:13414-13419.
54. Kim YH, Hu H, Guevara-Gallardo S, Lam MT, Fong SY, Wang RA. (2008) Artery and vein size is balanced by Notch and ephrin B2/EphB4 during angiogenesis. *Development* 135:3755-3764.
55. Egea J, Klein R. (2007) Bidirectional Eph-ephrin signaling during axon guidance. *Trends Cell Biol* 17:230-238.

56. Wu J, Luo H. (2005) Recent advances on T-cell regulation by receptor tyrosine kinases. *Curr Opin Hematol* 12:292-297.
57. Zhao C, Irie N, Takada Y, Shimoda K, Miyamoto T, Nishiwaki T, Suda T, Matsuo K. (2006) Bidirectional ephrinB2-EphB4 signaling controls bone homeostasis. *Cell Metab* 4:111-121.
58. Batlle E, Henderson JT, Beghtel H, van den Born MM, Sancho E, Huls G, Meeldijk J, Robertson J, van de Wetering M, Pawson T, Clevers H. (2002) Beta-catenin and TCF mediate cell positioning in the intestinal epithelium by controlling the expression of EphB/ephrinB. *Cell* 111:251-263.
59. Radisic M, Park H, Shing H, Consi T, Schoen FJ, Langer R, Freed LE, Vunjak-Novakovic G. (2004) Functional assembly of engineered myocardium by electrical stimulation of cardiac myocytes cultured on scaffolds. *Proc Natl Acad Sci U S A* 101:18129-18134.
60. Carpenedo RL, Bratt-Leal AM, Marklein RA, Seaman SA, Bowen NJ, McDonald JF, McDevitt TC. (2009) Homogeneous and organized differentiation within embryoid bodies induced by microsphere-mediated delivery of small molecules. *Biomaterials* 30:2507-2515.
61. Shroff H, Galbraith CG, Galbraith JA, Betzig E. (2008) Live-cell photoactivated localization microscopy of nanoscale adhesion dynamics. *Nat Methods* 5:417-423.

CHAPTER 2

ASTROCYTES REGULATE ADULT HIPPOCAMPAL NEUROGENESIS THROUGH EPHRIN-B SIGNALING

This chapter is a postprint of a paper submitted to and accepted for publication as

Ashton RS, Conway A, Pangarkar C, Bergen J, Lim KI, Shah P, Bissell M, Schaffer DV. (2012) Astrocytes Regulate Adult Hippocampal Neurogenesis through Ephrin-B Signaling. *Nat Neurosci* 15:1399-1406.

The copy of record is available at
http://www.nature.com/neuro/journal/v15/n10/full/nn.3212.html.

Abstract

Neurogenesis in the adult hippocampus involves activation of quiescent neural stem cells (NSCs) to yield transiently amplifying NSCs and progenitors, and ultimately neurons that affect learning and memory. This process is tightly controlled by microenvironmental cues, though few endogenous factors are known to regulate neuronal differentiation. While astrocytes have been implicated, their role in juxtacrine (i.e. cell-cell contact-dependent) signaling within NSC niches has not been investigated. We show that ephrin-B2 presented from rodent hippocampal astrocytes regulates neurogenesis *in vivo*. Furthermore, clonal analysis in NSC fate-mapping studies reveals a novel role for ephrin-B2 in instructing neuronal differentiation. Additionally, ephrin-B2 signaling, transduced by EphB4 receptors on NSCs, activates β-catenin *in vitro* and *in vivo* independent of Wnt signaling and upregulates proneural transcription factors. Ephrin-B2^{+} astrocytes thus promote neuronal differentiation of adult NSCs through juxtacrine signaling, findings that advance our understanding of adult neurogenesis and may have future regenerative medicine implications.

Introduction

In the mammalian brain, neurogenesis persists throughout adulthood in the subgranular zone (SGZ) of the hippocampal dentate gyrus [1] and the subventricular zone (SVZ) of the lateral ventricles [2]. Within these niches, neural stem cell (NSC) maintenance, proliferation, and differentiation are orchestrated by a delicate balance of microenvironmental cues. The importance of such instructive signals in the niche is supported by the absence of significant neurogenesis in the adult mammalian central nervous system (CNS) outside of these regions [3,4] and by the development of aberrant neurogenesis in patients with pathologies that disrupt the natural chemistry of the brain, for example epilepsy [5], inflammation [6], and neurodegenerative diseases [7].

In the SGZ, adult neurogenesis entails the activation of quiescent Type 1 NSCs to produce mitotic, multipotent Type 2a NSCs [8,9]; the differentiation of the Type 2a NSCs to

lineage-committed, proliferative Type 2b neuronal precursors and subsequently Type 3 neuroblasts; and the survival, migration, and maturation of neuroblasts as they differentiate into granule cells that synaptically integrate into the existing neural network [8,9,10]. Each of these stages is regulated by signals within the niche. For example, bone morphogenic protein [11] and Notch [12,13] signaling modulate the balance between quiescent and proliferative NSCs, and Sonic hedgehog [14], fibroblast growth factor-2 [15], vascular endothelial growth factor [16], and Wnt7a [17] regulate NSC proliferation.

While there is thus increasing knowledge of niche factors that regulate NSC division, significantly less is known about key signals that instruct cells in the SGZ to undergo neuronal differentiation [18,19]. Gamma aminobutyric acid (GABA) inputs from local neuronal circuitry [20] and systemic retinoic acid levels [21] modulate NSC neuronal fate commitment. Furthermore, while neuronal differentiation precedes gliogenesis during CNS development, adult hippocampal astrocytes directly induce neuronal differentiation of NSCs *in vitro* via both secreted and membrane-associated factors [22], and the former have since been found to include Wnt3a [23] and potentially additional secreted signals [19]. However, the membrane-bound astrocytic components [22] that may play critical roles in neuronal fate commitment *in vivo* remain unidentified.

Ephrins are a diverse class of glycophosphatidylinositol-linked (ephrinA1-6) and transmembrane (ephrinB1-3) cell surface ligands that bind Eph receptors (EphA1-10 and EphB1-6) on opposing cell membranes to initiate bidirectional signaling [24]. Ephrin/Eph signaling is traditionally known to control the spatial organization of cells and their projections by modulating intercellular attractive and repulsive forces [25]. For example, ephrin/Eph signaling instructs topographical mapping of hippocampo-septal and entorhino-hippocampal projections during development [26] and regulates neuronal dendrite spine morphogenesis and synaptogenesis of adult hippocampal neurons [27].

Recent studies have also indicated that ephrin/Eph signaling plays an earlier role in regulating stem cell behavior. For example, ephrin-A/EphA signaling promotes embryonic telencephalic NSC differentiation [28], and ephrin-B3/EphB3 signaling may exert an anti-proliferative effect on NSCs in the developing SVZ [29]. Within the adult CNS, infusion of ephrin-B2 or EphB2 ectodomains into the lateral ventricles induced SVZ NSC proliferation and disrupted neuroblast migration through the rostral migratory stream [30]. Also, signaling between ephrin-$A2^+$ neural stem cells, and $EphA7^+$ ependymal cells and putative stem cells, was shown to suppress proliferation of NSCs in the adult SVZ [31]. Within the adult SGZ, ephrin-$B3^+$ neurons in the granule cell layer have been proposed to regulate $EphB1^+$ NSC polarity, SGZ positioning, and proliferation [32]. Similarly, in *Efna5*$^{-/-}$ mice, a decrease in both the proliferation of NSCs and the survival/maturation of newborn neurons in the adult SGZ was observed [33]. Thus, ephrin/Eph signaling has been shown to affect the proliferation, migration, and survival of adult NSCs; however, its potential regulation of NSC fate commitment remains unknown.

Here, we demonstrate that ephrin-B2 presented by hippocampal astrocytes instructs neuronal differentiation of NSCs in the SGZ of the adult hippocampus. Furthermore, ephrin-B2/EphB4 forward signaling induces neuronal differentiation of NSCs by activating β-catenin, independent of Wnt signaling, and inducing transcription of proneural transcription factors. Thus, these findings describe a novel juxtacrine signaling mechanism by which astrocytes actively regulate neuronal differentiation of NSCs during adult neurogenesis.

Materials and Methods

Cell Culture

NSCs isolated from the hippocampi of 6-week-old female Fisher 344 rats (Charles River), were cultured as previously described [14] on poly-ornithine/laminin-coated plates in DMEM/F12 medium (Life Technologies) containing N2 supplement (Life Technologies) and 20 ng/mL FGF-2 (PeproTech), with subculturing upon reaching 80% confluency using Accutase (Phoenix Flow Systems). To induce differentiation, NSCs were cultured for five days in DMEM/F12/N2 medium supplemented with 2% fetal bovine serum (FBS, Life Technologies) and 1 μM retinoic acid (BIOMOL). Rat hippocampal astrocytes were isolated from Fisher 344 rats (Charles River) as previously described [22] and cultured on poly-ornithine/laminin-coated plates in DMEM/F12/N2 supplemented with 10% FBS, with subculture upon reaching 90% confluency using Trypsin EDTA (Mediatech, Inc.).

Fc-Ephrin-B2 Synthesis and Differentiation Assays

To generate Fc-ephrin-B2, mouse ephrin-B2/Fc (Sigma-Aldrich) was incubated at a 9:1 ratio (w/w) with a goat, anti-human IgG Fc antibody (Jackson ImmunoResearch USA) for 90 min at 4°C before immediate use. To differentiate NSC *in vitro*, eight-well chamber slides were seeded with $5x10^4$ cells per well in standard culture medium containing 20 ng/mL FGF-2. Next day, the medium was replaced with DMEM/F12 containing 0.5 ng/mL FGF-2 and various concentrations of Fc-ephrin-B2. Differentiation experiments were performed over a 4 day period with a 50% media change daily. Then, the cells were fixed using 4% paraformaldehyde (PFA, Sigma Aldrich) and stained using standard protocols (see below). To test the effect of Eph receptor blocking, NSCs were pre-incubated with goat anti-EphB4 or anti-EphB2 (1:50, Santa Cruz Biotechnology) for 30 minutes before addition of Fc-ephrin-B2 ligands.

Lentiviral and Retroviral Vector Construction

DNA cassettes containing either human or mouse U6 promoter driven expression of candidate shRNAs against rat *efnb2* (Gene ID: 306636) were constructed by PCR. The forward primer containing a *Pac* I site for cloning and the reverse primer containing the entire shRNA sequence were used to amplify the U6 promoter from template plasmids pFhU6ABCgUGW (unpublished) or pmU6 pro. PCR was performed using Phusion high fidelity polymerase (Finnzymes) under the following conditions: pre-incubation at 98°C for 2 min; 30 cycles, with 1 cycle consisting of 12 s at 98°C, 30 s at 55°C - 65°C, and 15 s – 25 s at 72°C; and the final extension step of 2 min at 72°C. The U6 sense primers were sense_hU6 (5'-AACAATTAATTAAAAGGTCGGGCAGGAAGAGGGCCTATT-3') and sense_mU6 (5'-AACAATTAATTAAATCCGACGCCGCCATCTCTAGGCC-3'). For a listing of the shRNA encoding antisense primers see **Table 1**. In parallel, a control shRNA cassette against *LacZ* was constructed [34] analogously, using pBS U6 shRNA β-gal as the template and with primers listed in **Table 1**. All PCR products were digested with *Pac* I and cloned into the pFUGW lentiviral vector [35] upstream of the human ubiquitin-C promoter and eGFP. pCLGPIT-GSK3β S9A encoding a constitutively active form of GSK3β (a gift of Ashley Fritz and Smita Agrawal) was constructed by amplifying the GSK3β sequence from rat NSC cDNA, inserting it into pCLGPIT, and subjecting the plasmid to a site-directed mutagenesis to introduce the S9A mutation. Lentiviral and retroviral vectors were packaged using standard methods as described elsewhere

[36,37]. Lastly, to validate functionality of the *efnb2* shRNA vectors, the mouse GFAP promoter [38] as well as the human GFAP promoter [39] was cloned into the digested pFUGW vector, replacing the ubiquitin promoter upstream of eGFP.

***Efnb2* shRNA**	**Primer Sequence**
h2	5'-AAAATTAATTAAAAAGCCAAATTTCTACCCGGACATCTCTTGAATGTCCGGGTAGAAATTTGGCGGTGTTTCGTCCTTTCCACAAGATATATAAAGCC-3'
h3 (#1)	5'-AAAATTAATTAAAAAGCCGCAGGAGACACCGCAAATCTCTTGAATTTGCGGTGTCTCCTGCGGCGGTGTTTCGTCCTTTCCACAAGATATATAAAGCC-3'
h4	5'-AAAATTAATTAAAAAGAGCCGACAGATGCACTATTTCTCTTGAAAATAGTGCATCTGTCGGCTCGGTGTTTCGTCCTTTCCACAAGATATATAAAGCC-3'
h5	5'-AAAATTAATTAAAAAGCAGACAAGAGCCATGAAGATCTCTTGAATCTTCATGGCTCTTGTCTGCGGTGTTTCGTCCTTTCCACAAGATATATAAAGCC-3'
m1 (#2)	**5'-**AAAATTAATTAAAAAGGCTAGAAGCTGGTACGAATTCTCTTGAAATTCGTACCAGCTTCTAGCCAAACAAGGCTTTTCTCCAAGGGATATTTATAGTCTC-3'
m2	5'-AAAATTAATTAAAAAGCCAAATTTCTACCCGGACATCTCTTGAATGTCCGGGTAGAAATTTGGCAAACAAGGCTTTTCTCCAAGGGATATTTATAGTCTC-3'
m5	5'-AAAATTAATTAAAAAGCAGACAAGAGCCATGAAGATCTCTTGAATCTTCATGGCTCTTGTCTGCAAACAAGGCTTTTCTCCAAGGGATATTTATAGTCTC-3'
***LacZ* sense**	5'-GGGGTTAATTAAAAGGTCGGGCAGGAAGAGGGC-3'
***LacZ* anti-sense**	5'-GGGGTTAATTAAAAAAAGTGACCAGCGAATACCTGTTCTC-3'

Table 1: shRNA primers for RNAi.

Ephrin-B2 RNAi Co-Cultures

To select effective shRNA sequences targeting *efnb2,* hippocampus-derived astrocytes were transduced with lentivirus encoding trial shRNA sequences at an MOI of 3 and cultured for four days. RNA isolated from astrocyte cultures was analyzed for *efnb2* expression using QPCR (see below and **Fig. 6**). For co-culture assays, hippocampus-derived astrocytes were transduced with lentivirus encoding shRNA sequences at an MOI of 3 and cultured for two days prior to a 3 day incubation in medium containing 20 μM cytosine arabinoside (AraC, Sigma-Aldrich) to deplete rapidly dividing astrocytes. Then, cells were returned to standard medium for 24 hours, before being subcultured onto 8-well chamber slides at a density of 70,000 cells/cm^2. NSCs were transduced with retrovirus encoding either pCLGPIT or pCLGPIT-GSK3β S9A at an MOI of 1 and cultured for two days before a 96-hour selection period in medium containing 1 μg/mL puromycin (Sigma-Aldrich). Next, NSCs were incubated in standard media containing 25 μM bromodeoxyuridine (BrdU, Sigma-Aldrich) for 48-hours. Then, the BrdU-labeled NSCs were seeded on top of a monolayer of astrocytes in 8-well chamber slides at a density of 70,000 cells/cm^2 in medium lacking FGF-2. Co-cultures were maintained for six days prior to fixation and analysis by immunocytochemistry.

In Vivo Gain and Loss of Function Studies

All animal protocols were approved by the Institutional Animal Care and Use Committee of the University of California Berkeley. Eight-week-old adult female Fisher 344 rats received daily 50 mg/kg intraperitoneal (i.p.) injections of BrdU (Sigma Aldrich) dissolved in saline to label mitotic cells, as previously described [14]. In Fc-ephrin-B2 studies, animals were anesthetized prior to 3 µL bilateral intrahippocampal stereotaxic injections of either PBS (Life Technologies), ephrin-B2 (14 µg/mL), Anti-Fc antibody (126 µg/mL), or Fc-ephrin-B2 (140 µg/mL) in PBS. The injection coordinates were -3.5 mm anteriorposterior and ± 2.5 mm mediolateral relative to bregma, and -3.0 mm dorsoventral relative to dura. Refer to **Fig. 3a** for injection time course. Unbiased stereology (Zeiss Axio Imager, software by MicroBrightfield) using the optical fractionator method was performed on eight, evenly distributed sections from each rat to estimate the total number of relevant cells throughout the entire hippocampus. In RNAi studies, rats received bilateral intrahippocampal injections of 3 µL of lentiviral solutions in PBS on day -19. The injection coordinates with respect to bregma were -3.5 mm anteriorposterior, -3.5 mm dorsoventral (i.e. from the dura), and ± 2.0 mm mediolateral. Refer to **Fig. 8a** for injection time course. Unbiased stereology was performed on eight GFP^+ hippocampal sections from each rat, and the number of selected cells was normalized by the volume of hippocampal tissue analyzed.

In Vivo Fate Mapping

Nestin-CreER^{T2} mice [40] (a kind gift from Amelia Eisch, UT Southwestern, Dallas, TX) and *R26-stop$^{fl/fl}$-lacZ* mice [41] (a kind gift from John Ngai, UC Berkeley, Berkeley, CA), both having a 100% C57/Bl6 background, were crossbreed twice to generate a homozygous *Nestin-CreER^{T2};R26-stop$^{fl/fl}$-lacZ* mosue strain. Geneotyping was performed using the following primers: Cre-F (5'-ACCAGCCAGCTATCAACTCG-3'), Cre-R (5'-TTACATTGGTCCAGCCACC-3'), 200bp; LacZ-F (5'-GTCAATCCGCCGTTTGTTCCCACG-3'), LacZ-R (5'-CCAGTACAGCGCGGCTGAAATCAT-3'), 400 bp; wtRosa-F (5'-GGAGCGGGAGAAATGGATATG-3'), wtRosa-R (5'- AAAGTCGCTCTGAGTTGTTAT-3'), 600bp. To induce recombination and label mitotic cells, 5 week old *Nestin-CreER^{T2};R26-stop$^{fl/fl}$-lacZ* mice were administered i.p. 180 mg/kg tamoxifen (SigmaAldrich) dissolved in corn oil and 50 mg/kg BrdU daily for three days prior to intrahippocampal injections of experimental solutions. 1 µL of Anti-Fc (126 µg/mL) and Fc-ephrin-B2 (140 µg/mL) in PBS were then administered at -2.12 mm anteriorposterior, -1.55 mm dorsoventral (from dura), and ± 1.5 mm mediolateral with respect to the bregma. Pre-determined groups of mice (balanced in male-to-female ratio) were sacrificed at Day 0 (Sham), 5, and 14 time points, and tissue collection and histology were performed.

In Vitro Validation of β-Catenin Reporter and dnWnt Vectors

NSCs were co-infected with 7xTcf-FFluc [42] (Tcf-Luc) and either LV-dnWnt-IRES-GFP [23] or LV-GFP and expanded in culture. After a 24-hour pulse with Wnt3a (200 ng/mL), cell lysates were collected and analyzed using Luc-Screen® Extended-Glow Luciferase Reporter Gene Assay System (Applied Biosystems) and a TD-20/20 luminometer (Turner BioSystems) to determine the relative level of β-catenin activation.

In Vivo β-Catenin Activation and Wnt-Independent Neurogenesis

Eight-week-old adult female Fisher 344 rats received bilateral, intrahippocampal, stereotaxic injections of 3 µL of a mixture of half 7xTcf-FFluc [42] (Tcf-Luc) and half LV-dnWnt-IRES-GFP [23] or LV-GFP (kind gifts from Fred Gage, Salk Institute, La Jolla, CA) lentiviral vectors on Day -17. Starting on Day -3, animals were intraperitoneally injected with BrdU (50 mg/kg) for three days prior to subsequent bilateral intrahippocampal stereotaxic injections of 3 uL of either Fc-ephrin-B2 (140 µg/mL) or PBS on Day 0. The injection coordinates with respect to the bregma were -3.5 mm anteriorposterior, -3.4 mm dorsoventral (from dura), and ± 1.8 mm mediolateral. Animals were sacrificed on Day 1 and half were sacrificed on Day 5 before brains were processed for histology and analyzed by stereology.

Immunostaining and Imaging

Cells cultures were fixed with 4% paraformaldehyde (PFA) for 10 minutes, blocked for 1 hour with 5% donkey serum (Sigma), permeabilized with 0.3% Triton X-100 (Calbiochem), and incubated for 48 hours with combinations of the following primary antibodies: mouse anti-nestin (1:1000, BD Pharmingen), rabbit anti-GFAP (1:250, Abcam), rabbit anti-βIII-Tubulin (1:250, Sigma), and rabbit anti-MBP (1:500, Santa Cruz). Appropriate Cy3-, Cy5-, or Alexa Fluor 488-conjugated secondary antibodies were used to detect primary antibodies (1:250, Jackson Immunoresearch; 1:250, Molecular Probes). TO-PRO-3 (10 µM, Life Technologies) or DAPI was used as the nuclear counterstain.

Animals were perfused with 4% PFA (Sigma), and brain tissue was extracted, stored in fixative for 24 hours, and allowed to settle in a 30% sucrose solution. Brains were coronally sectioned and immunostained using previously published protocols [14]. Primary antibodies used were mouse anti-BrdU (1:100, Roche), mouse anti-NeuN (1:100, Millipore), rat anti-BrdU (1:100, Abcam), goat anti-doublecortin (1:50, Santa Cruz Biotechnology), rabbit anti-GFAP (1:1000, Abcam), guinea pig anti-doublecortin (1:1000, Millipore), goat anti-ephrin-B2 (1:10, R&D Systems), rabbit anti-Sox2 (1:250, Millipore), goat anti-EphB4 (1:50, Santa Cruz), mouse anti-GFAP (1:2000, Advanced Immunochemical), rabbit anti-GFP (1:2000, Life Technologies), goat anti-GFP (1:200, Abcam), and rabbit anti-β-Gal (Gift from John Ngai). Appropriate Cy3-, Cy5-, or Alexa Fluor 488-conjugated secondary antibodies (1:125, Jackson Immunoresearch; 1:250, Life Technologies) were used. For sections stained with rat anti-BrdU, biotin-conjugated anti-rat IgG (1:250, Jackson Immunoresearch) was used as the secondary, which was then washed and incubated with Cy3-conjugated streptavidin (1:1000, Jackson Immunoresearch USA) for 2 hours to amplify the signal. DAPI (50 µg/mL, Invitrogen) was used as a nuclear counterstain. Sections were mounted on glass slides and analyzed using the optical fractionator method in unbiased stereological microscopy (Zeiss Axio Imager, software by MicroBrightfield) and/or imaged with either a Leica Microsystems confocal microscope or a Zeiss 510 Meta UV/VIS confocal microscope located in the CNR Biological Imagining Facility at the University of California Berkeley.

Western Blotting

NSCs were seeded at $2.5x10^5$ cells per well in a 6-well culture dish in standard culture medium containing 0.1 µg/mL FGF2. The following day, 10 µg/mL Fc-ephrin-B2 was added using a 50% media change. To test the effect of inhibition of the EphB4 receptor, NSCs were pre-incubated with goat anti-EphB4 (1:50, Santa Cruz Biotechnology) for 30 minutes before addition of Fc-ephrin-B2. Cell lysates were collected at various time intervals (0-24 hours after Fc-ephrin-B2 addition) and Western blotted as previously described [43]. On nitrocellulose

membranes, proteins were labeled using anti-active β-catenin (1:500, Millipore) and rabbit anti-total GSK-3β (1:1000, Cell Signaling) primary antibodies in combination with the appropriate HRP-conjugated secondary antibody (1:10,000, Pierce). SuperSignal West Dura Extended Duration Substrate (Pierce) was used to detect the protein bands, and after film development (Kodak Film Processor 5000RA), membranes were stripped and re-probed with rabbit anti-GAPDH (1:2500, Abcam).

RNA Isolation and QPCR

RNA samples were isolated using standard Trizol (Life Technologies) collection and ethanol precipitation. RNA samples were quantified using a NanoDrop Spectrophotomer ND-1000 (NanoDrop Technologies, Inc.), and equivalent amounts of RNA were added to QPCR reactions. Quantitative PCR was performed to probe for expression of nestin, GFAP, β-Tubulin III, and 18S mRNA using prior protocols [44]. For analysis of ephrin-B2 mRNA levels, QPCR was performed using a Taqman Gene Expression Assay (Applied Biosystems) for *efnb2* (#Rn01215895_m1) and for eukaryotic *18S* (#803026). All reactions were performed using a BioRad IQ5 Multicolor Real-Time Detection System, and target mRNA expression levels were normalized according to levels of 18S.

Statistical Analysis

Statistical significance of the results was determined using an ANOVA and multiple means comparison function (i.e. Tukey-Kramer Analysis) in MATLAB. Data are represented as means ± s.d.

Results

Ephrin-B2 and EphB4 Expression in the SGZ

In the SGZ, Type 1 NSCs express the SRY-box 2 (Sox2) transcription factor and stain for glial fibrilary acid protein (GFAP) and Nestin along radial granule cell layer (GCL)-spanning or horizontal processes [13]. Type 2a NSCs [9] remain $Sox2^+$ and $Nestin^+$ but downregulate GFAP expression, and fate-restricted, proliferative Type 2b neuronal precursors co-express Sox2 and doublecortin (DCX) while downregulating Nestin expression. The latter then mature into ($Sox2^-/DCX^+$) Type 3 neuroblasts, which migrate into the GCL to become neuronal specific nuclear protein (NeuN)-positive/DCX^- granule neurons [8,10,11,13]. Alternatively, Type 1 NSCs can differentiate into stellate, $Sox2^-/GFAP^+$, hippocampal astrocytes primarily located in the hilus adjacent to the SGZ [10].

As part of a candidate screen, we investigated ephrin-B2 expression within the hippocampal dentate gyrus. Ephrin-B2 antibodies consistently labeled $GFAP^+$ astrocytes in the hilus, the SGZ, and the molecular layer (**Fig. 1a**,**b**). In contrast, EphB4, an ephrin-B2 receptor, was expressed by $Sox2^+/DCX^-$, $Sox2^+/DCX^+$, $Sox2^-/DCX^+$, and $Sox2^+/GFAP^-$ cells in the SGZ, as well as on the majority of cells in the GCL (**Fig. 1a,c**,**d**). Therefore, EphB4 appears to be expressed in Type 2a ($Sox2^+/DCX^-/GFAP^-$) NSCs and persists as these cells become Type 2b neuronal precursors ($Sox2^+/DCX^+$), Type 3 neuroblasts ($Sox2^-/DCX^+$), and eventually granule neurons. Some Type 1 NSCs stained $EphB4^+$, though in many EphB4 was not expressed at levels detectable by immunostaining (data not shown). Overall, staining results indicate that astrocytes

are a source of ephrin-B2 ligand in the dentate gyrus and suggest that EphB4-expressing NSCs, neuronal precursors, and neuroblasts contact these ligand-expressing astrocytes (**Fig. 1e**,**f**).

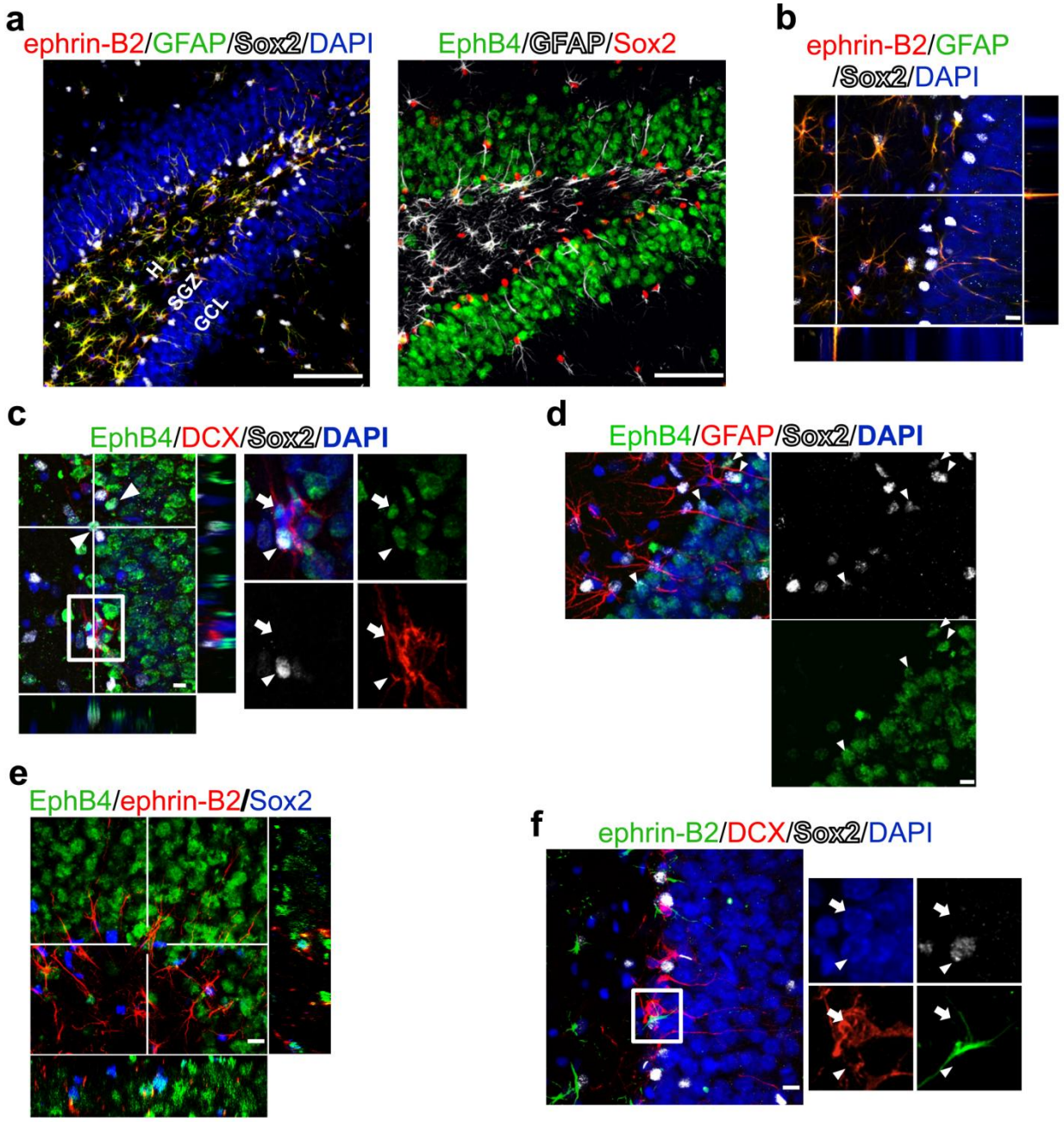

Figure 1: ***In vivo*****, SGZ Type 2a NSCs, Type 2b neuronal precursors, and Type 3 neuroblasts express EphB4, and hippocampal astrocytes express ephrin-B2.** (**a**) Staining of the hippocampal dentate gyrus showed that $GFAP^+$ hilar (H) astrocytes express ephrin-B2. In addition, cells in the SGZ and neurons in the granule cell layer (GCL) express $EphB4^+$ on the cell soma. Scale bar represents 100 µm. (**b**) $GFAP^+$ astrocytes adjacent to the SGZ co-express ephrin-B2. (**c,d**) EphB4 expression persists throughout NSC neuronal differentiation, including Type 2a NSCs ($Sox2^+/DCX^-/GFAP^-$), Type 2b neuronal precursors ($Sox2^+/DCX^+$), and Type 3 neuroblasts (DCX^+). (**c**) Confocal images show EphB4 expression in $Sox2^+/DCX^-$ cells (large arrowheads) in the SGZ. Magnified region depicts the presence of EphB4 expression on a $Sox2^+/DCX^+$ Type 2b neuronal precursor (small arrowhead) and a DCX^+ Type 3 neuroblast (arrow). (**d**) Confocal images also show EphB4 expression by $Sox2^+/GFAP^-$ cells (small

arrowheads); therefore, $Sox2^+/DCX^-/GFAP^-$ Type 2a NSCs also express EphB4. (**e**) Given the close proximity of ephrin-$B2^+$ astrocytes to $EphB4^+$ cells in the SGZ, ephrin-B2/EphB4 juxtacrine signaling is in a position to induce NSC differentiation into (**f**) $Sox2^+/DCX^+$ Type 2b neuronal precursors (small arrowhead) and subsequently $Sox2^-/DCX^+$ Type 3 neuroblasts (arrow). The scale bars represent 10 μm.

Ephrin-B2 Increases Neurogenesis *In Vitro* and *In Vivo*

Ephrin/Eph signaling begins with clustering of multiple ligand-receptor complexes at sites of cell-cell contact [24]. Thus to initially explore a possible role for ephrin-B2 in regulating NSC fate, antibody-clustered ephrin-B2/Fc fusion molecules (Fc-ephrin-B2) [45] were added to adult hippocampus-derived NSCs in culture and found to induce a strong, dose-dependent increase in NSC neuronal differentiation (**Fig. 2a**,**b**). No biological activity was observed with monomeric, unclustered ephrin-B2/Fc, consistent with previous findings [30,45], and no proliferative effect was observed under any conditions (data not shown). To investigate which receptor mediated Fc-ephrin-B2's activity, the NSCs were pre-incubated with an antibody against EphB2 or EphB4, two known ephrin-B2 receptors, before addition of Fc-ephrin-B2. Inhibition of EphB4, but not EphB2, significantly reduced Fc-ephrin-B2 induction of neuronal differentiation (**Fig. 2c**), indicating that EphB4 receptors mediate the proneuronal effect of Fc-ephrin-B2. RT-PCR and immunocytochemistry (ICC) results confirmed that hippocampus-derived NSCs express EphB4 receptors (**Fig. 2d**), in contrast to SVZ NSCs which reportedly do not express EphB4 [30].

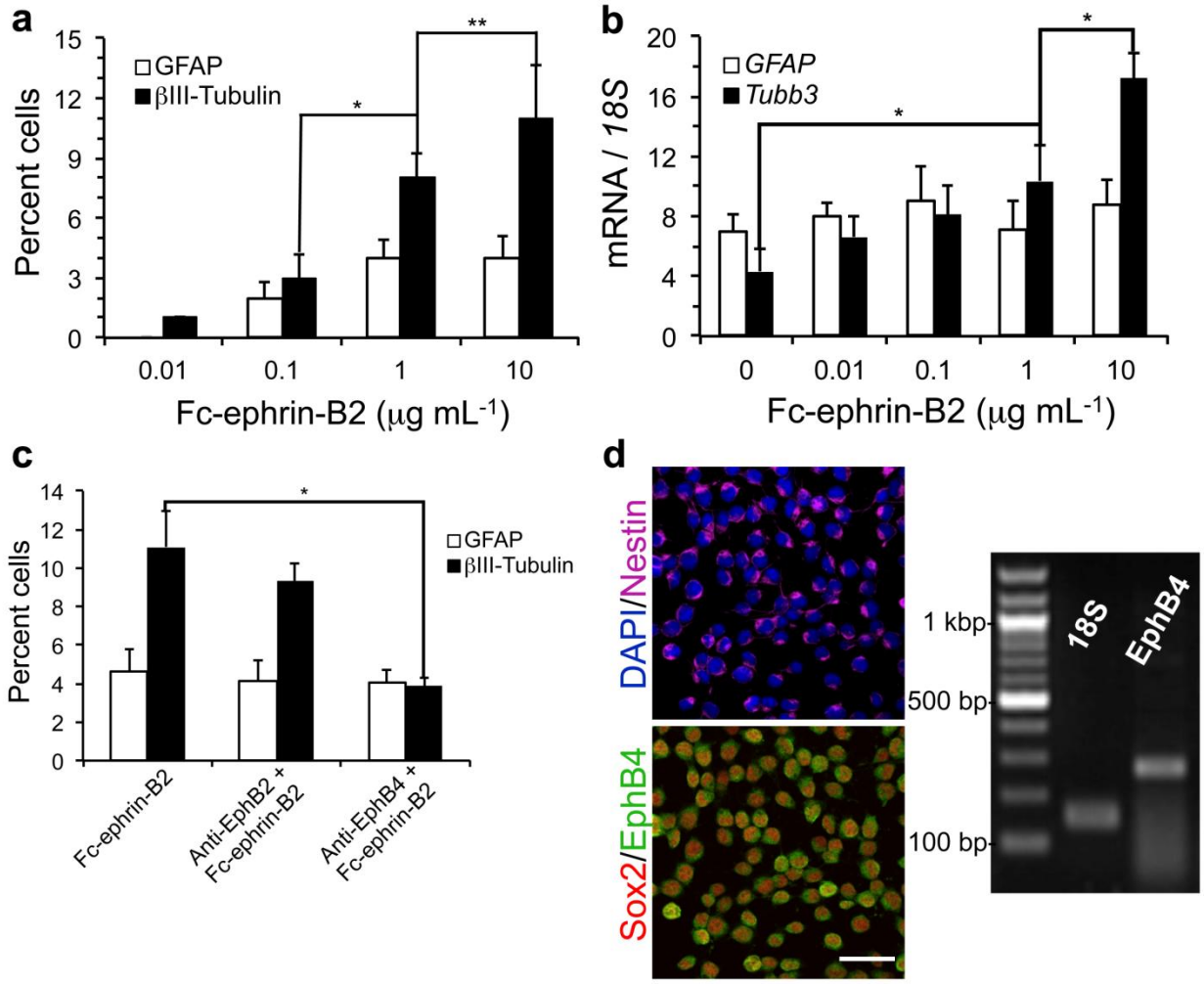

Figure 2: Fc-ephrin-B2 promoted the neuronal differentiation of NSCs *in vitro*. (**a,b**) Stimulation by Fc-Ephrin-B2 induced NSCs to undergo neuronal differentiation (βIII-Tubulin$^+$ or *Tubb3*) in a dose-responsive fashion as measured by immunocytochemistry and QPCR (n = 3, experimental replicates). Glial fibrilary acidic protein (GFAP) staining was slightly increased with ephrin-B2, but no increase in expression was observed by QPCR. (**c**) Blockage of ephrin-B2 receptors, EphB2 and EphB4, during Fc-ephrin-B2 (10 μg/mL) stimulation revealed that EphB4 mediates Fc-ephrin-B2's proneuronal effect on NSCs (n = 3, experimental replicates). ANOVA plus a multi-variable Tukey-Kramer analysis was conducted, with * indicating $P < 0.01$ and ** indicating $P < 0.05$. Data are represented as means ± s.d. (**d**) Nestin$^+$/Sox2$^+$ NSCs express EphB4 as demonstrated by immunocytochemistry and RT-PCR. Scale bar represents 100 μm.

Given the previous staining and *in vitro* results, we hypothesized that astrocytic ephrin-B2 actively promotes neuronal differentiation of NSCs in the SGZ through juxtacrine signaling, and therefore, we proceeded to investigate Fc-ephrin-B2 activity *in vivo*. Mitotic cells in the brain of adult rats were first labeled with BrdU, followed by bilateral hippocampal injections of PBS, non-clustered ephrin-B2, Anti-Fc antibody without ephrin-B2, or Fc-ephrin-B2 (**Fig. 3a**). Five days after injection, histology showed an increase in the number of BrdU$^+$ cells in the SGZ of animals injected with Fc-ephrin-B2 compared to animals treated with vehicle or clustering antibody controls (**Fig. 3c**), mirroring one report in the SVZ [30]. In addition, no difference in the percentage of BrdU$^+$ cells that co-stained as non-radial GFAP$^+$ astrocytes was observed

between experimental groups at Day 5 (**Fig. 4a**,**b**). However, there was a considerable increase in the proportion of $BrdU^+$ cells that co-stained for DCX in animals injected with Fc-ephrin-B2 (80.6% ± 0.87%) as compared to PBS (40.65% ± 4.15%), ephrin-B2 (50.3% ± 3.45%), and Anti-Fc (50.37% ± 9.28%) controls (**Fig. 3b**,**d**). These results indicate that ephrin-B2 signaling *in vivo* may regulate early stages of adult hippocampal neurogenesis by modulating NSC proliferation and/or differentiation, but further analysis is required to distinguish between these two possibilities.

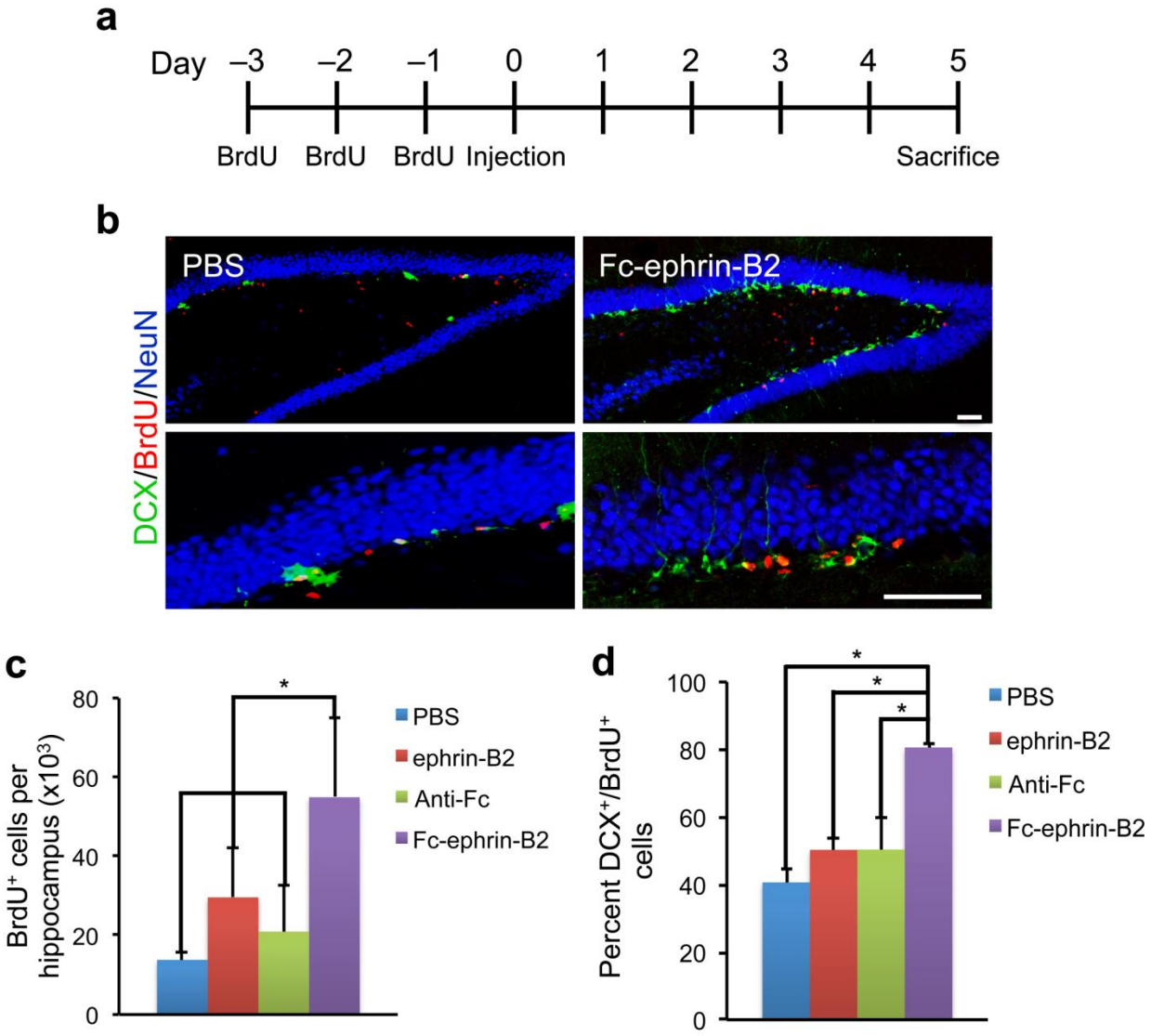

Figure 3: Intrahippocampal injection of Fc-ephrin-B2 increases neurogenesis in the SGZ. (**a**) Schematic of experimental time course. (**b**) Administration of Fc-ephrin-B2 into the hippocampus significantly increased neurogenesis as shown by representative confocal images of the dentate gyrus and SGZ (close-up). The scale bar represents 100 µm. (**c**) The injection of exogenous ephrin-B2 ligands increased $BrdU^+$ cell numbers compared to vehicle and constituent controls. (**d**) Only injection of Fc-ephrin-B2, but not its constituent controls, increased the percentage of $BrdU^+$ cells that co-stained for DCX in the SGZ (n = 3 brains, analyzed 8 hippocampal sections per brain). * indicates $P < 0.01$, and ** indicates $P < 0.05$; ± s.d.

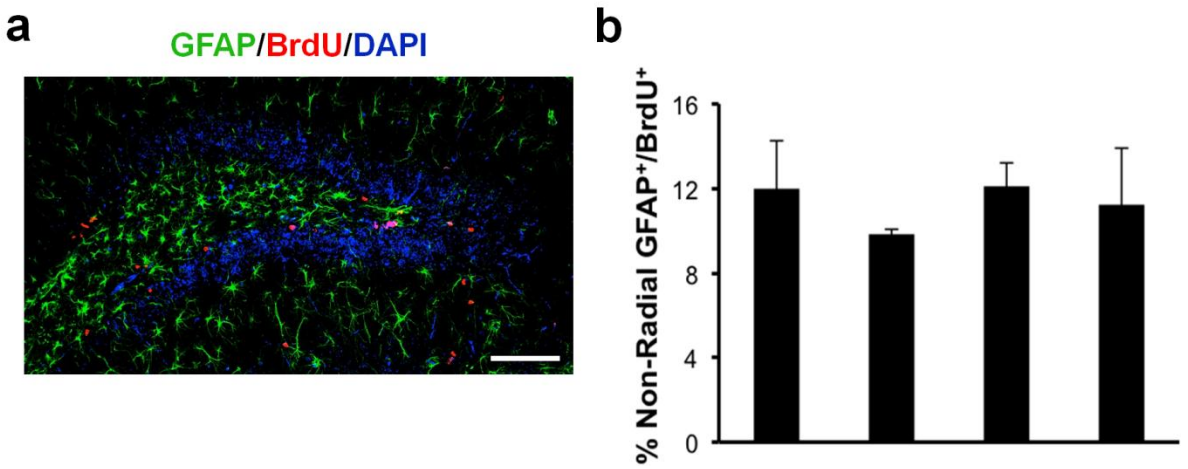

Figure 4: Fc-ephrin-B2 does not affect gliogenesis *in vivo*. (**a**) In general, only a small fraction of $BrdU^+$ cells co-labeled as astrocytes ($GFAP^+$). (**b**) The percentage of radial, $GFAP^+/BrdU^+$, Type 1 NSCs and non-radial $GFAP^+/BrdU^+$ astrocytes was not affected by Fc-ephrin-B2 induced signaling (n = 4 experimental replicates ± s.d.).

Astrocytic Ephrin-B2 Regulates Neurogenesis *In Vitro*

Exogenous ephrin-B2 elevates hippocampal neurogenesis, and astrocytes expressing ephrin-B2 contact NSCs in the hippocampus; however, it remains unclear whether astrocytic ephrin-B2 regulates NSC fate. Previous studies have shown that hippocampal astrocytes promote neuronal differentiation of co-cultured NSCs through secretion of soluble Wnt3a and by unidentified membrane-bound signaling molecules [22,23].To determine whether ephrin-B2 is a key component of this membrane-associated activity, we first verified its expression in cultured hippocampal astrocytes. Consistent with the *in vivo* results (**Fig. 1**), QPCR revealed that hippocampus-derived astrocytes express ephrin-B2 mRNA at levels three orders of magnitude higher than cultured NSCs (**Fig. 5a**). Notably, cultured NSCs down-regulate EphB4 and up-regulate ephrin-B2 expression upon astrocytic differentiation, yet maintain EphB4 expression on their soma upon neuronal differentiation into DCX^+ immature neurons (**Fig. 5b**).

We then analyzed whether RNAi-mediated knockdown of ephrin-B2 in hippocampal astrocytes could compromise their ability to induce neuronal differentiation of NSCs in co-culture. We screened five candidate anti-*efnb2* shRNA sequences expressed under a human and/or a mouse U6 promoter upstream of a human ubiquitin-C promoter eGFP expression cassette (**Fig. 6**). Upon lentiviral delivery, QPCR analysis indicated that two shRNA constructs (*efnb2* shRNA #1 and #2) could knockdown ephrin-B2 mRNA levels in astrocytes by approximately 90 and 85%, respectively (**Fig. 7a**). Next, BrdU-labeled NSCs (<95%) were seeded on near-confluent layers of mitotically inactivate astrocytes, that were naïve or expressing *efnb2* shRNA #1, #2, or *LacZ* shRNA, and the co-cultures were immunostained after six days. NSC proliferation was insignificant in all experimental groups. However, the percentage of βIII-$Tubulin^+/BrdU^+$ cells increased from 6.79 ± 0.62% in NSC-only control cultures to 14.2 ± 0.55% in NSC/ naïve astrocyte co-cultures (**Fig. 7b**), levels consistent with a prior NSC-astrocyte co-culture study [22], and the neuronally differentiated NSCs were primarily located in close proximity to astrocytes (**Fig. 7c**). A similar proneuronal effect was maintained by astrocytes expressing the *LacZ* shRNA (15.4 ± 1.12%); however, knockdown of ephrin-B2 expression within *efnb2* shRNA #1 and #2 astrocytes decreased their neuronal instructive potential by ~70%, i.e. to 9.09 ± 0.39% and 9.51 ± 0.11% βIII-$Tubulin^+/BrdU^+$ cells, respectively.

Intriguingly, this decrease in NSC neuronal differentiation due to ephrin-B2 knockdown is comparable to the previously observed ~55% loss when NSCs were cultured in astrocyte-conditioned medium rather than in co-culture [22]. Furthermore, antibody blockage of EphB4 receptors in the co-culture assay also significantly inhibited the proneuronal effect of naïve astrocytes, resulting in only 10.75 ± 0.87% of NSCs differentiating into βIII-Tubulin^{+}/BrdU^{+} neurons. Ephrin-B2 is thus a key membrane-presented factor that hippocampal astrocytes employ to instruct neuronal differentiation of NSCs *in vitro*, and EphB4 receptors on NSCs transduce this signal.

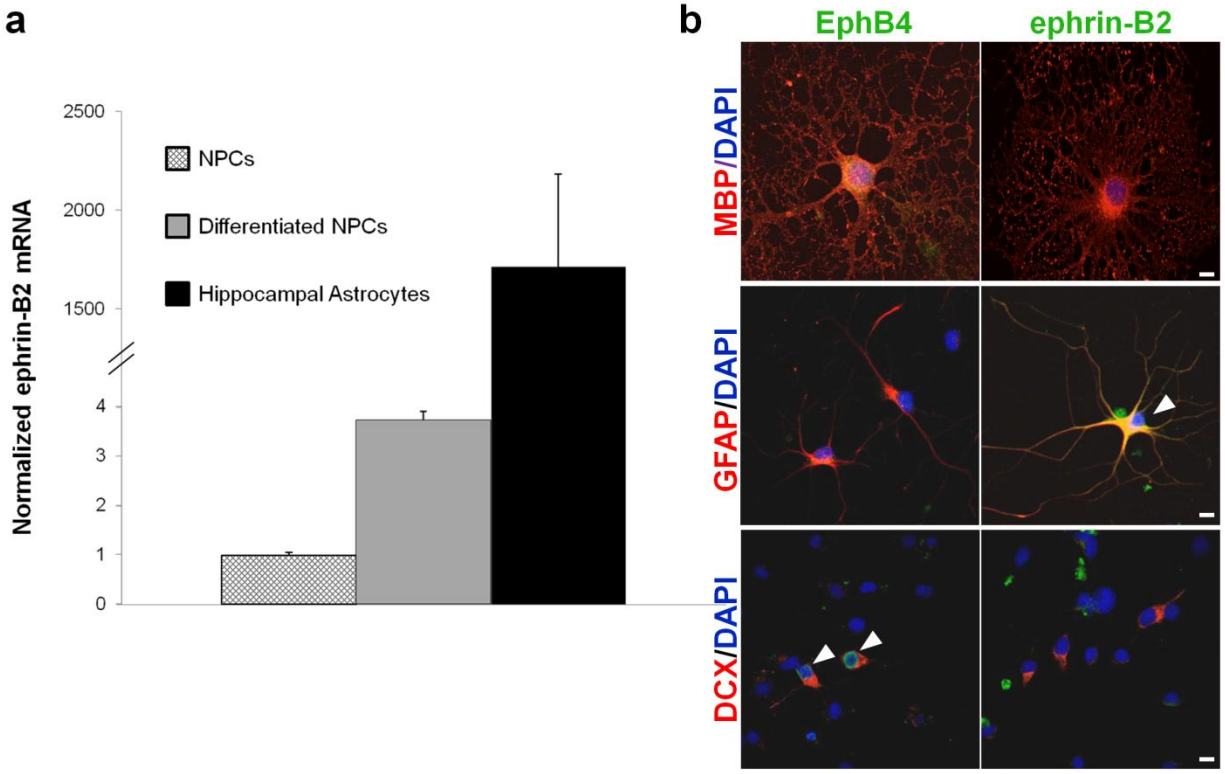

Figure 5: In vitro analysis of ephrin-B2 expression in hippocampus-derived astrocytes and differentiated NSCs. (**a**) Using QPCR, we compared *efnb2* expression levels in cultures of NSCs, differentiated NSCs, and hippocampus-derived astrocytes. Hippocampus-derived astrocytes express *efnb2* at levels three order-of-magnitude higher than NSCs, and it appears as though *efnb2* expression increased as the fraction and maturity of astrocytes in the cell population also increased. Data is normalized to NSC *efnb2* expression level (n = 3, technical replicates ± s.d.). (**b**) NSCs were differentiated into oligodendrocytes (MBP^{+}), astrocytes (GFAP^{+}), and immature neurons (DCX^{+}) and stained for expression of ephrin-B2 and EphB4. NSCs differentiated into astrocytes down-regulated EphB4 and up-regulated ephrin-B2 expression, while NSCs differentiated into neurons still expressed EphB4 on the cell soma. NSCs differentiated into oligodendrocytes did not express high levels of either ephrin-B2 or EphB4. The scale bar represents 10 μm.

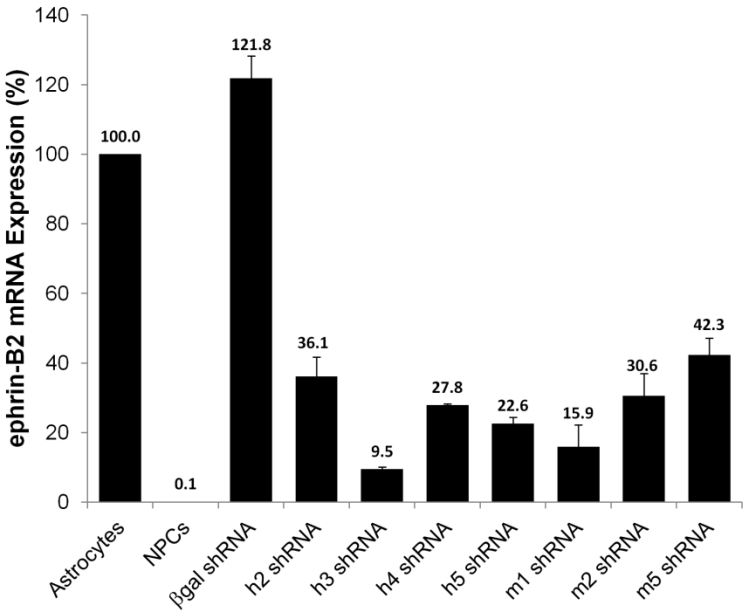

Figure 6: Screen for effective shRNA targeting *efnb2*. QPCR analysis of hippocampus-derived astrocytes expressing shRNA sequences designed to knockdown expression of *efnb2*. Five shRNA sequences were tested using human or mouse U6 promoters. Naïve astrocytes, NSCs, and astrocytes expressing a shRNA sequence targeting *LacZ* mRNA were used as controls, and data was normalized to *efnb2* expression of non-infected astrocytes (n = 3, technical replicates ± s.d.).

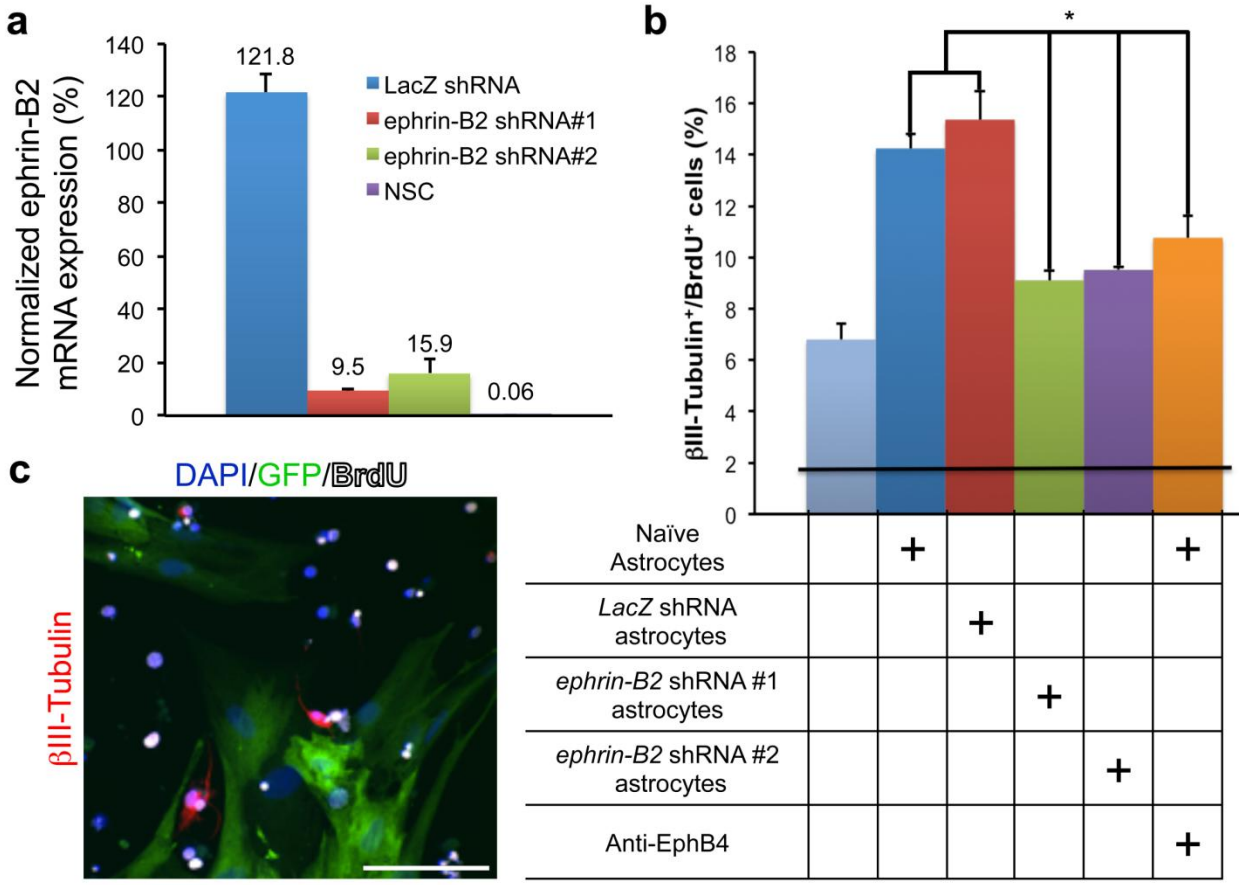

Figure 7: Ephrin-B2 RNAi decreases the proneuronal effect of hippocampus-derived astrocytes *in vitro*. (**a**) *Efnb2* shRNA lentiviral vectors (#1 and #2) significantly inhibit *efnb2* expression in hippocampus-derived astrocytes. Expression levels were measured by QPCR and normalized to *efnb2* expression in non-infected hippocampus-derived astrocytes (i.e. 100%). Also, hippocampus-derived astrocytes express orders of magnitude more *efnb2* than NSCs (n = 3, technical replicates). (**b**) Naïve astrocytes and astrocytes expressing a control *LacZ* shRNA promoted neuronal differentiation of NSCs, compared to NSC-only cultures. However, knockdown of astrocyte *efnb2* expression, or antibody blockage of NSC EphB4 receptors, significantly diminished the proneuronal effect of hippocampus-derived astrocytes, as demonstrated by the decrease in the percentage of βIII-Tubulin$^+$/BrdU$^+$ NSCs to levels closer to those in NSC-only cultures (n = 4, experimental replicates). The solid black line indicates the level of βIII-Tubulin$^+$/BrdU$^+$ cells at the start of the experiment. (**c**) Representative confocal image of BrdU-labeled NSCs differentiated into βIII-Tubulin$^+$ neurons after co-culture with lentiviral vector-expressing, i.e. GFP$^+$, astrocytes. NSCs adjacent to astrocytes had a higher propensity for neuronal differentiation. Scale bar represents 100 µm. * indicates $P < 0.01$; ± s.d.

Loss of Astrocytic Ephrin-B2 Decreases Neurogenesis in SGZ

To determine whether endogenous ephrin-B2 signaling promotes neuronal differentiation *in vivo*, adult rats were injected intrahippocampally with lentiviral vectors encoding *efnb2* shRNA #1, #2, or control *LacZ* shRNA. After two weeks, mitotic cells in the SGZ were labeled with BrdU, and tissue samples were collected after five additional days (**Fig. 8a**). Within GFP$^+$ regions of the hippocampus, ephrin-B2 levels from rats treated with the *efnb2* shRNA constructs were dramatically lower than in sections from PBS or *LacZ* shRNA treated rats, which exhibited ephrin-B2 expression in patterns similar to GFAP staining (**Fig. 8b**). We noted that neurons rather than astrocytes expressed GFP in the lentiviral vector-infected hippocampi; however, it was later confirmed through administration of an otherwise identical lentiviral vector in which

the human ubiquitin-C promoter was replaced with a GFAP promoter [22] that the low GFP expression initially observed in astrocytes was due to the ubiquitin promoter (**Fig. 9a**,**b**). In either case, the U6 promoter driving the shRNA expression mediated strong ephrin-B2 knockdown in hippocampal astrocytes (**Fig. 8b** and **Fig. 9c)**.

Next, $BrdU^+$ and $DCX^+/BrdU^+$ cells in the SGZ were quantified within GFP^+ hippocampi (**Fig. 8c**). In contrast to results obtained after administration of exogenous ephrin-B2, no significant difference in the number of $BrdU^+$ cells/mm^3 was observed in *efnb2* shRNA #1 (33.2 ± 11.3%) and #2 (22.5 ± 2.50%) vs. *LacZ* shRNA control animals (29.0 ± 7.20%, **Fig. 8d**), importantly indicating that endogenous ephrin-B2 signaling does not by itself regulate the proliferation of NSCs and Type 2b neuronal precursors. However, consistent with the proneuronal effect of Fc-ephrin-B2 *in vitro* and *in vivo*, the percentage of $BrdU^+$ cells that co-stained for DCX was significantly lower in animals treated with *efnb2* shRNA #1 (32.3 ±4.95%) and #2 (41.6 ± 3.41%) compared to *LacZ* shRNA (59.4 ± 2.33%, **Fig. 8e**). Therefore, knockdown of ephrin-B2 expression in hippocampal astrocytes decreased neurogenesis in the adult SGZ.

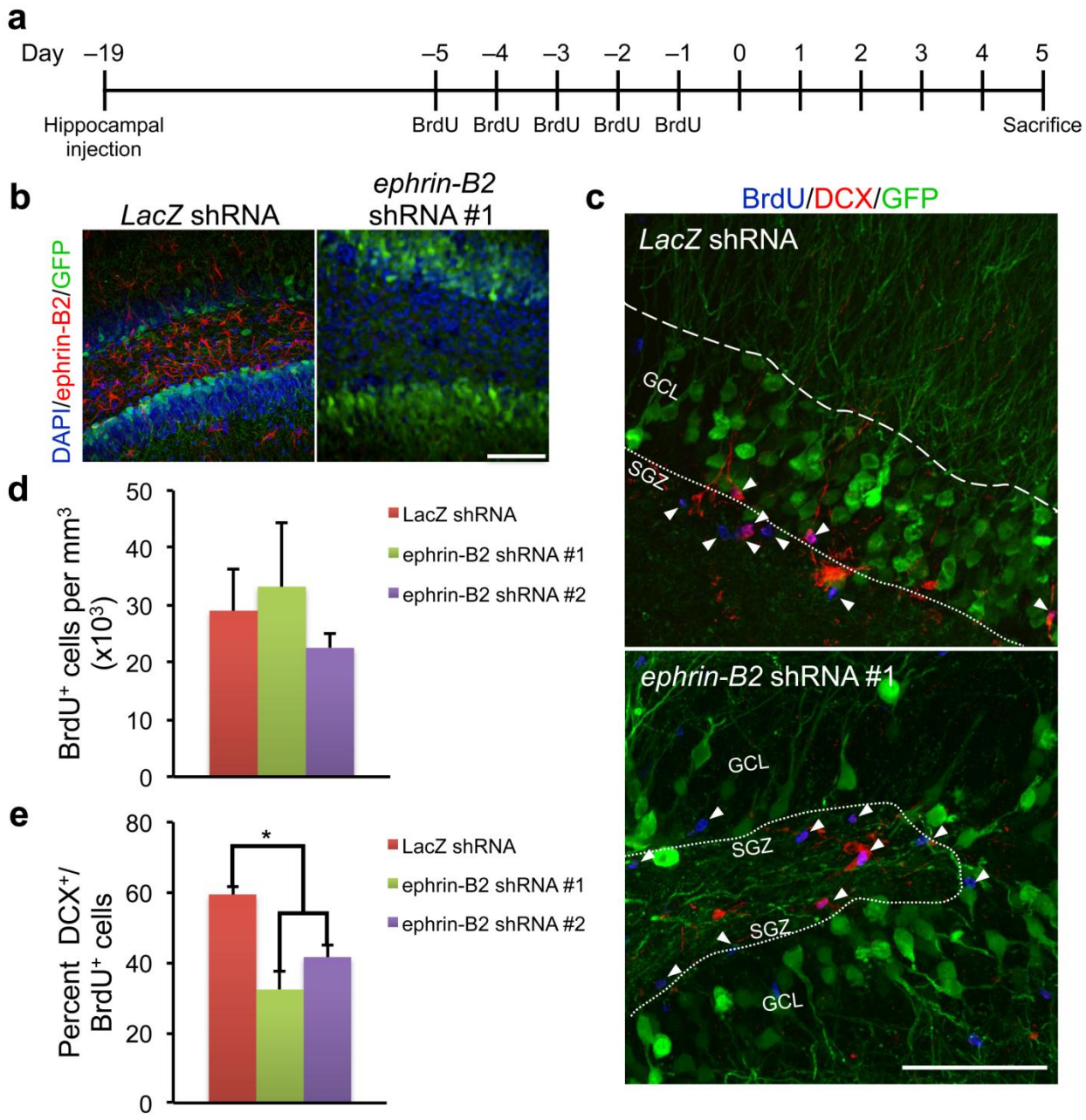

Figure 8: Ephrin-B2 RNAi decreases neuronal differentiation of BrdU$^+$ cells in the SGZ. (**a**) Schematic of experimental time course. (**b**) Regions of the hippocampus transduced with lentiviral vector (GFP$^+$) carrying *efnb2* shRNA #1 and #2 (data not shown) showed considerably less ephrin-B2 staining than hippocampi transduced with *LacZ* shRNA lentivirus injected rats. (**c**) Representative confocal images showing decreased neuronal differentiation, i.e. DCX$^+$ co-staining, of BrdU$^+$ (arrowheads) cells in the SGZ of rats injected with lentivirus encoding *efnb2* shRNA. Scale bars represent 100 µm. (**d,e**) Knockdown of ephrin-B2 in the hippocampal niche did not affect BrdU$^+$ cell numbers, but it did result in a significant decrease in the percentage of BrdU$^+$ cells that co-stained for DCX in the SGZ (n = 4 brains, analyzed 8 hippocampal sections per brain). This suggests that endogenous ephrin-B2 signaling regulates neuronal differentiation of NSCs. * indicates $P < 0.01$; ± s.d; dotted line marks SGZ/Hilus boundary and dashed line marks GCL/MCL boundary.

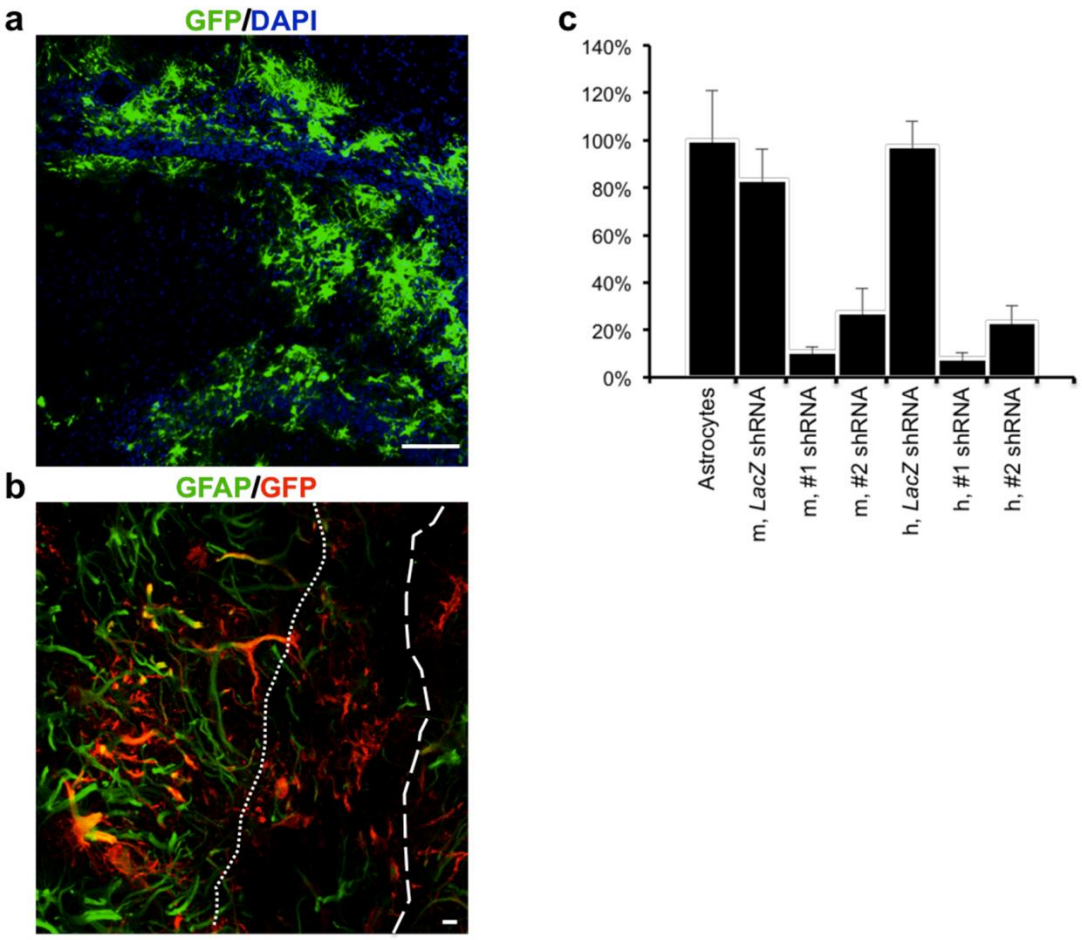

Figure 9: Validation of astrocytic shRNA expression. (**a,b**) We hypothesized that selective expression of GFP in hippocampal neurons (see **Figure 5**) was due to low activity of the ubiquitin-C promoter in astrocytes, not inactivity of the U6 promoter-shRNA cassette or a neuronal tropism of the lentiviral vector. The ubiquitin-C promoter was replaced by a mouse (m) and a human (h) GFAP promoter, and as evidenced by histology, the new shRNA vectors were expressed by $GFAP^+$ astrocytes proving that prior localization of GFP expression to neurons was an artifact of the ubiquitin-C promoter. Dotted line marks SGZ/Hilus boundary and dashed line marks GCL/MCL boundary. (**c**) QPCR analysis of shRNA vector-expressing astrocytes in culture demonstrated sustained effectiveness of the *efnb2* shRNA #1 and #2 vectors (n = 3, technical replicates ± s.d.).

Ephrin-B2 Signaling Instructs NSC Neuronal Differentiation

To gain insight into whether neural stem and/or progenitor cell populations are modulated by ephrin-B2, we developed an inducible, conditional, reporter mouse strain to map the fate of $Nestin^+$ NSCs in response to exogenous ephrin-B2. *Nestin-CreER^{T2}* [40] and *R26-stop$^{fl/fl}$-lacZ* [41] mouse strains were bred to generate mice in which tamoxifen administration induces *lacZ* expression in $Nestin^+$ cells via a transient recombination event. Using adult *Nestin-CreER^{T2}; R26-stop$^{fl/fl}$-lacZ* mice, cells were co-labeled by BrdU and tamoxifen injections prior to an intrahippocampal injection of Fc-ephrin-B2 or the Anti-Fc antibody control, and tissue sections were collected at day 0 from sham mice and at day 5 and 14 post-treatment (**Fig. 10a**). Quiescent and mitotic cells in the SGZ were labeled $\beta\text{-Gal}^+$ and $BrdU^+$ in a near clonal fashion on day 0 (43.6 ± 7.95% of $\beta\text{-Gal}^+$ cells were also $BrdU^+$; 3.89 ± 1.00% of $BrdU^+$ cells were also $\beta\text{-Gal}^+$), and these cells expanded, differentiated, and migrated into the GCL over the 14-day observation

period (**Fig. 10b-h**). At the population level, β-Gal$^+$ hippocampal cells initially (day 0) consisted of Type 1 and 2a Nestin$^+$/Sox2$^+$ NSCs (90.7 ± 1.79%), and a large fraction of β-Gal$^+$ cells were specifically Type 1, radial, GFAP$^+$/Sox2$^+$ NSCs (53.8 ± 5.49%, **Fig. 10b-f**). By day 5, the total number of β-Gal$^+$ cells had increased, but to the same extent in Fc-ephrin-B2 and Anti-Fc groups (**Fig. 11a**). At this time point, however, a larger fraction of the β-Gal$^+$ cell population in Fc-ephrin-B2 injected mice had shifted from Type 1 and 2a NSCs to neuronal fate committed Type 2b DCX$^+$/Sox2$^+$ precursors and even more so to Type 3 DCX$^+$/NeuroD1$^+$ neuroblasts, as compared to Anti-Fc injected mice (**Fig. 10d,e**). By day 14, the total number of β-Gal$^+$ cells was again consistent between experimental groups, but the increase in neuronal fated, β-Gal$^+$ cells in Fc-ephrin-B2 versus Anti-Fc injected mice persisted as Type 2b and Type 3 cells matured into NeuN$^+$ GCL neurons (**Fig. 11a** and **Fig. 10d-f**).

To gain further insights into the early fate decisions that ephrin-B2 modulates [10], we analyzed individual β-gal$^+$ cell clusters that are likely clonal. This quantification was conducted at day 5 in Nestin/Sox2 co-stained hippocampal sections (a total of 916 and 1145 cell clusters analyzed in n = 4 Anti-Fc control and n = 5 Fc-ephrin-B2 treated brains, respectively). Type 1 (**1**) and Type 2a (**2a**) cells were identified by Nestin$^+$/Sox2$^+$ co-staining and distinguished by morphology, and β-gal$^+$/Nestin$^-$/Sox2$^-$ cells were deemed astrocytes (**A**) or other neuronal cells (**N**, presumably neuronal precursors, neuroblasts, or mature neurons) by morphology and positioning relative to the GCL (**Fig. 10i**). We observed that the vast majority of clonal β-gal$^+$ cell clusters contained 3 or fewer cells. Importantly the average number of cells per cluster was 1.55 ± 0.03 and 1.54 ± 0.04 cells in Anti-Fc and Fc-ephrin-B2 sections respectively, again indicating that Fc-ephrin-B2 did not enhance proliferation of Type 1 or Type 2a cells, in contrast to the previously observed increase in BrdU$^+$ cells with Fc-ephrin-B2 (**Fig. 3c**). Furthermore, the cell phenotype distribution of the β-gal$^+$ cell clusters mirrored the overall, population-level results (**Fig. 11b** and **Fig. 10b-f**). Specifically, the clearest result was that Fc-ephrin-B2 induced a significant decrease in the percentage of single Type 1 and single Type 2a cells and a corresponding increase in the number of single N cells (**Fig. 10i**). Likewise, there was a statistically significant decrease in the overall number of doublets containing a Type 1 cell (1 + X) or a Type 2a cell (2a + X), accompanied by an increase in the number of N + N doublets. These results are consistent with the interpretation that the ephrin-B2 induced the conversion of Type 1 and 2a cells toward more differentiated phenotypes, either with or without a cell division event. Finally, there was no significant change in the percentage of astrocyte-containing clonal β-gal$^+$ cell clusters, as anticipated due to the low levels of gliogenesis previously observed in this experimental paradigm (**Fig. 4**). In summary, these results demonstrate that ephrin-B2 signaling significantly increases the commitment of Type 1 and Type 2a NSCs to a neuronal fate.

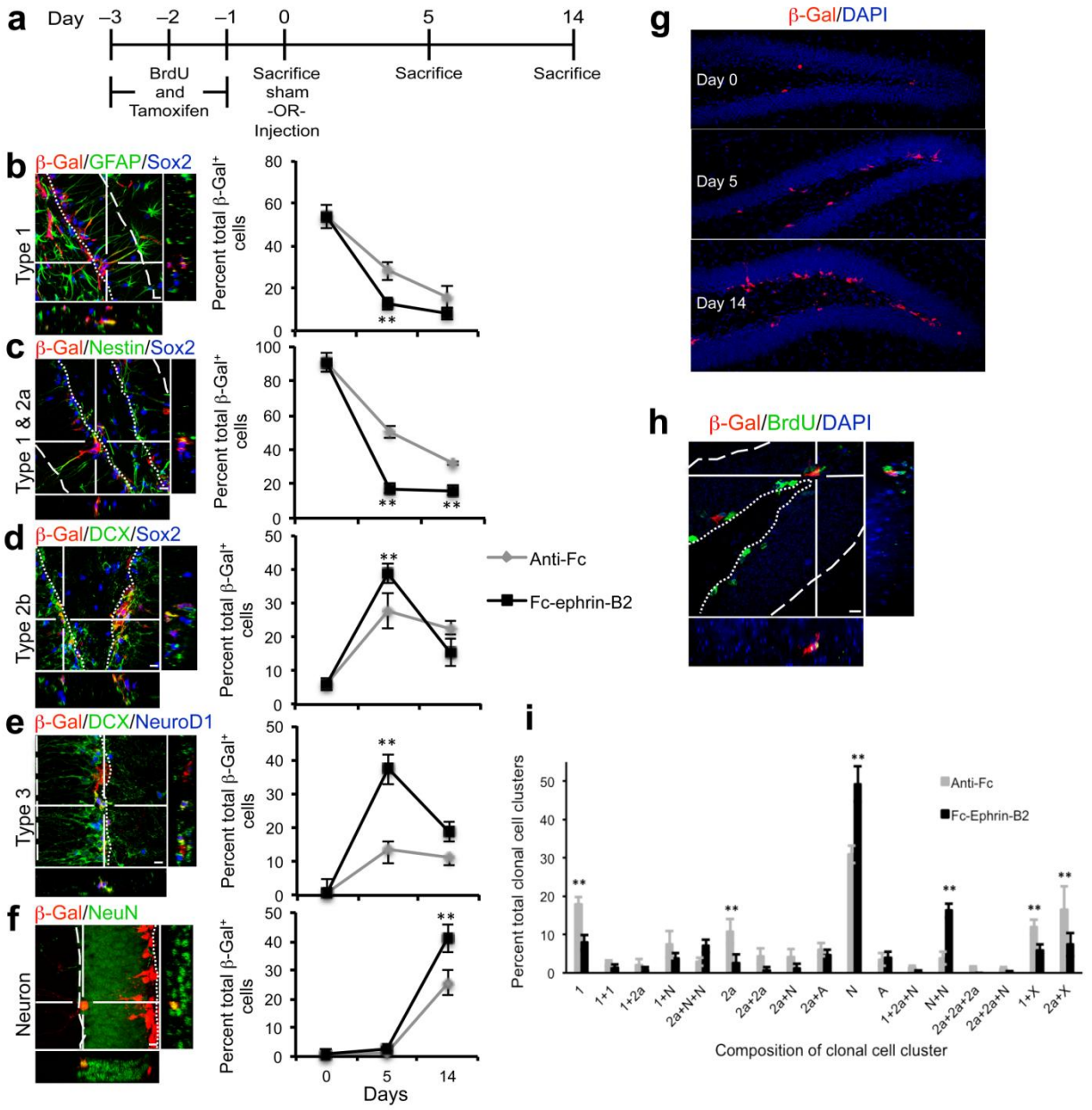

Figure 10: Lineage tracing of ephrin-B2-induced NSC differentiation. (**a**) Time course where (**b**,**c**) initially 90.7 ± 1.79% of β-Gal$^+$ cells were Nestin$^+$/Sox2$^+$, and 53.8 ± 5.49% were GFAP$^+$ along radial process (Type 1 NSCs). (**d,e**) By day 5, 38.7 ± 2.73% and 37.3 ± 4.51% of β-Gal$^+$ cells were Sox2$^+$/DCX$^+$ and DCX$^+$/NeuroD1$^+$, respectively, in Fc-ephrin-B2 injected mice vs. 27.7 ± 5.16% and 13.8 ± 4.38% in Anti-Fc controls. (f) At day 14, 41.1 ± 4.86% of β-Gal$^+$ cells were NeuN$^+$ for Fc-ephrin-B2 vs. 25.6 ± 4.24% for controls. (**g,h**) Representative sections where β-Gal$^+$ and BrdU$^+$ cells proliferated and differentiated over 14 days. (i) Compared to Anti-Fc, Fc-ephrin-B2 decreased the number of single Type 1 ("1", 8.01 ± 1.91% vs. 17.8 ± 1.93%) and Type 2a NSCs ("2a", 2.51 ± 2.34% vs. 10.8 ± 3.22%) and increased single neuroblast or neurons ("N", 49.2 ± 4.57% vs. 30.9 ± 2.28%). Furthermore, ephrin-B2 decreased the number of doublets containing a Type 1 ("1+X", 5.95 ± 1.47% vs. 11.8 ± 2.03%) or Type 2 ("2a+X", 7.37 ± 3.00% vs. 16.5 ± 6.03%) cell and increased neuroblasts or neuron doublets ("N+N",16.3 ± 1.82% vs. 3.87 ± 1.65%). Cluster size (1.55 ± 0.03 vs. 1.54 ± 0.04) and overall β-Gal$^+$ cell numbers (**Fig. 11**) were indistinguishable in Fc-ephrin-B2 vs. control mice. Thus, ephrin-B2 signaling increases neuronal differentiation without altering proliferation. ** $P < 0.05$; ± s.d; Five sections (10 hemispheres) analyzed in $n = 4$ Anti-Fc and 5 Fc-ephrin-B2 brains; dotted vs. dashed lines mark SGZ/Hilus vs. GCL/MCL boundaries.

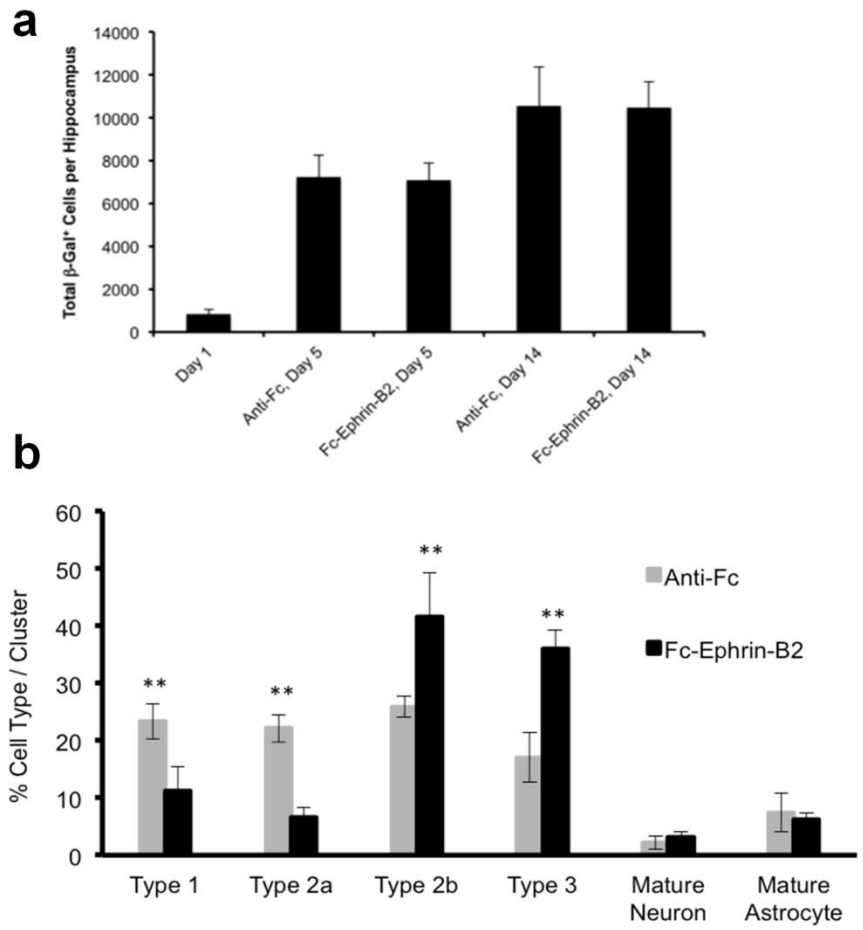

Figure 11: Effect of Fc-ephrin-B2 on Nestin$^+$ (β-gal$^+$) NSCs. (**a**) In fate mapping experiments using *Nestin-CreER^{T2}; R26-stop$^{fl/fl}$-lacZ* mice, the proliferative rate of recombined cells was consistent between Anti-Fc and Fc-ephrin-B2 experimental groups indicating that the increase in BrdU$^+$ cells observed in **Fig. 3c** was not due to ephrin-B2 induced proliferation of Nestin$^+$ NSCs (n = 4 experimental replicates ± s.d.). (**b**) Analysis of cell phenotype amongst clonal β-gal$^+$ cell clusters at Day 5 showed a similar distribution as observed at the population level in **Fig. 10d-h** and no significant change in levels of gliogenesis between Anti-Fc and Fc-ephrin-B2 treated groups. ** indicates $P < 0.05$; n = 4 brains, analyzed 8 hippocampal sections per brain.

Wnt-Independent Induction of NSC Neuronal Differentiation

Activation of the canonical Wnt pathway elevates levels of β-catenin, followed by its nuclear translocation and association with Tcf/Lef transcription factors. Recently, this pathway was shown to regulate adult NSC differentiation by transcriptionally activating the proneural transcription factor NeuroD1 [23,46]. In zebrafish paraxial mesoderm, ephrin/Eph forward signaling recruits β-catenin to adherens junctions [47], and EphB receptors are known transcriptional targets of β-catenin/Tcf signaling in stem cells in the mammalian gut [48]. However, to our knowledge, ephrin/Eph signaling has not previously been shown to activate β-catenin signaling. Notably, we found that Fc-ephrin-B2 stimulation progressively increased the levels of intracellular active β-catenin in cultured NSCs over a 24 hour period (**Fig. 12a**), initially detectable at 4 hours and rising to maximal levels by 24 hours. To determine whether this increased active β-catenin was mediated by EphB4, NSCs were pre-incubated with anti-EphB4 antibody prior to Fc-ephrin-B2 addition. As observed in previous experiments (**Fig.**

2c,**4b**), EphB4 blockage decreased NSC responses to ephrin-B2 signaling and correspondingly limited the intracellular accumulation of active β-catenin (**Fig. 12b**).

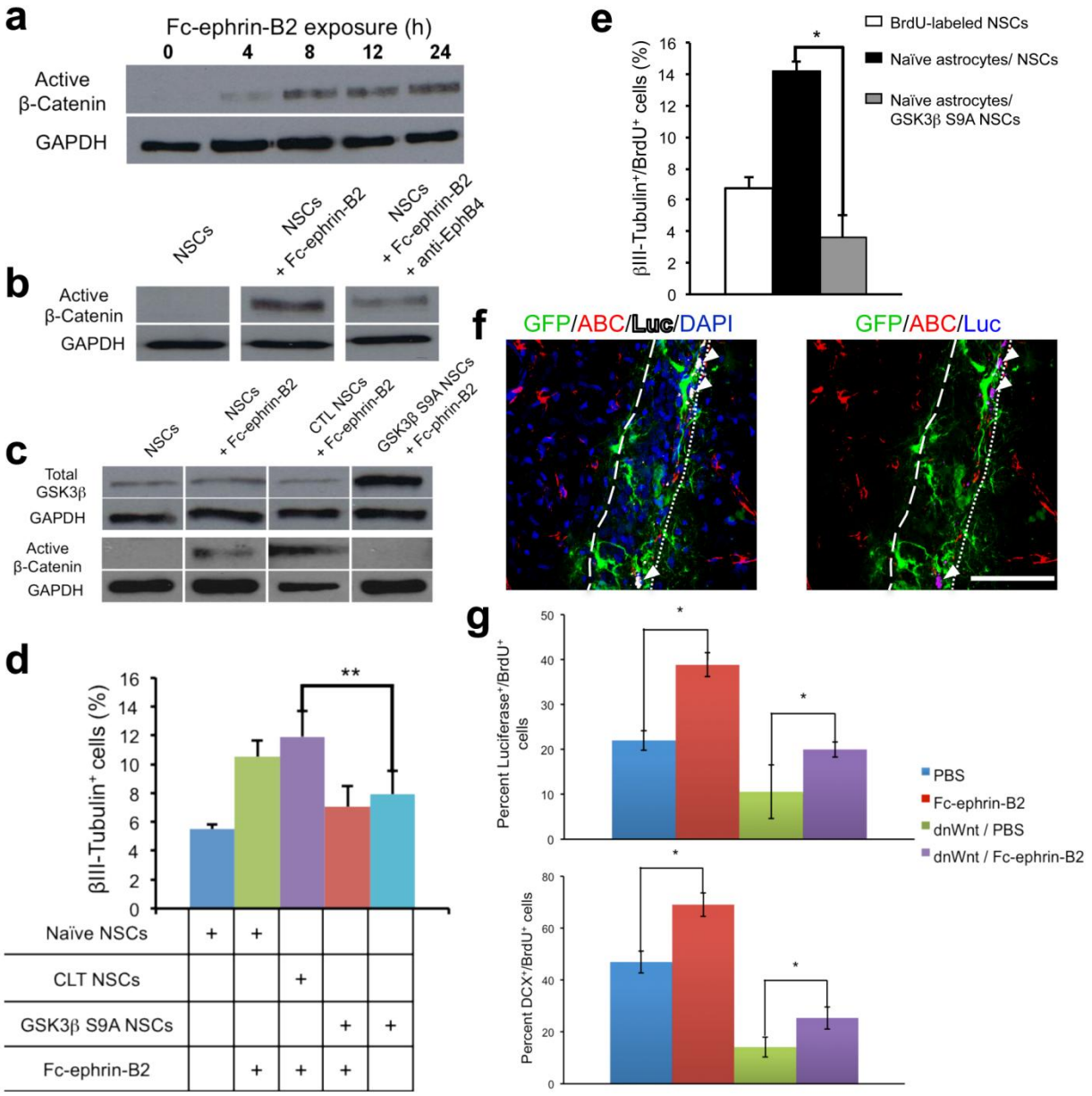

Figure 12: Ephrin-B2 instructs neuronal differentiation by activating β-catenin independent of Wnt signaling. (**a**) Fc-ephrin-B2 (10 µg/mL) induced active β-catenin accumulation in NSCs over a 24 hours. (**b**) However, blocking the EphB4 receptor compromised Fc-ephrin-B2 induction of β-catenin accumulation. (**c**) NSCs expressing a constitutively active GSK3β, GSK3β S9A, did not accumulate β-catenin in response to Fc-ephrin-B2 (10 µg/mL for 24 hours), in contrast to naïve or empty vector control NSCs (CTL NSCs). (**d**) Constitutive degradation of β-catenin in GSK3β S9A NSCs decreased NSCs differentiation into βIII-Tubulin$^+$ neurons in response to Fc-ephrin-B2 (10 µg/mL) vs. empty vector control NPCs (CTL NPCs) (n = 3 experimental replicates). (**e**) The lack of β-catenin signaling in GSK3β S9A NSCs also nullified the proneuronal effect of hippocampus-derived, ephrin-B2 expressing astrocytes in co-culture (n=4, experimental repeats). (**f**) In mice co-infected with Tcf-Luc and dnWnt-IRES-GFP constructs, cells in the SGZ still expressed active β-catenin (ABC) and Luciferase (arrowheads) 24 hours after Fc-ephrin-B2 injection. Scale bar represents 100 µm. (**g**) In hippocampi co-infected with Tcf-Luc and either dnWnt-

IRES-GFP or IRES-GFP construct, then injected with Fc-ephrin-B2 or PBS, Fc-ephrin-B2 increased the percentage of SGZ $BrdU^+$ cells with active β-catenin signaling 24 hours post-injection and the percentage of $DCX^+/BrdU^+$ cells by day 5 even with dnWnt present (n=4 brains, 8 sections per brain). Ephrin-B2 thus activates β-catenin signaling and enhances adult neurogenesis independent of Wnt signaling. * indicates $P < 0.01$; ** indicates $P < 0.05$; ± s.d; dotted vs. dashed lines mark SGZ/Hilus vs. GCL/MCL boundaries.

In the canonical Wnt pathway, intracellular β-catenin levels are directly regulated by glycogen synthase kinase-3 beta (GSK3β), which phosphorylates and thereby marks β-catenin for proteasomal degradation [49]. To determine whether elevated β-catenin activity is required for ephrin-B2's proneuronal effect, we generated NSCs expressing a constitutively active form of GSK3β (GSK3β S9A) [50]. Upon stimulation with Fc-ephrin-B2, both naïve NSCs and NSCs carrying a control empty retroviral vector (CTL NSCs) exhibited increased levels of active β-catenin (**Fig. 12c**), consistent with prior results (**Fig. 12a**). However, GSK3β S9A NSCs were unable to accumulate β-catenin in response to ephrin-B2 signaling. Furthermore, unlike naïve cells, GSK3β S9A NSCs resisted neuronal differentiation when stimulated with Fc-ephrin-B2 or co-cultured with ephrin-B2 expressing naïve astrocytes, demonstrating that increased active β-catenin levels are required for ephrin-B2's proneuronal effect (**Fig. 12d,e**).

These results raise the possibility that ephrin-B2's pro-neuronal effect could involve Wnt ligand mediated activation of β-catenin. To determine whether ephrin-B2 signaling indirectly activates β-catenin via upregulation of soluble Wnts *in vivo*, lentiviruses encoding a Tcf-Luc construct that reports β-catenin activity [42] and either a dnWnt-IRES-GFP [23] (dominant negative Wnt) or IRES-GFP (control) cassette were used. We first confirmed that lentiviral mediated expression of the soluble dnWnt by cultured NSCs significantly decreased luciferase reporter expression upon incubation of the cells with Wnt3a (**Fig. 13**). β-catenin reporter vector, as well as vector expressing dnWnt or GFP alone, was then co-administered *in vivo*. After two weeks, mitotic cells in the rat hippocampi were labeled with BrdU, and Fc-ephrin-B2 or PBS was administered by intrahippocampal injection. After 24 hours, in animals injected with Tcf-Luc and IRES-GFP constructs, Fc-ephrin-B2 increased the number of $Luc^+/BrdU^+$ cells, which also co-stained for active β-catenin (ABC) indicating that ephrin-B2 stimulates β-catenin signaling *in vivo* (**Fig. 12f**,**g**). Furthermore, administration of the dnWnt-IRES-GFP vector with the Tcf-Luc vector knocked down the number of $Luc^+/BrdU^+$ cells proportionally in the Fc-ephrin-B2 and PBS injected groups, indicating that Wnt signaling is active in the hippocampus, but that ephrin-B2 still stimulates β-catenin signaling even when Wnt is inhibited. Consistent with these results, dnWnt reduced the number of newborn neurons in both the Fc-ephrin-B2 and PBS injected animals by day 5, but the former still showed a significantly higher number of $DCX^+/BrdU^+$ cells than the latter (**Fig. 12g**). Thus, ephin-B2 signaling does not apparently activate β-catenin through a soluble Wnt intermediate, and it can increase adult neurogenesis in the absence of Wnt signaling.

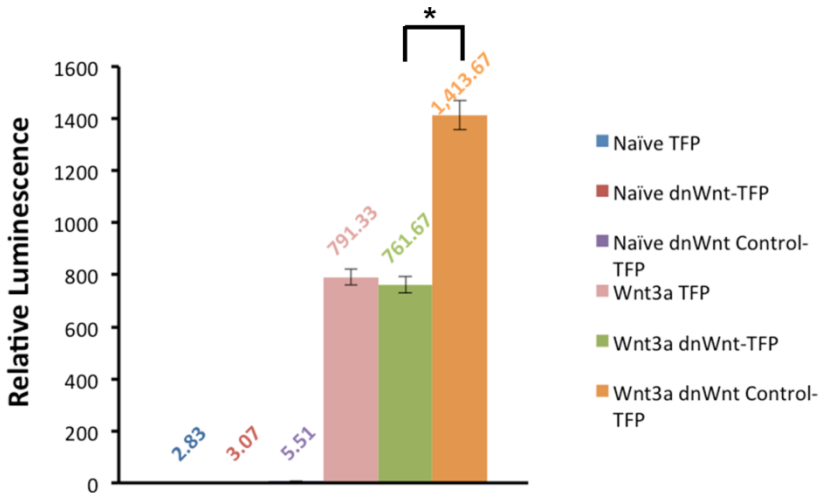

Figure 13: In vitro validation of lentiviral vectors encoding Tcf-Luc reporter (TFP), dnWnt-IRES-GFP (dnWnt), and IRES-GFP (dnWnt Control) cassettes. Naïve NSCs, NSCs infected with TFP vector, and NSCs co-infected with TFP and either dnWnt or dnWnt control vectors were assayed for their ability to report β-catenin signaling, as evidenced by luciferase expression, in response to a 24-hour incubation in Wnt3a supplemented (200 ng/mL) or standard media. No Luc expression was observed in the absence of Wnt3a, and a significant decrease in Wnt3a-induced Luc reporting was observed in NSCs expressing dnWnt as compared to the dnWnt control construct, thus validating proper activity of the three constructs (n = 3 technical replicates ± s.d.). * indicates a $P < 0.01$.

Finally, in NSC cultures stimulated with Fc-ephrin-B2, we observed a significant increase in the transcription of both *Mash1* (*Ascl1*) and *Neurod1*, proneural transcription factors previously shown to play roles in adult hippocampal neurogenesis [46,51] (**Fig. 14a**,**b**). This mRNA upregulation presumably occurs within the subset of cells that undergo neuronal differentiation. Therefore, our collective results strongly indicate that hippocampal astrocytes instruct neuronal differentiation of EphB4^{+} NSCs through juxtacrine ephrin-B2/EphB4 forward signaling, which induces the expression of proneural transcription factors via a β-catenin-dependent and soluble Wnt independent mechanism.

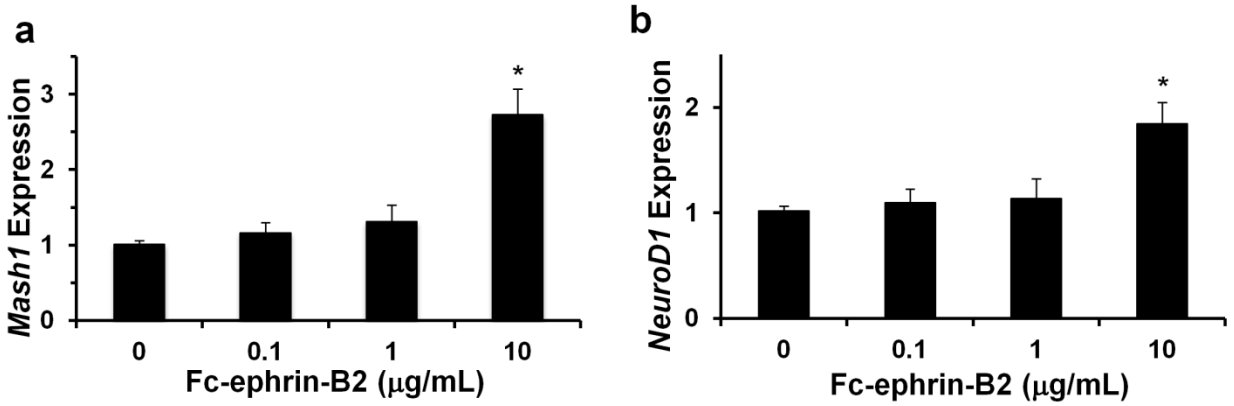

Figure 14: Fc-ephrin-B2 induces expression of Mash1 and NeuroD1 in NSCs *in vitro*. (**a**,**b**) Similar to experiments in Figure 1, Fc-ephrin-B2 stimulation also induced a dose-dependent increase in the expression of two proneural transcription factors, Mash1and NeuroD1, known to play important roles in adult hippocampal neurogenesis (n = 3, technical replicates ± s.d.). * indicates $P < 0.01$.

Discussion

Stem cell niches present repertoires of signals that control cell maintenance, proliferation, and differentiation. Recent studies have identified several factors that regulate cell maintenance and proliferation within the adult NSC niche; however, few cues have been found to induce differentiation. Furthermore, whereas numerous soluble cues have been found to regulate adult neurogenesis, cell-cell interactions in the niche have in general been less studied. We have found that ephrin-B2 presented from hippocampal astrocytes activates β-catenin signaling in NSCs, upregulates the expression of key proneural transcription factors, and instructs their neuronal differentiation (**Fig. 15**).

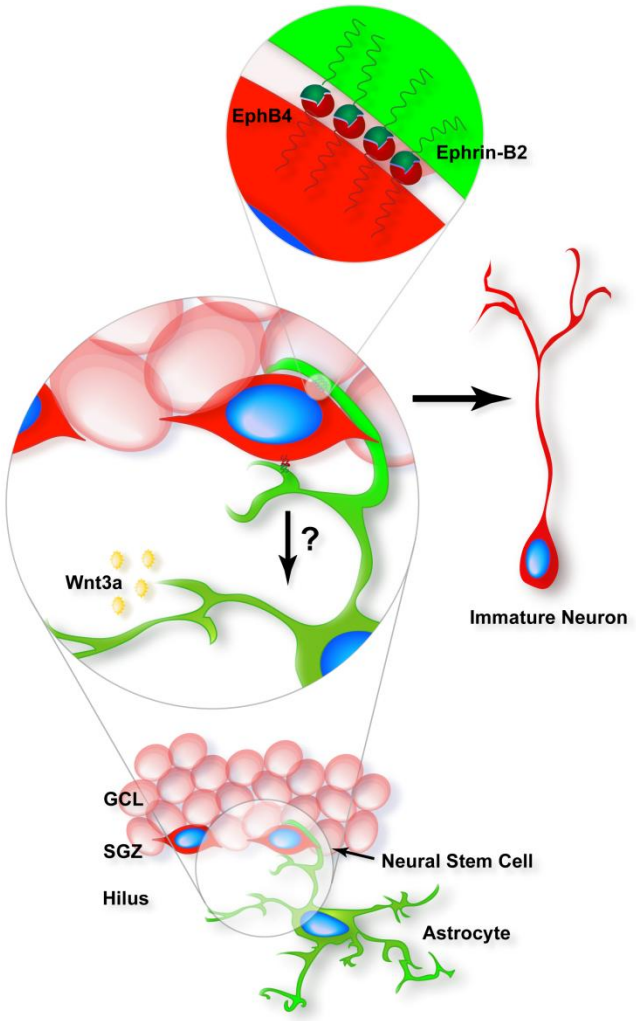

Figure 15: Proposed model of ephrin-B2 signaling in regulating adult neurogenesis. In the SGZ, ephrin-B2+ hippocampal astrocytes induce neuronal differentiation of Sox2+/EphB4+ NSCs through juxtacrine ephrin-B2/EphB4 forward signaling via a β-catenin dependent mechanism. However, the effect EphB4/ephrin-B2 reverse-signaling on hippocampal astrocytes remains unknown.

Hippocampal astrocytes, but not astrocytes derived from non-neurogenic regions of the central nervous system, regulate neurogenesis [22], and a recent expression profiling analyzed the differential expression of factors that underlie this activity [19]. However, ephrin-B2 was not represented on the Affymetrix chip used for this important comparative gene expression study, and cues dependent on cell-cell contact between the stem cells and hippocampal astrocytes have not been explored. The importance of ephrins and their receptors in axon guidance, neural tissue patterning, and synapse formation is well established [24]; however, less is known about their role in regulating adult NSCs. Several studies have shown that ephrin/Eph signaling can affect NSC proliferation [31,32,33,52]; however, these important studies did not address the potential for ephrins and Ephs to regulate stem cell differentiation within the brain. This work thus represents the first case of ephrin/Eph-family regulation of NSC neuronal lineage commitment in the adult CNS.

We have shown that endogenous ephrin-B2 is expressed by astrocytes in close proximity to adult NSCs, shRNA-mediated knockdown of the endogenous ephrin-B2 substantially lowers the fraction of newborn cells that become DCX+ neuronal precursors, and exogenous addition of ephrin-B2 induces the conversion of Type 1 and 2a NSCs toward Type 2b precursors and subsequently neurons (**Fig. 2,5,6**). Furthermore, lineage tracing analysis revealed a decrease in single Type 1 and Type 2a cells and an increase in the number of single neuroblasts and neurons in the presence of ephrin-B2, as well as a decrease in the number of cell doublets containing a Type 1 or 2a cell with a corresponding increase in the number of neuroblast and neuron doublets (**Fig. 10**). These results are consistent with ectopic ephrin-B2 inducing β-catenin signaling and upregulation of proneural transcription factors (**Fig. 12 and Fig. 14a,b**) to induce NSC differentiation independent of cell division. Collectively, our results indicate that juxtacrine signaling between astrocytes and NSCs provides a mechanism for the niche to locally control NSC differentiation. Prior results have investigated the importance of Notch and EphB2 signaling in modulating the properties of neighboring cells in the NSC niche [53] and the importance of Notch in maintaining Type 1 NSCs [13,54]. Together, these results increasingly establish cell contact-dependent signaling as a critical mechanism for locally regulating multiple stages in adult neurogenesis.

Ephrin/Eph signaling is generally known to be bidirectional, such that the Eph-presenting cell can activate signaling within the ephrin ligand-expressing cell [24]. We find that adult NSCs significantly upregulate ephrin-B2 and downregulate EphB4 expression upon differentiation into astrocytes *in vitro*, yet retain EphB4 expression upon neuronal differentiation (**Fig. 5b**). Ephrin/Eph signal feedback from the differentiating NSC to neighboring cells could thus represent a mechanism to dynamically remodel the signaling environment of the niche, analogous to GDF11-dependent negative feedback from neurons to neural progenitors in the olfactory epithelium [55] or EGF-dependent feedback from neural progenitors to neural stem cells in the SVZ [56]. In addition, ephrin and Eph expression dynamics could help control cell differentiation following NSC symmetric or asymmetric division [8] and thereby contribute to maintaining or modulating the cellular composition of the niche. The potential of ephrin signaling in general to support self-renewing, asymmetric cell division – i.e. to generate a stem cell and a differentiated progeny – is virtually unexplored, as there is only one report of ephrin mediated regulation of asymmetric stem cell division, in the ascidian embryo [57].

Type 1 NSCs were depleted upon ephrin-B2 administration (**Fig. 10**), indicating that they may be direct targets of this ligand's signaling. However, while some type 1 cells expressed levels of EphB4 detectable by immunostaining and upregulated β-catenin signaling upon ephrin-

B2 addition, nearly all type 2a cells did so, and additional work will be needed to determine whether the observed differentiation of type 1 cells in response to ephrin-B2 is direct and/or indirect. In addition, while ephrin-B2 knockdown did not impact cell proliferation (**Fig. 8d**), and ephrin-B2 protein administration did not affect the proliferation of genetically-labeled, Nestin-expressing stem and progenitor cells (**Fig. 10** and **Fig. 11**), ephrin-B2 addition did result in the expansion of cells pre-labeled with BrdU in the rat brain. It is thus conceivable that in addition to its clear role in inducing the differentiation of NSCs at the expense of stem cell maintenance or self-renewing cell divisions (**Fig. 10**), ephrin-B2 could also modulate the expansion of later stage neuroblasts that are strongly labeled with BrdU, a possibility that could be explored in future work.

In summary, our findings reveal ephrin-B2, a transmembrane factor known for its role in cell and tissue patterning, as a key regulator of adult hippocampal neurogenesis, the first known function of an Eph-family protein in regulating neuronal lineage commitment of NSCs in the adult CNS. Additionally, hippocampal astrocytes are the source of the ephrin-B2 signal, which further supports the emerging view that astroglia are active and essential regulators of an increasing number of adult CNS functions, including remodeling the neurogenic niche through local cellular interactions. Moreover, the discovery that ephrin-B2 signals through β-catenin adds further understanding to the interconnected and likely synergistic nature by which niche factors regulate adult neurogenesis. Finally, this work may have future applications in modulating NSC function for treating brain injury and neurodegenerative disease.

Acknowledgements

This research was supported by NIH grant EB007295, LBL LDRD grant 3668DS, and CIRM training grant T1-00007. We also thank Russell Fletcher for his guidance in mouse breeding and geneotyping.

References

1. Eriksson PS, Perfilieva E, Bjork-Eriksson T, Alborn AM, Nordborg C, Peterson DA, Gage FH. (1998) Neurogenesis in the adult human hippocampus. *Nat Med* 4:1313-1317.
2. Lois C, Alvarez-Buylla A. (1994) Long-distance neuronal migration in the adult mammalian brain. *Science* 264:1145-1148.
3. Spalding KL, Bhardwaj RD, Buchholz BA, Druid H, Frisen J. (2005) Retrospective birth dating of cells in humans. *Cell* 122:133-143.
4. Manganas LN, Zhang X, Li Y, Hazel RD, Smith SD, Wagshul ME, Henn F, Benveniste H, Djuric PM, Enikolopov G, Maletic-Savatic M. (2007) Magnetic resonance spectroscopy identifies neural progenitor cells in the live human brain. *Science* 318:980-985.
5. Jessberger S, Zhao C, Toni N, Clemenson GD, Jr., Li Y, Gage FH. (2007) Seizure-associated, aberrant neurogenesis in adult rats characterized with retrovirus-mediated cell labeling. *J Neurosci* 27:9400-9407.
6. Ekdahl CT, Claasen JH, Bonde S, Kokaia Z, Lindvall O. (2003) Inflammation is detrimental for neurogenesis in adult brain. *Proc Natl Acad Sci U S A* 100:13632-13637.

7. Tattersfield AS, Croon RJ, Liu YW, Kells AP, Faull RL, Connor B. (2004) Neurogenesis in the striatum of the quinolinic acid lesion model of Huntington's disease. *Neuroscience* 127:319-332.
8. Suh H, Consiglio A, Ray J, Sawai T, D'Amour KA, Gage FH. (2007) In vivo fate analysis reveals the multipotent and self-renewal capacities of Sox2+ neural stem cells in the adult hippocampus. *Cell Stem Cell* 1:515-528.
9. Suh H, Deng W, Gage FH. (2009) Signaling in adult neurogenesis. *Annu Rev Cell Dev Biol* 25:253-275.
10. Bonaguidi MA, Wheeler MA, Shapiro JS, Stadel RP, Sun GJ, Ming GL, Song H. (2011) In vivo clonal analysis reveals self-renewing and multipotent adult neural stem cell characteristics. *Cell* 145:1142-1155.
11. Mira H, Andreu Z, Suh H, Lie DC, Jessberger S, Consiglio A, San Emeterio J, Hortiguela R, Marques-Torrejon MA, Nakashima K, Colak D, Gotz M, Farinas I, Gage FH. (2010) Signaling through BMPR-IA regulates quiescence and long-term activity of neural stem cells in the adult hippocampus. *Cell Stem Cell* 7:78-89.
12. Ehm O, Goritz C, Covic M, Schaffner I, Schwarz TJ, Karaca E, Kempkes B, Kremmer E, Pfrieger FW, Espinosa L, Bigas A, Giachino C, Taylor V, Frisen J, Lie DC. (2010) RBPJkappa-dependent signaling is essential for long-term maintenance of neural stem cells in the adult hippocampus. *J Neurosci* 30:13794-13807.
13. Lugert S, Basak O, Knuckles P, Haussler U, Fabel K, Gotz M, Haas CA, Kempermann G, Taylor V, Giachino C. (2010) Quiescent and active hippocampal neural stem cells with distinct morphologies respond selectively to physiological and pathological stimuli and aging. *Cell Stem Cell* 6:445-456.
14. Lai K, Kaspar BK, Gage FH, Schaffer DV. (2003) Sonic hedgehog regulates adult neural progenitor proliferation in vitro and in vivo. *Nat Neurosci* 6:21-27.
15. Jin K, Sun Y, Xie L, Batteur S, Mao XO, Smelick C, Logvinova A, Greenberg DA. (2003) Neurogenesis and aging: FGF-2 and HB-EGF restore neurogenesis in hippocampus and subventricular zone of aged mice. *Aging Cell* 2:175-183.
16. Cao L, Jiao X, Zuzga DS, Liu Y, Fong DM, Young D, During MJ. (2004) VEGF links hippocampal activity with neurogenesis, learning and memory. *Nat Genet* 36:827-835.
17. Qu Q, Sun G, Li W, Yang S, Ye P, Zhao C, Yu RT, Gage FH, Evans RM, Shi Y. (2010) Orphan nuclear receptor TLX activates Wnt/beta-catenin signalling to stimulate neural stem cell proliferation and self-renewal. *Nat Cell Biol* 12:31-40; sup pp 31-39.
18. Gage FH, Coates PW, Palmer TD, Kuhn HG, Fisher LJ, Suhonen JO, Peterson DA, Suhr ST, Ray J. (1995) Survival and differentiation of adult neuronal progenitor cells transplanted to the adult brain. *Proc Natl Acad Sci U S A* 92:11879-11883.
19. Barkho BZ, Song H, Aimone JB, Smrt RD, Kuwabara T, Nakashima K, Gage FH, Zhao X. (2006) Identification of astrocyte-expressed factors that modulate neural stem/progenitor cell differentiation. *Stem Cells Dev* 15:407-421.
20. Tozuka Y, Fukuda S, Namba T, Seki T, Hisatsune T. (2005) GABAergic excitation promotes neuronal differentiation in adult hippocampal progenitor cells. *Neuron* 47:803-815.
21. Jacobs S, Lie DC, DeCicco KL, Shi Y, DeLuca LM, Gage FH, Evans RM. (2006) Retinoic acid is required early during adult neurogenesis in the dentate gyrus. *Proc Natl Acad Sci U S A* 103:3902-3907.

22. Song H, Stevens CF, Gage FH. (2002) Astroglia induce neurogenesis from adult neural stem cells. *Nature* 417:39-44.
23. Lie DC, Colamarino SA, Song HJ, Desire L, Mira H, Consiglio A, Lein ES, Jessberger S, Lansford H, Dearie AR, Gage FH. (2005) Wnt signalling regulates adult hippocampal neurogenesis. *Nature* 437:1370-1375.
24. Pasquale EB. (2005) Eph receptor signalling casts a wide net on cell behaviour. *Nat Rev Mol Cell Biol* 6:462-475.
25. Knoll B, Drescher U. (2002) Ephrin-As as receptors in topographic projections. *Trends in Neurosciences* 25:145-149.
26. Martinez A, Soriano E. (2005) Functions of ephrin/Eph interactions in the development of the nervous system: emphasis on the hippocampal system. *Brain Res Brain Res Rev* 49:211-226.
27. Xu NJ, Sun S, Gibson JR, Henkemeyer M. (2011) A dual shaping mechanism for postsynaptic ephrin-B3 as a receptor that sculpts dendrites and synapses. *Nat Neurosci* 14:1421-1429.
28. Aoki M, Yamashita T, Tohyama M. (2004) EphA receptors direct the differentiation of mammalian neural precursor cells through a mitogen-activated protein kinase-dependent pathway. *J Biol Chem* 279:32643-32650.
29. del Valle K, Theus MH, Bethea JR, Liebl DJ, Ricard J. (2011) Neural progenitors proliferation is inhibited by EphB3 in the developing subventricular zone. *Int J Dev Neurosci* 29:9-14.
30. Conover JC, Doetsch F, Garcia-Verdugo JM, Gale NW, Yancopoulos GD, Alvarez-Buylla A. (2000) Disruption of Eph/ephrin signaling affects migration and proliferation in the adult subventricular zone. *Nat Neurosci* 3:1091-1097.
31. Holmberg J, Armulik A, Senti KA, Edoff K, Spalding K, Momma S, Cassidy R, Flanagan JG, Frisen J. (2005) Ephrin-A2 reverse signaling negatively regulates neural progenitor proliferation and neurogenesis. *Genes Dev* 19:462-471.
32. Chumley MJ, Catchpole T, Silvany RE, Kernie SG, Henkemeyer M. (2007) EphB receptors regulate stem/progenitor cell proliferation, migration, and polarity during hippocampal neurogenesis. *J Neurosci* 27:13481-13490.
33. Hara Y, Nomura T, Yoshizaki K, Frisen J, Osumi N. (2010) Impaired hippocampal neurogenesis and vascular formation in ephrin-A5-deficient mice. *Stem Cells* 28:974-983.
34. Qin XF, An DS, Chen IS, Baltimore D. (2003) Inhibiting HIV-1 infection in human T cells by lentiviral-mediated delivery of small interfering RNA against CCR5. *Proc Natl Acad Sci U S A* 100:183-188.
35. Lois C, Hong EJ, Pease S, Brown EJ, Baltimore D. (2002) Germline transmission and tissue-specific expression of transgenes delivered by lentiviral vectors. *Science* 295:868-872.
36. Yu JH, Schaffer DV. (2006) Selection of novel vesicular stomatitis virus glycoprotein variants from a peptide insertion library for enhanced purification of retroviral and lentiviral vectors. *J Virol* 80:3285-3292.
37. Lim KI, Klimczak R, Yu JH, Schaffer DV. (2010) Specific insertions of zinc finger domains into Gag-Pol yield engineered retroviral vectors with selective integration properties. *Proc Natl Acad Sci U S A* 107:12475-12480.

38. Greenberg KP, Geller SF, Schaffer DV, Flannery JG. (2007) Targeted transgene expression in muller glia of normal and diseased retinas using lentiviral vectors. *Invest Ophthalmol Vis Sci* 48:1844-1852.
39. Lawlor PA, Bland RJ, Mouravlev A, Young D, During MJ. (2009) Efficient gene delivery and selective transduction of glial cells in the mammalian brain by AAV serotypes isolated from nonhuman primates. *Mol Ther* 17:1692-1702.
40. Battiste J, Helms AW, Kim EJ, Savage TK, Lagace DC, Mandyam CD, Eisch AJ, Miyoshi G, Johnson JE. (2007) Ascl1 defines sequentially generated lineage-restricted neuronal and oligodendrocyte precursor cells in the spinal cord. *Development* 134:285-293.
41. Soriano P. (1999) Generalized lacZ expression with the ROSA26 Cre reporter strain. *Nat Genet* 21:70-71.
42. Fuerer C, Nusse R. (2010) Lentiviral vectors to probe and manipulate the Wnt signaling pathway. *PLoS One* 5:e9370.
43. Peltier J, O'Neill A, Schaffer DV. (2007) PI3K/Akt and CREB regulate adult neural hippocampal progenitor proliferation and differentiation. *Dev Neurobiol* 67:1348-1361.
44. Peltier J, Agrawal S, Robertson MJ, Schaffer DV. (2010) In vitro culture and analysis of adult hippocampal neural progenitors. *Methods Mol Biol* 621:65-87.
45. Davis S, Gale NW, Aldrich TH, Maisonpierre PC, Lhotak V, Pawson T, Goldfarb M, Yancopoulos GD. (1994) Ligands for EPH-related receptor tyrosine kinases that require membrane attachment or clustering for activity. *Science* 266:816-819.
46. Kuwabara T, Hsieh J, Muotri A, Yeo G, Warashina M, Lie DC, Moore L, Nakashima K, Asashima M, Gage FH. (2009) Wnt-mediated activation of NeuroD1 and retro-elements during adult neurogenesis. *Nat Neurosci* 12:1097-1105.
47. Barrios A, Poole RJ, Durbin L, Brennan C, Holder N, Wilson SW. (2003) Eph/Ephrin signaling regulates the mesenchymal-to-epithelial transition of the paraxial mesoderm during somite morphogenesis. *Curr Biol* 13:1571-1582.
48. Batlle E, Henderson JT, Beghtel H, van den Born MM, Sancho E, Huls G, Meeldijk J, Robertson J, van de Wetering M, Pawson T, Clevers H. (2002) Beta-catenin and TCF mediate cell positioning in the intestinal epithelium by controlling the expression of EphB/ephrinB. *Cell* 111:251-263.
49. Kim WY, Wang X, Wu Y, Doble BW, Patel S, Woodgett JR, Snider WD. (2009) GSK-3 is a master regulator of neural progenitor homeostasis. *Nat Neurosci* 12:1390-1397.
50. Stambolic V, Woodgett JR. (1994) Mitogen inactivation of glycogen synthase kinase-3 beta in intact cells via serine 9 phosphorylation. *Biochem J* 303 (Pt 3):701-704.
51. Elmi M, Matsumoto Y, Zeng ZJ, Lakshminarasimhan P, Yang W, Uemura A, Nishikawa SI, Moshiri A, Tajima N, Agren H, Funa K. (2010) TLX activates MASH1 for induction of neuronal lineage commitment of adult hippocampal neuroprogenitors. *Mol Cell Neurosci*.
52. Jiao JW, Feldheim DA, Chen DF. (2008) Ephrins as negative regulators of adult neurogenesis in diverse regions of the central nervous system. *Proc Natl Acad Sci U S A* 105:8778-8783.
53. Nomura T, Goritz C, Catchpole T, Henkemeyer M, Frisen J. (2010) EphB signaling controls lineage plasticity of adult neural stem cell niche cells. *Cell Stem Cell* 7:730-743.

54. Ables JL, Decarolis NA, Johnson MA, Rivera PD, Gao Z, Cooper DC, Radtke F, Hsieh J, Eisch AJ. (2010) Notch1 is required for maintenance of the reservoir of adult hippocampal stem cells. *J Neurosci* 30:10484-10492.
55. Wu HH, Ivkovic S, Murray RC, Jaramillo S, Lyons KM, Johnson JE, Calof AL. (2003) Autoregulation of neurogenesis by GDF11. *Neuron* 37:197-207.
56. Aguirre A, Rubio ME, Gallo V. (2010) Notch and EGFR pathway interaction regulates neural stem cell number and self-renewal. *Nature* 467:323-327.
57. Picco V, Hudson C, Yasuo H. (2007) Ephrin-Eph signalling drives the asymmetric division of notochord/neural precursors in Ciona embryos. *Development* 134:1491-1497.

CHAPTER 3

MULTIVALENT LIGANDS TO CONTROL STEM CELL FATE

Abstract

There is currently significant interest in designing nanostructured materials that can interact with cells and regulate key cellular functions [1,2,3]. We demonstrate for the first time the design of potent multivalent conjugates that can organize stem cell receptors into nanoscale clusters and control stem cell fate, both *in vitro* and *in vivo*. The ectodomain of ephrin-B2, normally an integral membrane protein ligand, was conjugated to a soluble biopolymer to yield multivalent nanoscale conjugates that potently induced signaling in neural stem cells and promoted their neuronal differentiation both in culture and within the brain. Furthermore, synthetic multivalent conjugates of ephrin-B1 strongly enhanced human embryonic and induced pluripotent stem cell differentiation into functional dopaminergic neurons. Multivalent bioconjugates thus represent a powerful tool for controlling stem cell fate *in vitro* and *in vivo*. These results also highlight the potential of nanoscale therapeutics that interact with target cells and elicit desired cellular responses.

Introduction

Multivalent interactions, involving the simultaneous binding of multiple ligands on one entity to multiple receptors on another, are ubiquitous in biology and include cell-cell binding, viral and bacterial attachment to cellular surfaces, and antibody opsonization of pathogens [4,5,6]. Cellular signal transduction also often begins with the multivalent binding of ligands, either secreted or cell-surface tethered, to target cell receptors, leading to receptor clustering. Many growth factors and morphogens that play critical roles in regulating cell function and fate involve multivalent interactions. For instance, integral and peripheral membrane ligands often form multimeric assemblies upon binding cognate receptors on neighboring cell surfaces and thereby induce juxtacrine signaling. These systems include ephrins and Eph receptors [7], Delta/Jagged and Notch receptors [8], stem cell factor (SCF) and c-kit receptor [9], Fas ligand and receptor [10], Flt ligands and receptors [11], neuroligins and neurexins [12], myelin-derived proteins Nogo and MAG [13,14], and others. Analogously, some soluble signaling factors such as Sonic hedgehog (Shh) [15] are post-translationally modified and assembled to yield oligomeric nanoparticles that can freely diffuse and induce signaling. Moreover, many growth factors (e.g., fibroblast growth factor (FGF) [16], transforming growth factor-β (TGF-β) [17], Hedgehogs (Hh) [18], vascular endothelial growth factor (VEGF) [19], etc.) contain heparin or other extracellular matrix (ECM) binding domains, and their resulting immobilization onto the ECM modifies signal potency, potentially via modulating ligand nanoscale organization or clustering.

Cellular mechanisms that orchestrate ligand oligomerization are complex, and the capacity to control multivalent interactions and thereby modulate key signaling events within living systems is therefore currently very limited. In particular, post-translational modifications involved in ligand assembly [20], peripheral or integral membrane ligands whose ectodomains alone cannot

oligomerize [8,21], and intricate interactions with the ECM [16,17,18,19] are difficult to imitate with recombinant or synthetic ligands. Ligand clustering can be achieved via antibody-induced grouping, though this method is not well-controlled, efficient, or readily reproducible. The use of synthetic multivalent ligands is thus a promising approach to elucidate fundamental mechanisms [4,5] in cellular signaling, such as the role of receptor-ligand cluster size and number in cellular signaling. Moreover, synthetic multivalent ligands could serve as both potent therapeutics and powerful biological tools if they could be used to control stem cell fate *in vitro* and *in vivo*.

Adult neural stem cells (NSC) represent an important class of therapeutically relevant cells, persist in specific regions of the brain, and have the capacity to generate new neurons and glia throughout life. Furthermore, NSC-mediated neurogenesis has been implicated in learning and memory, mood regulation, and neurological disorders [22,23,24,25,26]. In addition, human pluripotent stem cells (hPSCs) – which include human embryonic stem cells (hESCs) and induced pluripotent stem cells (hiPSCs) – have the capacity to differentiate into all cells of the adult body and therefore offer broad potential for cell replacement therapy and modeling human disease. We have recently found that ephrin-Eph signaling regulates both the neuronal differentiation of adult hippocampal NSCs [27] and the differentiation of hESCs into dopaminergic neurons [28], the cells lost in Parkinson's disease. The design of molecules that regulate ephrin-Eph signaling in NSCs and hPSCs could therefore advance both basic biology and therapeutic applications.

Here, we demonstrate the design of multivalent ephrin ligands that induce Eph receptor clustering, activate downstream signaling, and thereby potently regulate NSC differentiation *in vitro* and *in vivo*, as well as hESC and hiPSC differentiation *in vitro*. This strong capacity to regulate cell fate offers implications for fundamental biological investigation, pharmacology and toxicology screens, cell replacement therapies, and other regenerative medicine approaches to restore organ function [29,30].

Materials and Methods

Recombinant Protein Production, Purification, and Bioconjugation

Murine ephrin-B2 ectodomain sequence (amino acids 31-227) was amplified from the plasmid pcDNA3.1-ephrin-B2-hFc (a kind gift from T. Miyamoto, Keio University), and human ephrin-B1 ectodomain sequence (amino acids 28-237) was amplified from pALTER-MAX (a kind gift from H. Sugimura, Hamamatsu University). A C-terminal hexahistidine tag and cysteine were added during PCR, followed by insertion into the bacterial expression plasmid pBAD. Protein was expressed in bacteria and purified as previously described [31]. Protein purity was assessed by confirmation of a single band following SDS-PAGE. Purified ephrin-B2 or ephrin-B1 was conjugated to 800 kDa hyaluronic acid (HA) (Genzyme) or to a range of monodisperse molecular weight HAs (Hyalose) through a two-step reaction using carbodiimide chemistry at the HA carboxylate group and a maleimide reaction at the protein C-terminal cysteine [31]. In the first step, 3,3´-*N*-(ε-Maleimidocaproic acid) hydrazide (EMCH, Pierce, 1.2 mg/mL), *N*-hydroxysulfosuccinimide (Sulfo-NHS, Pierce, 2.8 mg/mL), and 1-ethyl-3-(3-dimethylaminopropyl) carbodiimide hydrochloride (EDC, Pierce, 10 mg/mL) were added to a 3 mg/mL solution of HA in 0.1 M 2-(*N*-morpholino)ethanesulfonic acid (MES) (Sigma) buffer pH 6.5 and allowed to react at 4 °C for 4 hours. The solution was then dialyzed into pH 7.0 PBS containing 10% glycerol and 2 mM EDTA. Recombinant ephrin-B2 or ephrin-B1 was reduced

using Tris(2-carboxyethyl)phosphine hydrochloride (TCEP) (Pierce) in 200-fold molar excess and reacted at 4 °C for 5 minutes. Activated HA-EMCH was then added at desired molar ratios with reduced ephrin-B2 or ephrin-B1 and allowed to react at 4 °C overnight. The ephrin-conjugated HA was dialyzed with 100 kDa MWCO tubing (Spectrum Labs) in pH 7.0 PBS containing 2 mM EDTA to remove unreacted ephrin. Purified ephrin and HA-conjugated ephrin protein concentrations were measured using a BCA assay, and valencies were verified using SEC-MALS as previously described [31].

Murine ephrin-B2 (amino acids 31-227) to be expressed in mammalian cells was cloned into pN1-eYFP (a kind gift from J. Groves, UC Berkeley) CMV expression vector and was modified to remove the eYFP portion as well as include a sequence of ten histidines directly after an added cysteine residue at the C-terminus. The expression vector was transfected into HEK 293T cells using polyethylenimine (Polysciences Inc.) as previously described [32]. The protein was purified from cell supernatant with gravity flow column containing Nickel-Agarose beads (Qiagen Inc.) at 4 °C. Mammalian ephrin-B2 was conjugated to HA in the same protocol as bacterial ephrin-B2 described above. Fluorescently-labeled ephrin-B2 conjugates were created by reacting purified recombinant ephrin-B2 with an Alexa Fluor 488 or 647 5-SDP ester (Molecular Probes) at a 3:2 (w/w) ratio for 24 hours at 4 °C with constant vortexing. Labeled protein was then immediately reduced using TCEP and conjugated as described above.

Cell Culture and Differentiation

NSCs were cultured as previously described [33]. For differentiation studies, 8-well chamber slides were seeded with $2x10^4$ cells per well in standard culture medium containing 0.1 ng/mL FGF-2. For the subsequent 6 days, ephrin-B2 was added at the desired molar concentration, and daily 50% media changes were performed. For Western blotting and qPCR experiments, cells were seeded at $2.5x10^5$ cells per well in a 6-well culture dish in standard media containing 0.1 ng/mL FGF-2. The following day, conjugates or controls were added at 200 nM ephrin-B2 concentration, and a 50% media change was performed. For β-catenin activation studies, cell lysate was collected 24 hours later, and a luciferase assay (Promega) was quantified using a luminometer (TD-20/20, Turner BioSystems). For qPCR, cells were differentiated for 6 days total with daily 50% media changes. To achieve a highly differentiated group as a positive control, a combination of retinoic acid at 1 μM and FBS at 2% (v/v) were used (RA/FBS). For EphB4 clustering studies, cells were seeded at a cell density of $7x10^4$ cells/cm^2 onto 0.17 mm thick, 25 mm diameter glass coverslips in 6-well plates, then fluorescent conjugates were added at 200 nM ephrin-B2 concentration before being placed at 4 °C on an orbital rocker for 4 hours before fixation, staining, and imaging. EphB4 cluster properties were quantified using ImageJ.

Rat hippocampal astrocytes were isolated as described [34] and cultured on poly-ornithine/laminin-coated plates in DMEM/F-12 media containing N2 supplement and 10% FBS. For co-culture experiments, astrocytes were seeded in 8-well chamber slides at a cell density of $7x10^4$ cells/cm^2 in standard culture medium and incubated overnight. Wells were then carefully washed with medium lacking FBS and FGF-2 two times before seeding EphB4-Dendra2 mutant NSCs at a density of $7x10^4$ cells/cm^2. Cells were allowed to adhere and initiate ligand/receptor clustering for 4 hours at 37 °C before fixing, immunostaining, and imaging.

hESC lines H1 (NIH registry no. WA01) and HSF6 (originally NIH no. UC06) were used for ephrin-B1 conjugate hESC experiments. During the course of the study, HSF6 cells were taken off NIH federal registry, so H1s were subsequently used in their place. The fibroblast derived iPSC line (a kind gift from George Q. Daley, Children's Hospital Boston, Boston, MA) was used

for ephrin-B1 conjugate iPSC experiments. Cells were cultured as previously described [35]. For differentiation studies, passaged cells were resuspended in X-VIVO 10 media (Lonza) supplemented with 10 ng/mL FGF-2, triturated to form cell aggregates of roughly 50 µm in diameter, and cultured in Costar Ultra-Low attachment plates (Corning) for 3 days. Free-floating embryoid bodies (EBs) were then collected and plated into poly-ornithine/laminin-coated 6-well plates with fresh media at a density of roughly 25 EBs per well. The next day, a 50% medium change was performed, excluding FGF-2, and the differentiation factors – SDF-1 (100 ng/mL), PTN (100 ng/mL), IGF-2 (100 ng/mL), ephrin-B1 (1 µg/mL), and heparin (100 µg/mL) – were added. Cells were cultured for 14 to 28 days with 50% medium changes every two days to replenish the SPIE factors. For the proliferation study, cells were incubated with 10 µg/mL BrdU (Sigma) for 20-24 hours before fixation and staining.

Antibody-Clustered Ephrin-B Formation

To create clustered ephrin-B2 and ephrin-B1 complexes (Fc-ephrin-B), recombinant mouse ephrin-B/Fc chimera (R&D Systems) were incubated with goat anti-human IgG, Fc-fragment specific, (Jackson ImmunoResearch) antibody at a 1:9 ratio (w/w) for 90 min at 4 °C. Complexes were used immediately after clustering.

Retroviral vector construction and NSC transduction

To perform super-resolution microscopy, a mutant NSC line expressing an EphB4-Dendra2 fusion protein was created. In short, murine EphB4 cDNA (a kind gift from J. Groves, UC Berkeley) and cDNA for the photoconvertible protein Dendra2 (a kind gift from Lana Bosanac, Tjian Lab, UC Berkeley) was cloned into the retroviral vector CLPIT. Retroviral vectors were packaged using standard methods as previously described [36]. NSCs were infected at an MOI of 1 and selected using puromycin (1 µg/mL).

Stereotactic Injections

All animal protocols were approved by the University of California, Berkeley Animal Care and Use Committee and conducted in accordance with National Institutes of Health guidelines. 8-week-old adult female Fisher 344 rats were intraperitoneally injected with BrdU (50 mg/kg) for three days prior to surgery. On the fourth day, each animal was anesthetized using a ketamine/xylazine cocktail, and underwent bilateral intrahippocampal stereotactic injections of 3 µL of either HA (4.6 nM), Fc-ephrin-B2 (100 nM ephrin-B2), or 1:22 HA:Ephrin-B2 (100 nM ephrin-B2). The injection coordinates with respect to the bregma were -3.5 mm anteriorposterior, -3.3 mm dorsoventral (from dura), and ± 1.8 mm mediolateral. Before the injections, the animals received a buprenorphine/meloxicam cocktail in saline as an analgesic and to avoid dehydration. Directly after the surgery a 1 mL intraperitoneal injection of yohimbine in saline was administered to counteract the effects of xylazine. Another injection of buprenorphine in saline was given 6-8 hours post surgery as additional analgesic. Animals were allowed to recover for 5 days prior to sacrifice. On the sixth day, the rats were perfused with 4% PFA and the brains were extracted, stored in fixative for 24 hours, and then allowed to settle in a 30% sucrose solution.

Immunostaining

Coronal brain sections (40 µm) were processed, stored, and stained as previously described [37]. Primary antibodies used were mouse anti-BrdU (1:100, Roche), guinea pig anti-DCX (1:1000, Millipore), goat anti-EphB4 (1:50, Santa Cruz Biotechnology), and goat anti-ephrin-B2 (1:10,

R&D Systems). Appropriate Cy3-, Dylight 649-, Alexa Fluor 488-, or Alexa Fluor 647-conjugated secondary antibodies (1:250, Jackson ImmunoResearch, Molecular Probes) were used to detect primary antibodies. DAPI (20 μg/mL, Invitrogen) was used as a nuclear counterstain. To co-stain for ephrin-B2 and EphB4, sections were primary stained for EphB4, secondary stained, then fixed with 4% PFA for 50 minutes, washed, then stained with ephrin-B2 which was pre-labeled with an Alexa Fluor 488 or 647 monoclonal antibody labeling kit (Molecular Probes). Sections were then mounted on glass slides, and either stereological analysis (Stereo Investigator, MBF Biosciences) or confocal microscopy (LSM 710, Zeiss) was performed. In short, using an optical fractionator method, BrdU+ and DCX+ cells were counted in a Systematic Randomly Sampled (SRS) set of unbiased virtual volumes inside the subgranular zone and granular cell layer of both the left and right sides of the hippocampus. An estimate of the total number of DCX+/BrdU+ cells in the hippocampus was then generated.

Cells cultures were fixed with 4% paraformaldehyde for 10 minutes, blocked for 1 hour with 5% donkey serum (Sigma), permeabilized with 0.3% Triton X-100 (Calbiochem), and incubated for 48 hours with combinations of the following primary antibodies: mouse anti-nestin (1:1000, Abcam), mouse anti-βIII-Tubulin (1:250, Sigma), rabbit anti-βIII-Tubulin (1:1000, Covance), rat anti-BrdU (1:100, Abcam), mouse anti-Map2 (1:500, Millipore), and rabbit anti-TH (1:500, Pel-Freez). Appropriate Cy3-, Cy5-, Alexa Fluor 488, or Alexa Fluor 647-conjugated secondary antibodies were used to detect primary antibodies. DAPI was used as a nuclear counterstain. For the hESC proliferation experiment, cells were pretreated for BrdU labeling as previously described [38] before primary staining. The percentage of antibody-labeled cells was determined by manually evaluating at least 1,000 cells at randomly sampled sites throughout the culture well.

Super-Resolution Microscopy

Fixed cultures incubated with fluorescent conjugate and/or immunostained with fluorescent antibodies were subsequently incubated with 100 nm Tetraspeck fluorescent beads (Life Technologies) in PBS at a 1:2000 (v/v) dilution to act as reference points during imaging to later use for drift correction in image reconstruction. The sample coverslips were then placed in an Attofluor cell chamber (Life Technologies) and incubated in cold, freshly made pH 8.0 buffer containing 100 mM cysteamine (Sigma), 50 mM Tris, 10 mM NaCl, 10% (wt/v) glucose, 560 μg/mL glucose oxidase (Sigma), and 34 μg/mL catalase (Sigma). Using a microscope (TE2000, Nikon) with adaptive optics for 3D localization [39], a piezoelectric stage, and highly inclined thin illumination capability [40], photoactivatable localization microscopy (PALM) [41] was performed to detect EphB4-Dendra2 [42] simultaneously with direct stochastic optical reconstruction microscopy (dSTORM) [43] to detect Alexa Fluor 647-tagged ephrin-B2 conjugates, as previously described. Sub-diffraction limit images were then reconstructed using QuickPALM then quantified using ImageJ.

Quantitative Reverse Transcription Polymerase Chain Reaction (qRT-PCR)

RNA was isolated from differentiated cells using standard Trizol (Invitrogen) collection and ethanol precipitation techniques. Samples were quantified using a NanoDrop Spectrophotomer (ND-1000, NanoDrop Technologies), and equivalent amounts of RNA were added to quantitative PCR (qPCR) reactions. QPCR was performed as previously described [44] to probe for expression of various markers and 18S control mRNA. Neuronal subtype qPCR was performed using validated probes from Applied Biosystems. All reactions were performed using

a Bio-Rad iQ5 Multicolor Real-Time PCR Detection System, and target mRNA expression levels were normalized to 18S mRNA levels for relative comparison.

For PCR product amplification, equal amounts of differentiated hESC cDNA were combined with *Taq* DNA Polymerase and forward and reverse primers for *En1* and ran for 40 cycles in a thermocycler (iCycler, Bio-Rad) with an annealing temperature of 55 °C. PCR products were then ran on a 3% agarose gel and imaged (ChemiDoc XRS, Bio-Rad).

Western Blotting

Cell lysates were collected in RIPA buffer (1% IGEPAL, 0.1% SDS, in 0.05 M PBS) containing various protease inhibitors 24 hours after ephrin-B2 addition. Lysate protein concentration was determined using a BCA Protein Assay (Pierce), ran on a 10% SDS-PAGE gel, then transferred onto a nitrocellulose membrane. Nonspecific protein binding was blocked using 5% milk, then the membrane was incubated in rabbit anti-active-β-catenin (1:1000, Cell Signaling) at 4°C overnight. An appropriate HRP-conjugated secondary antibody (1:10,000, Pierce) was then added after washing to bind the primary antibody. Supersignal West Dura Extended Duration Substrate (Pierce) was used to detect protein bands. After film development (Kodak Film Processor 5000RA), membranes were stripped and reprobed with rabbit anti-GAPDH (1:2500, Abcam). Blot intensities were quantified and normalized to GAPDH using ImageJ.

Flow Cytometry

Naïve NSCs were placed in amber 1.5 mL Eppendorf tubes at a cell density of $4.0x10^5$ cells per mL and incubated with a range of concentrations of Alexa Fluor 647-tagged ephrin-B2 conjugate (800 kDa HA, 1:9 HA:Eprin-B2 final molar ratio) for 4 hours at 4 °C. The samples were then run on a flow cytometer (LSRFortessa, BD Biosciences) and conjugate-bound cells were detected using a 633 nm laser and PMT detector.

High Performance Liquid Chromatography (HPLC)

Conditioned media from differentiated hESCs was collected as previously described [45] and catecholamines were extracted and concentrated using a kit (Chromsystems) before analysis on an HPLC with an electrochemical detector (ECD) was performed.

Statistical Analysis

Statistical significance of the results was determined using an ANOVA and multiple means comparison function (Tukey-Kramer method) in MATLAB with an alpha level of 0.05. All error bars are reported in s.d. from the mean, with $n = 3$ unless otherwise noted.

Results

Multivalent Ephrin-B2 Enhances Neuronal Differentiation of NSCs *In Vitro*

To create synthetic multivalent ligands with potentially high potencies, recombinantly produced ephrin-B2 extracellular domain was conjugated at a range of stoichiometries to high molecular weight hyaluronic acid (HA) – a well-characterized biopolymer present throughout the body and in particular within the brain – using EDC/Sulfo-NHS chemistry, as previously described [31] (**Fig. 1a,b**). The results are ~100 nm polymeric conjugates [46]. Valencies – estimated using a BCA assay and further quantified with size exclusion chromatography coupled with multi-angle

light scattering (SEC-MALS) (**Fig. 1c**) – ranged in this synthesis from 2 to 25 ephrin molecules per HA chain.

Based on the recently discovered role of ephrin-B2 signaling in regulating the neuronal lineage commitment of adult NSCs *in vitro* and *in vivo* [27], we investigated the activity of the multivalent conjugates at various concentrations in NSC culture. At a given concentration of ephrin-B2 ectodomain molecules, increasing the valency of the HA:Ephrin-B2 conjugates progressively elevated neuronal differentiation (**Fig. 1d,e**). Strikingly, compared to antibody-clustered ligand, the 1:22, 1:12, and 1:8 valency conjugates induced similar levels of neuronal differentiation at 37-, 26-, and 9-fold lower protein concentrations, respectively. In contrast to the current antibody clustered form, where studying ephrin biology currently requires high ligand concentrations of these low potency molecules, the multivalent ligands are potent agonists, with potentially reduced cost. Next, the addition of monomeric ephrin-B2 in tenfold molar excess to Fc-ephrin-B2 wells blocked differentiation, further establishing that ephrin clustering is required for activity. Finally, the results were further validated by quantifying mRNA levels of the neuronal marker *Tubb3* (**Fig. 1f**).

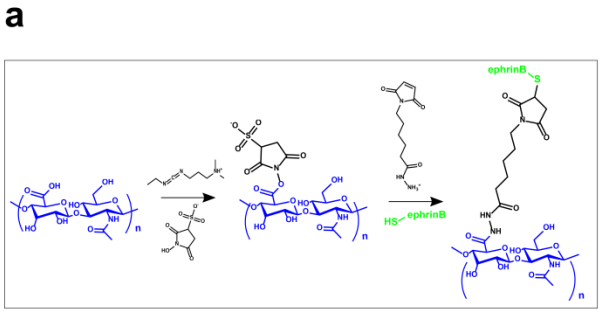

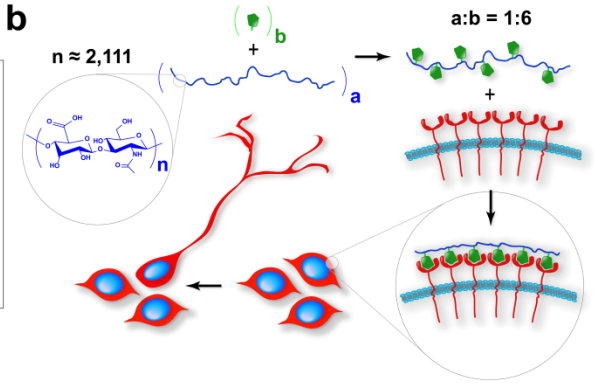

c

Initial HA:Ephrin-B2 Molar Ratio	Final Ephrin-B2 Molar Ratio	
	BCA	*SEC-MALS*
1:0	0	0
1:1	0.77	2.71
1:5	1.75	4.55
1:10	8.20	7.94
1:20	12.04	11.82
1:40	22.78	25.84

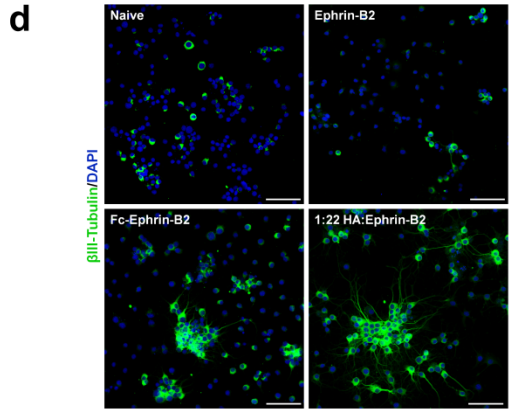

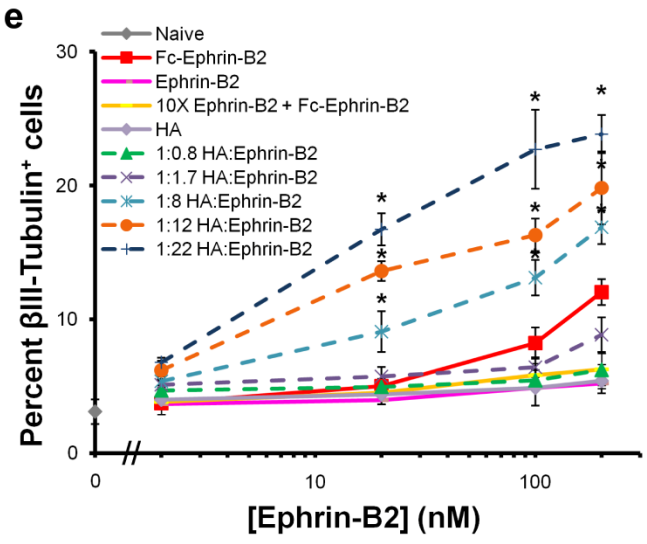

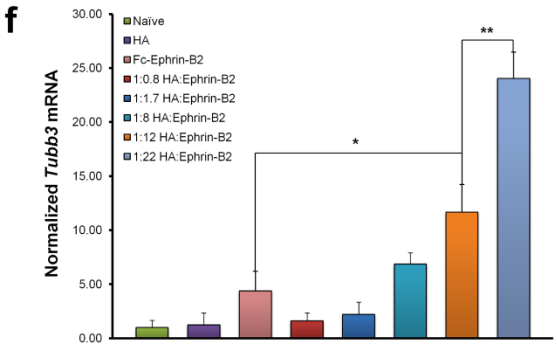

Figure 1: Multivalent ephrin-B2 enhances neuronal differentiation of NSCs *in vitro*. (a) Chemical mechanism of HA functionalization and recombinant protein conjugation. **(b)** Schematic of protein conjugation to linear HA and subsequent clustering of receptors upon introduction to cells. **(c)** Comparative BCA vs. SEC-MALS analysis for a range of ephrin-B2 bioconjugate valencies. **(d)** Representative images of cultured NSCs differentiated for 6 days in media alone (naïve) or in the presence of unclustered ephrin-B2, antibody clustered Fc-ephrin-B2, or multivalent 1:22 HA:Ephrin-B2, then immunostained for the neuronal marker βIII-Tubulin (green) and total nuclei (blue). Scale bars, 100 μm. **(e)** Quantification of the total fraction of neurons after 6 days of NSC differentiation in the presence of ephrin-B2 conjugates (dashed lines) or controls (solid lines), as assessed by immunostaining. * $P < 0.05$ compared to Fc-ephrin-B2 at corresponding ephrin-B2 concentrations. **(f)** qPCR for the neuronal transcript *Tubb3* after 6-day differentiation. * $P = 0.0159$, ** $P = 0.0037$.

Multivalent Ephrin-B2 Enhances Receptor Clustering

We compared the ability of natural and synthetic ligands to cluster Eph receptors. Since ephrin-B2 presented from astrocytes regulates the neuronal differentiation of adult NSCs [27], we analyzed Eph-ephrin localization in NSCs in contact with hippocampal astrocytes. Punctate staining of both ephrin-B2 and its receptor EphB4 was observed at cell-cell junctions (**Fig. 2a**), which was significantly more prevalent on NSCs when in contact with astrocytes (**Figs. 2b, 3a**). Co-localization of the ligand and receptor was also observed at NSC-astrocyte contacts in the hippocampus of the adult brain (**Fig. 2c**), where NSCs reside.

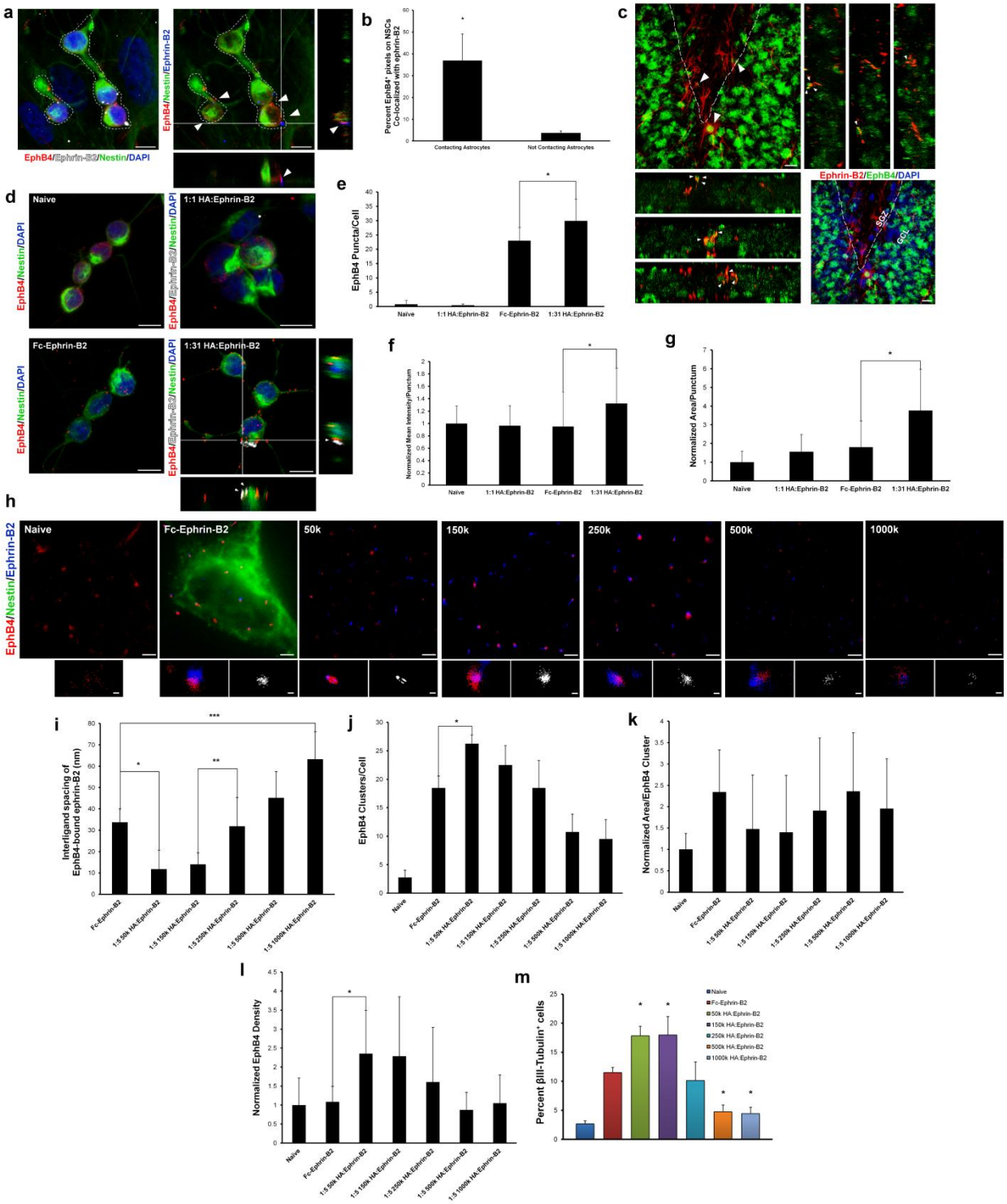

Figure 2: Multivalent ephrin-B2 enhances receptor clustering. (a) Representative image of EphB4 and ephrin-B2 clustering on the surface of NSCs and hippocampal astrocytes, respectively, in co-culture. **(b)** Quantification of percent of the total number of EphB4^{+} pixels on the NSC membrane which co-localized with ephrin-B2 pixels from astrocytes. * P = 0.0218. **(c)** EphB4 receptor clustering on the surface of multiple cells in the hippocampal subgranular zone (SGZ) upon contact with ephrin-B2^{+} astrocytes. **(d)** Representative images of NSCs incubated with fluorescently labeled ephrin-B2 bioconjugates (white) for 4 hours at 4 °C and immunostained for their cognate

receptor EphB4 (red), the neural stem cell marker nestin (green), and total nuclei (blue). Scale bars, 10 μm. **(e)** Quantification of total number of EphB4 puncta per cell after incubation with ephrin-B2, either antibody-clustered or a new preparation of conjugate. * P = 0.024. **(f)** Normalized mean EphB4 signal intensity per punctum after incubation with ephrin-B2. * P = 0.001. **(g)** Normalized area per EphB4 punctum after incubation with ephrin-B2. * $P = 5.33 \times 10^{-9}$. **(h)** Representative reconstructed super-resolution images of EphB4-Dendra2 (red) NSCs incubated with fluorescently labeled ephrin-B2 bioconjugates (blue) for 4 hours at 4 °C immunostained for the neural stem cell marker nestin (green). Magnified images of representative EphB4/ephrin-B2 clusters are shown below whole cell images, with co-localized pixels indicated in white. Large scale bars, 1000 nm; small scale bars, 100 nm. **(i)** Quantification of average interligand spacing between individual EphB4-co-localized ephrin-B2 molecules, with a constant value of 16 nm per pixel. * $P = 1.80 \times 10^{-6}$. ** P = 0.0006. *** $P = 1.22 \times 10^{-6}$. **(j)** Quantification of total number of EphB4 clusters per cell after incubation with fluorescent ephrin-B2. * P = 0.0009. **(k)** Normalized area per EphB4 cluster after incubation with fluorescent ephrin-B2. * $P = 5.33 \times 10^{-9}$. **(l)** Normalized number of ephrin-B2-co-localized EphB4 pixels per unit area after incubation with ephrin-B2. * P = 0.0015. **(m)** Immunostaining quantification of the total fraction of neurons after 6 days of NSC differentiation in the presence of Alexa Fluor 647 tagged ephrin-B2 conjugates of varying HA backbone molecular weight (M_w) and antibody-clustered Fc-ephrin-B2 control, all at 200 nM protein concentration. * $P < 0.02$ compared to Fc-ephrin-B2.

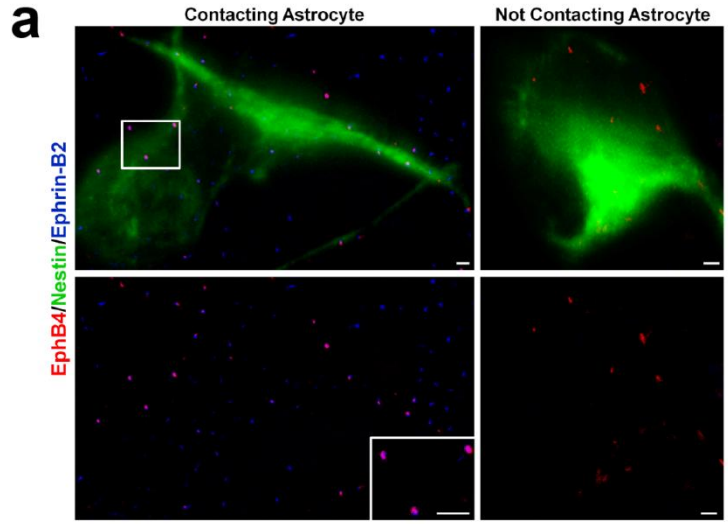

Figure 3: Ligand and receptor clustering in NSC/astrocyte co-culture. (a) Representative reconstructed super-resolution images of EphB4 and ephrin-B2 clustering on the surface of EphB4-Dendra2 NSCs which are or are not in contact with hippocampal astrocytes in co-culture. Large scale bars, 1000 nm; small scale bars, 100 nm.

We therefore analyzed whether the multivalent conjugates could emulate this natural process of receptor-ligand assembly. Fluorescently-labeled ephrin-B2 conjugates were synthesized and incubated with NSCs, at 4 ºC to block endocytosis (**Fig. 2d**). EphB4 localization was diffuse across the cell membrane in the absence of ephrin-B2 or with low ratio conjugates, whereas EphB4 puncta were observed in the presence of highly multivalent conjugates or antibody-clustered ligand. Additionally, while low ephrin-B2 valency conjugates yielded fewer and smaller EphB4 clusters than antibody-clustered ligand, high valency conjugates showed more (**Figs. 2e, 4b**), larger (**Figs. 2f, 4c**), and more dense (**Figs. 2g, 4d**) EphB4 clusters in close proximity to fluorescently tagged ephrin-B2. Ligand multivalency therefore modulates both the number and the size of receptor clusters.

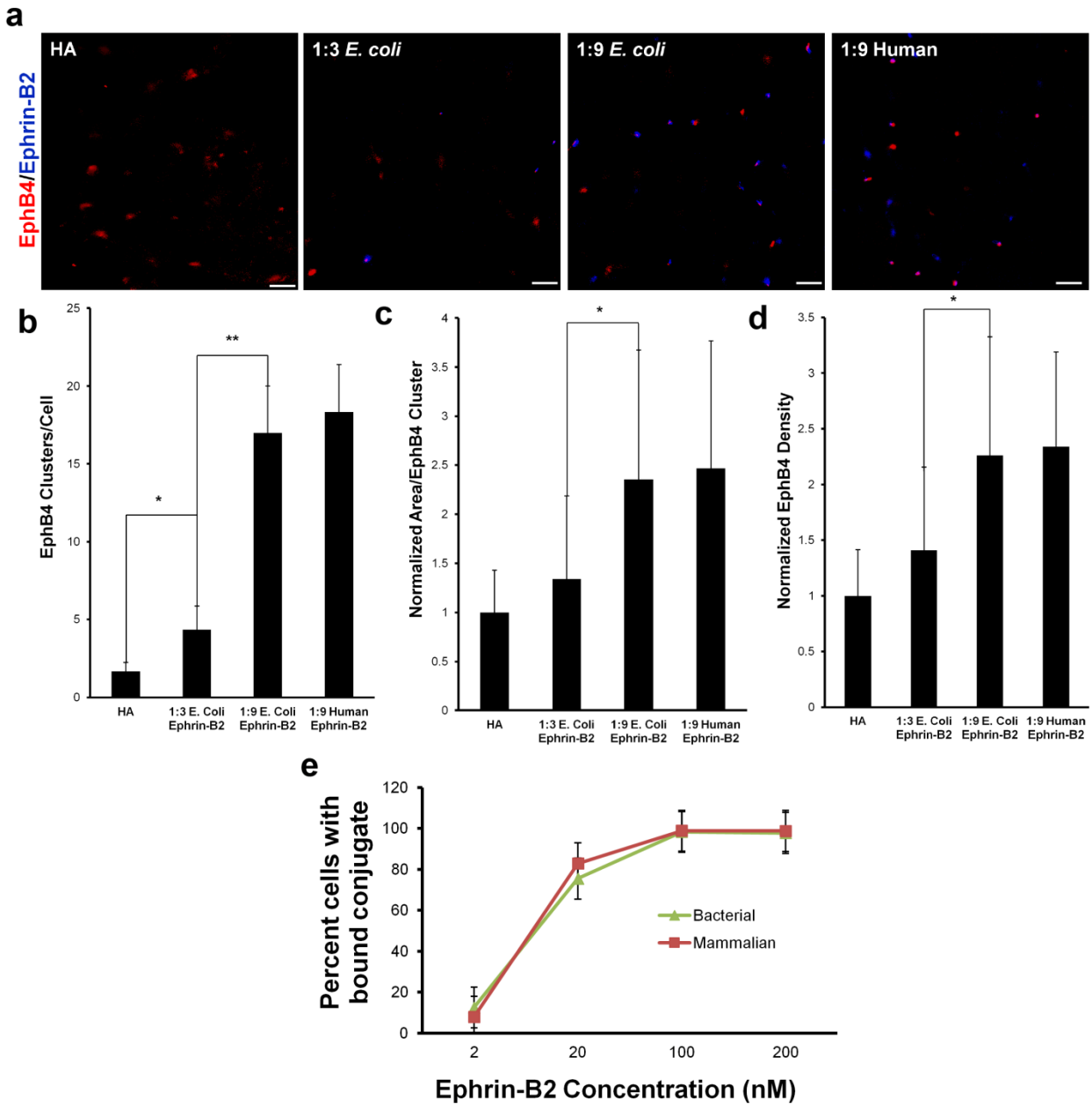

Figure 4: Effects of ephrin-B2 expression system on EphB4 receptor binding and clustering. (a) Representative reconstructed super-resolution images of EphB4-Dendra2 (red) NSCs incubated with fluorescently labeled ephrin-B2 bioconjugates (blue) containing protein produced in either *E. coli* or human 293T HEK cells for 4 hours at 4 °C. Scale bars, 1000 nm. (b) Quantification of total number of EphB4 clusters per cell after incubation with fluorescent ephrin-B2. * $P = 0.0474$. ** $P = 0.0029$. (c) Normalized area per EphB4 cluster after incubation with fluorescent ephrin-B2. * $P = 0.0355$. (d) Normalized number of ephrin-B2-co-localized EphB4 pixels per unit area after incubation with ephrin-B2. * $P = 0.0337$. (e) Percent of NSCs with cell membrane-bound fluorescently labeled ephrin-B2 bioconjugates as assessed by flow cytometry after incubation with conjugates for 4 hours at 4 °C.

To ensure the post-translational modifications on recombinant ephrin-B2 produced in mammalian cells did not differentially affect binding to EphB4 receptors on the NSC membrane compared to ephrin-B2 produced in *E. coli*, we performed a quantitative cell binding assay. We

incubated fluorescently tagged ephrin-B2 conjugates (1:9 HA:Ephrin-B2 final molar ratio) with NSCs for 4 hours at 4 ºC and performed flow cytometry. Our results indicate that the protein sequence and post-translational modifications arising from the different expression systems do not significantly affect ephrin binding to its receptor (**Fig. 4e**).

Next, to determine the effect of ligand density on NSC differentiation and cell receptor clustering, we acquired commercially available monodisperse hyaluronic acid (HA) molecules of varying molecular weights (MWs), then conjugated recombinant ephrin-B2 extracellular domains which we had tagged with fluorescent Alexa Fluor 647 molecules. Conjugations were performed such that the conjugates of varying MWs possessed equal molar amounts of fluorescently-tagged protein (1:5 HA:Ephrin-B2 final molar ratio). In this way, ligand spacing was controllably varied, with the high MW conjugates possessing greater interligand spacing compared to lower MW conjugates. Adult rat NPCs were then cultured at 37° C in the presence of the conjugates for 6 days and the levels of neuronal differentiation was quantified. Lower MW conjugates showed significantly higher levels of neuronal differentiation compared to antibody-clustered Fc-ephrin-B2, while higher MW conjugates showed significantly less differentiation (**Fig. 2m**).

Furthermore, in an attempt to quantify the interligand spacing of the differing MW conjugates, we performed super-resolution microscopy on mutant NPCs incubated with fluorescent conjugates for 4 hours at 4° C to obtain single molecule resolution. We used a mutant NPC line expressing an EphB4-Dendra2 [42] fusion protein to be able to perform photoactivatable localization microscopy (PALM) [41] in combination with direct stochastic optical resolution microscopy (dSTORM) [43] of Alexa Fluor 647-tagged HA:Ephrin-B2 conjugates. We observed that lower MW HA conjugates possessed significantly closer interligand spacing compared to high MW conjugates (**Fig. 2i**). Furthermore, conjugates with closer ephrin-B2 interligand spacing were able to form more, larger, and denser EphB4 clusters than conjugates with farther ephrin-B2 interligand spacing (**Fig. 2j-l**). These results thus indicate that increased ligand density is necessary to increase nanoscale receptor clustering and subsequent cellular responses, such as neuronal differentiation.

Multivalent Ephrin-B2 Enhances Downstream Signaling

Ephrin-B2 induces neuronal differentiation by activating the transcriptional co-activator β -catenin [27]. Western blotting quantitatively indicated that higher valency conjugate activated β-catenin significantly more than antibody-clustered Fc-ephrin or HA alone (**Fig. 5a,b**). Furthermore, a β-catenin responsive promoter-reporter construct, delivered with a lentiviral vector, showed a higher quantitative level of reporter activation with increasing valency, which at a 1:31 valency was substantially greater than antibody-clustered Fc-ephrinB2 (**Fig. 5c**). Finally, β-catenin drives neuronal differentiation via transcriptional activation of the proneural transcription factor *NeuroD1* [47], and multivalent ephrin-B2 conjugates with increasing valency again progressively induced higher levels of expression of this important target (**Fig. 5d**).

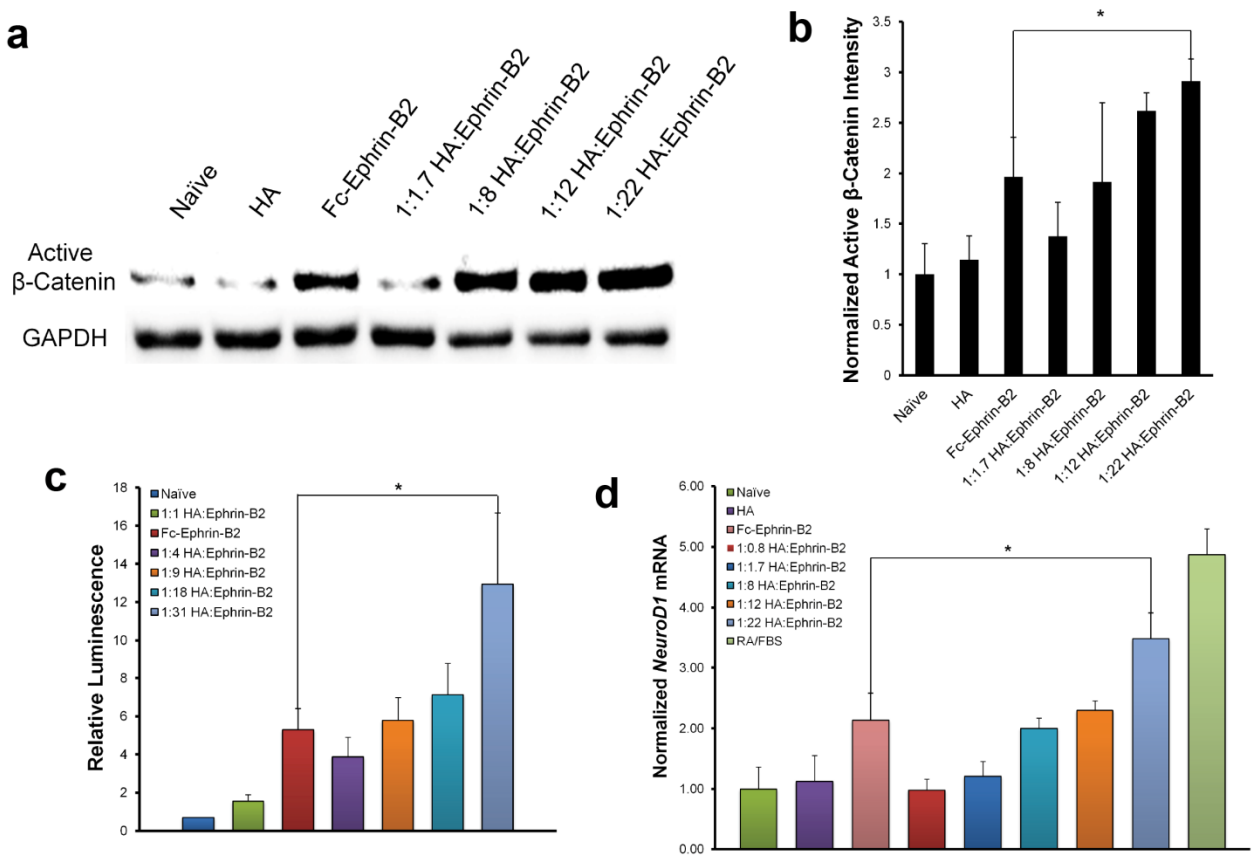

Figure 5: Multivalent ephrin-B2 enhances downstream signaling. (a) Representative Western blot for active β-catenin and GAPDH, as a loading control, in NSC lysate after 24 hour incubation with ephrin-B2 bioconjugates. **(b)** Quantification of the levels of β-catenin activation normalized to GAPDH. * P = 0.0217. **(c)** Quantification of β-catenin activation in NSCs after 24-hour incubation with fluorescently labeled ephrin-B2 bioconjugates at 37 °C, as assessed by upregulation of the transgenic luciferase reporter for β-catenin activity. * P = 0.0267. **(d)** qPCR for the intermediate transcriptional target of neurogenesis *NeuroD1* after 6 day differentiation. The RA/FBS group is described in detail in the Methods section. * P = 0.0192.

Multivalent Ephrin-B2 Enhances *In Vivo* Neurogenesis

Multivalent conjugates may have strong utility not only *in vitro* but also *in vivo*. To investigate the latter, multivalent ephrin-B2 was administered into the hippocampal region of the adult rodent brain to analyze its ability to modulate endogenous NSC function. Bromodeoxyuridine (BrdU) was administered to label dividing cells, followed by stereotactic injection of the ephrin-B2 conjugate and controls (**Fig. 6a**). After 5 days, the fractions of newly born cells (BrdU+) that had differentiated into neurons (DCX+) was quantified in tissue sections [27]. Antibody-clustered ligand showed a modest 20% increase over the uninjected sham brain and HA control at the ephrin levels administered; however, the same number of ephrin-B2 domains incorporated into the highly multivalent conjugate yielded a substantial 60% increase in neurogenesis in the brain (**Fig. 6b,c**). These data demonstrate that nanoscale organization in the presentation of this ligand greatly enhances its ability to elicit cellular responses both *in vitro* and *in vivo*.

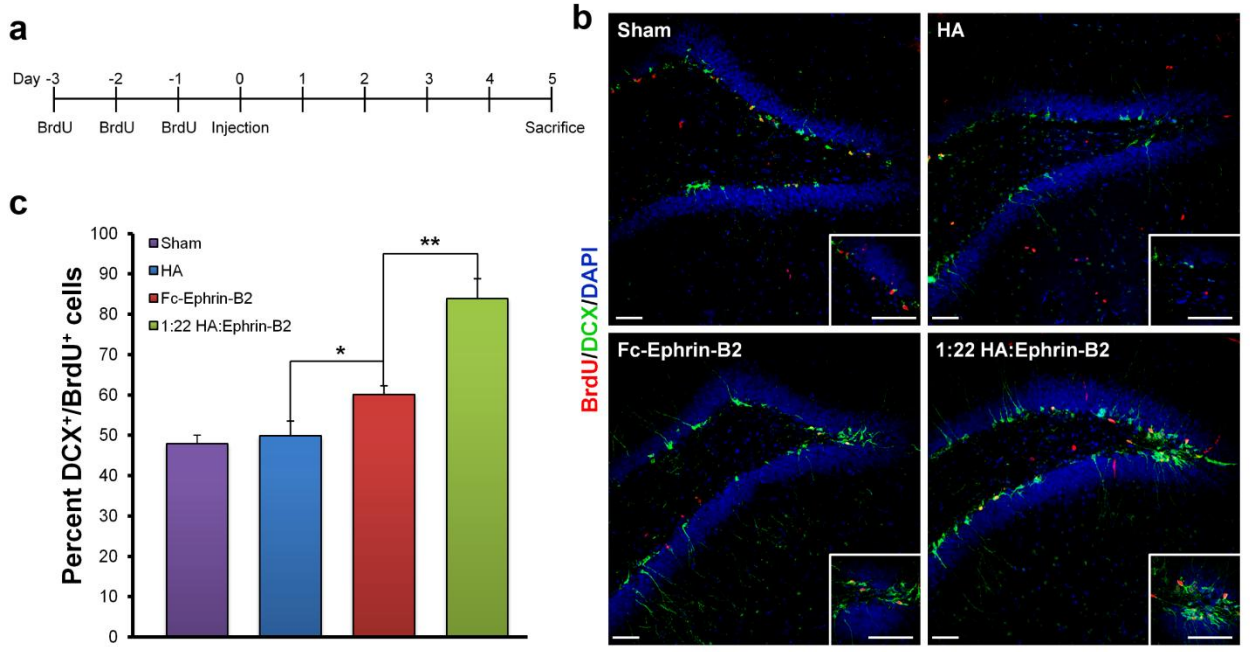

Figure 6: Multivalent ephrin-B2 enhances *in vivo* neurogenesis. (a) Schematic of experimental time course. **(b)** Representative image of adult rat hippocampal sections 5 days after stereotactic injections, immunostained for BrdU (red) to label dividing cells, DCX (green) to label immature neurons, and DAPI to stain nuclei (blue). Scale bars, 100 μm. **(c)** Quantification of the overall fraction of newborn hippocampal cells that underwent neuronal differentiation using stereological estimation. * $P = 0.0136$, ** $P = 0.0015$.

Multivalent Ephrin-B1 Enhances Neuronal Differentiation and Midbrain Specification of hESCs

We next assessed the generality of this approach with both human embryonic and human induced pluripotent stem cells, two important classes of stem cells with the capacity to differentiate into all tissues of an adult organism. Vazin et al. have shown that unclustered ephrin-B1 – in combination with soluble stromal cell-derived factor-1 (SDF-1), pleiotrophin (PTN), and IGF-2, a blend known as SPIE – enhances hESC differentiation into midbrain dopaminergic (DA) neurons [28], which have been considered as cell replacement therapies for Parkinson's disease (PD) [48]. By analogy with ephrin-B2, we synthesized multivalent ephrin-B1 conjugates. Using conjugates of varying valency, along with the other components of SPIE, hESCs were first differentiated within embryoid bodies (EB) and then toward DA neurons for 14-18 days (**Fig. 7a**). After 15 days, transcripts for the midbrain-specific marker *En1* increased with higher valency (**Fig. 7b**), and QPCR showed that both the pan-neuronal marker *Tubb3* and the dopaminergic marker *TH* progressively increased with conjugate valency (**Fig. 7c**).

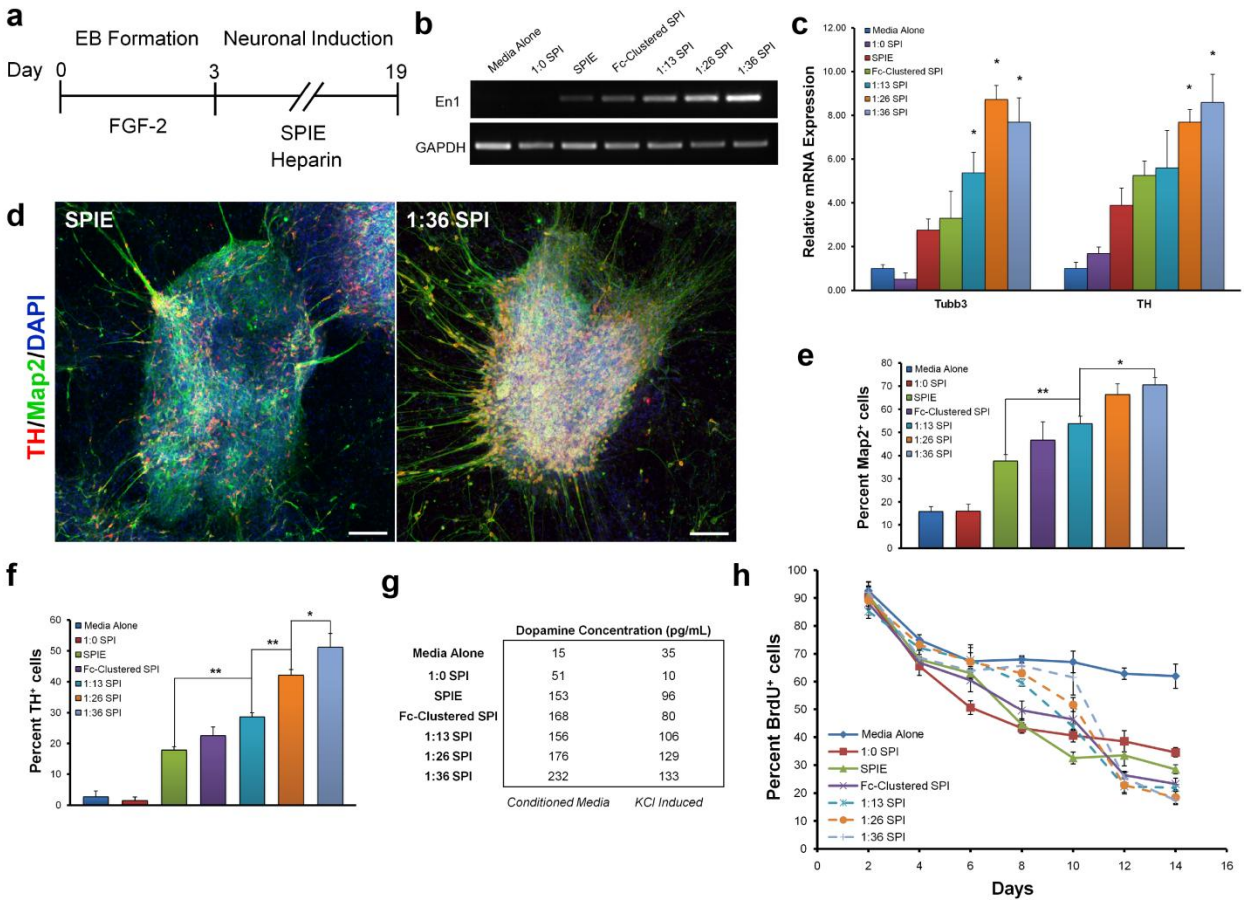

Figure 7: Multivalent ephrin-B1 enhances neuronal differentiation and midbrain specification of hESCs. (a) Schematic of experimental time course. **(b)** RT-PCR analysis of midbrain-specific marker *En1* expression vs. control *G3PDH*, from HSF6 hESCs differentiated for 15 days post-EB formation with ephrin-B1 conjugates or controls. **(c)** qPCR for the pan-neuronal marker *Tubb3* and the dopaminergic marker *TH* after 15-day differentiation of H1 hESCs with ephrin-B1 conjugates or controls. * $P < 0.05$ compared to SPIE for corresponding neuronal marker. **(d)** Representative images of cultured H1 hESCs differentiated for 18 days post-EB formation with the SPI factors, heparin, and either Fc-ephrin-B1 or multivalent 1:36 HA:Ephrin-B1. Immunostaining for total neurons (green), dopaminergic neurons (red), and total nuclei (blue). Scale bars, 100 μm. **(e)** Quantification of the fraction of total neurons after differentiation of H1 hESCs in the presence of ephrin-B1 conjugates or controls, as assessed by immunostaining. * $P = 0.0181$, ** $P = 0.0029$. **(f)** Quantification of the fraction of dopaminergic neurons after differentiation of H1 hESCs in the presence of ephrin-B1 conjugates or controls, as assessed by immunostaining. * $P = 0.0328$, ** $P = 0.0004$. **(g)** Quantification of the fraction of mitotic cells on various days over the 14 day course of HSF6 hESC differentiation in the presence of ephrin-B1 conjugates (dashed lines) or controls (solid lines). **(h)** Quantification of total dopamine levels in cultures of H1 hESCs differentiated for 4 weeks in the presence of ephrin-B1 conjugates or controls, as assessed by HPLC with electrochemical detection.

Immunostaining was then conducted to quantify cell differentiation into a DA lineage. After 15-18 days of differentiation in ephrin following post-embryoid body (EB) formation, hESC and derived cultures exhibited substantially higher proportions of cells expressing both the pan-neuronal (Map2) and the dopaminergic neuron marker (TH) with increasing conjugate valency, compared to antibody-clustered ephrin-B1 (**Fig. 7d,e,f**). Importantly, we achieved similar results with hiPSCs (**Fig. 8a,b**). Since contaminating cells within dopaminergic grafts can be associated with adverse events in clinical trials [49], approaches to improve DA neuron purity are significant. Furthermore, to assess the functional properties of the differentiated DA neurons,

levels of the neurotransmitter dopamine were measured, either in conditioned medium or upon addition of KCl to induce synaptic neurotransmitter release. Dopamine levels increased with increasing valency and were greater with highly multivalent conjugates than antibody-clustered groups (**Fig. 7g**), consistent with the observed higher DA differentiation levels observed with the conjugates.

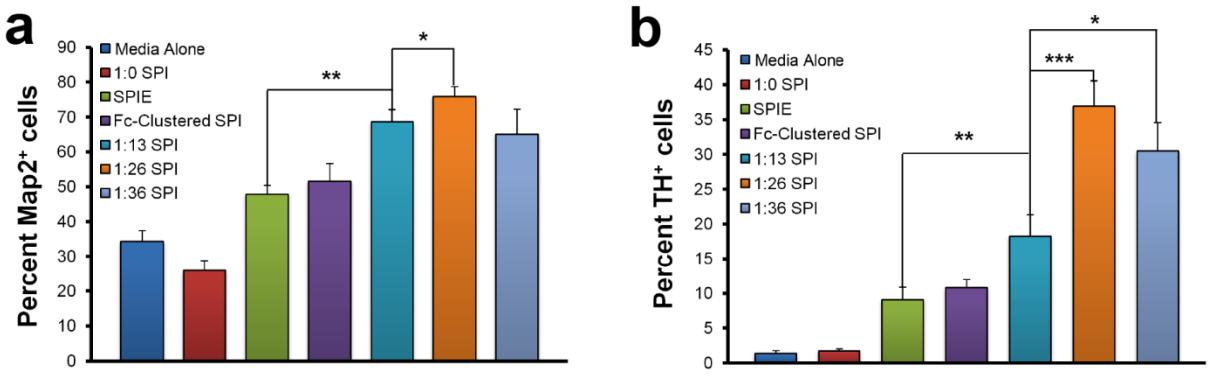

Figure 8: Multivalent ephrin-B1 enhances neuronal differentiation of iPSCs. (a) Quantification of the fraction of neurons after differentiation of hiPSCs with ephrin-B1 conjugates or controls, as assessed by immunostaining. Valencies were quantified using BCA assay. * P = 0.0524, ** P = 0.0012. (b) Quantification of the fraction of dopaminergic neurons after hiPSC differentiation in the presence of ephrin-B1 conjugates or controls, as assessed by immunostaining. * P = 0.0143, ** P = 0.0116, *** P = 0.0025.

As an initial assessment of how multivalent ephrin affects differentiating cultures, at various times over 14 days, cells received a 24 hour pulse of bromodeoxyuridine (BrdU) to quantify DNA synthesis. Cells with multivalent ephrin-B1 remained mitotically active longer than cultures with unclustered ephrin-B1 or no SPIE factors, indicating enhanced proliferation of intermediate neuronal progenitors may enhance the number of DA neurons in fully differentiated cultures (**Fig. 7h**). These results indicate that ephrin effects on dopaminergic differentiation are complex, and the multivalent conjugates will enable future mechanistic investigation of the role of this signaling system in DA neuron generation.

Discussion

This study demonstrates that multivalency greatly enhances the bioactivity of ligands that regulate stem cell behavior, and multivalent conjugates thus have utility for both mechanistic investigation in stem cell and developmental biology *in vitro* and *in vivo*, as well biotechnological applications. Other examples of important signaling systems that regulate stem cell fate include Delta/Jagged, which can activate the Notch receptor in an clustering-dependent manner [8]. Moreover, differential oligomerization of the angiogenic factor angiopoietin 1 modulates the trafficking and subsequent downstream signaling of its endothelial tyrosine kinase receptor Tie2 [50]. Receptor oligomerization also plays apparent roles in SCF and c-kit [9], Flt [11], TGF-β receptor [51], and Sonic hedgehog [15] signal transduction.

Studying the mechanistic role of receptor complex assembly in these and other signaling systems could greatly benefit from nanoscale synthetic ligands that potently activate receptors in a biomimetic fashion. For example, the effects of many receptor-ligand complex properties – including the number of receptor clusters per cell, cluster size, ligand scaffold, inter-receptor

distance within an oligomer, and induced heteroligomerization of different receptors into the same cluster – on biological activity in stem or other cells can now be systematically varied and studied *in vitro* or *in vivo*. Furthermore, nanoscale multivalent conjugates could potentially activate these systems more potently, and thus less expensively. Finally, this platform has biotechnological and biomedical applications, including in cell culture systems, bioactive materials, and drug delivery technologies.

Acknowledgements

We thank Agnieszka Ciesielska (Bankiewicz Lab, UCSF) for help with HPLC analysis of dopamine. We also thank Tandis Vazin for help with designing the ephrin-B1 experiments, Dawn P. Spelke for cloning the EphB4-Dendra2 retroviral vector, Nikhil A. Rode for conducting the SEC-MALS experiment, and Kevin E. Healy and Ravi S. Kane for providing critical feedback on the manuscript. This work was supported by NIH R21 EB007295 and California Institute for Regenerative Medicine grant RT2-02022 and a training grant fellowship from CIRM (T1-00007).

References

1. Jiang W, Kim BY, Rutka JT, Chan WC. (2008) Nanoparticle-mediated cellular response is size-dependent. *Nat Nanotechnol* 3:145-150.
2. Mannix RJ, Kumar S, Cassiola F, Montoya-Zavala M, Feinstein E, Prentiss M, Ingber DE. (2008) Nanomagnetic actuation of receptor-mediated signal transduction. *Nat Nanotechnol* 3:36-40.
3. McMurray RJ, Gadegaard N, Tsimbouri PM, Burgess KV, McNamara LE, Tare R, Murawski K, Kingham E, Oreffo RO, Dalby MJ. (2011) Nanoscale surfaces for the long-term maintenance of mesenchymal stem cell phenotype and multipotency. *Nat Mater* 10:637-644.
4. Mammen M, Choi S.-K. & Whitesides, G.M. (1998) Polyvalent Interactions in Biological Systems: Implications for Design and Use of Multivalent Ligands and Inhibitors. *Angew. Chem. Int. Ed.* 37: 2754-2794.
5. Kiessling LL, Gestwicki JE, Strong LE. (2000) Synthetic multivalent ligands in the exploration of cell-surface interactions. *Curr Opin Chem Biol* 4:696-703.
6. Vance D, Shah M, Joshi A, Kane RS. (2008) Polyvalency: a promising strategy for drug design. *Biotechnol Bioeng* 101:429-434.
7. Pasquale EB. (2005) Eph receptor signalling casts a wide net on cell behaviour. *Nat Rev Mol Cell Biol* 6:462-475.
8. Artavanis-Tsakonas S, Rand MD, Lake RJ. (1999) Notch signaling: cell fate control and signal integration in development. *Science* 284:770-776.
9. Broudy VC, Lin NL, Buhring HJ, Komatsu N, Kavanagh TJ. (1998) Analysis of c-kit receptor dimerization by fluorescence resonance energy transfer. *Blood* 91:898-906.
10. Holler N, Tardivel A, Kovacsovics-Bankowski M, Hertig S, Gaide O, Martinon F, Tinel A, Deperthes D, Calderara S, Schulthess T, Engel J, Schneider P, Tschopp J. (2003) Two adjacent trimeric Fas ligands are required for Fas signaling and formation of a death-inducing signaling complex. *Mol Cell Biol* 23:1428-1440.
11. Barleon B, Totzke F, Herzog C, Blanke S, Kremmer E, Siemeister G, Marme D, Martiny-Baron G. (1997) Mapping of the sites for ligand binding and receptor dimerization at the

extracellular domain of the vascular endothelial growth factor receptor FLT-1. *J Biol Chem* 272:10382-10388.
12. Ko J, Zhang C, Arac D, Boucard AA, Brunger AT, Sudhof TC. (2009) Neuroligin-1 performs neurexin-dependent and neurexin-independent functions in synapse validation. *EMBO J* 28:3244-3255.
13. Barton WA, Liu BP, Tzvetkova D, Jeffrey PD, Fournier AE, Sah D, Cate R, Strittmatter SM, Nikolov DB. (2003) Structure and axon outgrowth inhibitor binding of the Nogo-66 receptor and related proteins. *EMBO J* 22:3291-3302.
14. Filbin MT. (2003) Myelin-associated inhibitors of axonal regeneration in the adult mammalian CNS. *Nat Rev Neurosci* 4:703-713.
15. Vyas N, Goswami D, Manonmani A, Sharma P, Ranganath HA, VijayRaghavan K, Shashidhara LS, Sowdhamini R, Mayor S. (2008) Nanoscale organization of hedgehog is essential for long-range signaling. *Cell* 133:1214-1227.
16. Ye S, Luo Y, Lu W, Jones RB, Linhardt RJ, Capila I, Toida T, Kan M, Pelletier H, McKeehan WL. (2001) Structural basis for interaction of FGF-1, FGF-2, and FGF-7 with different heparan sulfate motifs. *Biochemistry* 40:14429-14439.
17. Haudenschild DR, Hong E, Yik JH, Chromy B, Moergelin M, Snow KD, Acharya C, Takada Y, Di Cesare PE. (2011) Enhanced activity of TGF-beta1 bound to cartilage oligomeric matrix protein. *J Biol Chem* 286:43250-43258.
18. Chang SC, Mulloy B, Magee AI, Couchman JR. (2011) Two distinct sites in sonic Hedgehog combine for heparan sulfate interactions and cell signaling functions. *J Biol Chem* 286:44391-44402.
19. Krilleke D, Ng YS, Shima DT. (2009) The heparin-binding domain confers diverse functions of VEGF-A in development and disease: a structure-function study. *Biochem Soc Trans* 37:1201-1206.
20. Callejo A, Culi J, Guerrero I. (2008) Patched, the receptor of Hedgehog, is a lipoprotein receptor. *Proc Natl Acad Sci U S A* 105:912-917.
21. Davis S, Gale NW, Aldrich TH, Maisonpierre PC, Lhotak V, Pawson T, Goldfarb M, Yancopoulos GD. (1994) Ligands for EPH-related receptor tyrosine kinases that require membrane attachment or clustering for activity. *Science* 266:816-819.
22. Balu DT, Lucki I. (2009) Adult hippocampal neurogenesis: Regulation, functional implications, and contribution to disease pathology. *Neuroscience & Biobehavioral Reviews* 33:232-252.
23. Blurton-Jones M, Kitazawa M, Martinez-Coria H, Castello NA, Müller F-J, Loring JF, Yamasaki TR, Poon WW, Green KN, LaFerla FM. (2009) Neural stem cells improve cognition via BDNF in a transgenic model of Alzheimer disease. *Proceedings of the National Academy of Sciences*.
24. Sahay A, Scobie KN, Hill AS, O'Carroll CM, Kheirbek MA, Burghardt NS, Fenton AA, Dranovsky A, Hen R. (2011) Increasing adult hippocampal neurogenesis is sufficient to improve pattern separation. *Nature* advance online publication.
25. Zhang C-L, Zou Y, He W, Gage FH, Evans RM. (2008) A role for adult TLX-positive neural stem cells in learning and behaviour. *Nature* 451:1004-1007.
26. Zhao C, Teng EM, Summers RG, Jr., Ming G-l, Gage FH. (2006) Distinct Morphological Stages of Dentate Granule Neuron Maturation in the Adult Mouse Hippocampus. *J. Neurosci.* 26:3-11.

27. Ashton RS, Conway A, Pangarkar C, Bergen J, Lim KI, Shah P, Bissell M, Schaffer DV. (in press) Astrocytes regulate adult hippocampal neurogenesis through ephrin-B signaling. *Nat Neurosci*.
28. Vazin T, Becker KG, Chen J, Spivak CE, Lupica CR, Zhang Y, Worden L, Freed WJ. (2009) A novel combination of factors, termed SPIE, which promotes dopaminergic neuron differentiation from human embryonic stem cells. *PLoS One* 4:e6606.
29. Yamanaka S. (2009) Elite and stochastic models for induced pluripotent stem cell generation. *Nature* 460:49-52.
30. Grskovic M, Javaherian A, Strulovici B, Daley GQ. (2011) Induced pluripotent stem cells--opportunities for disease modelling and drug discovery. *Nat Rev Drug Discov* 10:915-929.
31. Wall ST, Saha K, Ashton RS, Kam KR, Schaffer DV, Healy KE. (2008) Multivalency of Sonic hedgehog conjugated to linear polymer chains modulates protein potency. *Bioconjug Chem* 19:806-812.
32. Akinc A, Thomas M, Klibanov AM, Langer R. (2005) Exploring polyethylenimine-mediated DNA transfection and the proton sponge hypothesis. *J Gene Med* 7:657-663.
33. Lai K, Kaspar BK, Gage FH, Schaffer DV. (2003) Sonic hedgehog regulates adult neural progenitor proliferation in vitro and in vivo. *Nat Neurosci* 6:21-27.
34. Song H, Stevens CF, Gage FH. (2002) Astroglia induce neurogenesis from adult neural stem cells. *Nature* 417:39-44.
35. Keung AJ, Asuri P, Kumar S, Schaffer DV. (2012) Soft microenvironments promote the early neurogenic differentiation but not self-renewal of human pluripotent stem cells. *Integr Biol (Camb)*.
36. Lim KI, Klimczak R, Yu JH, Schaffer DV. (2010) Specific insertions of zinc finger domains into Gag-Pol yield engineered retroviral vectors with selective integration properties. *Proc Natl Acad Sci U S A* 107:12475-12480.
37. Kempermann G, Kuhn HG, Gage FH. (1997) More hippocampal neurons in adult mice living in an enriched environment. *Nature* 386:493-495.
38. Peltier J, Conway A, Keung AJ, Schaffer DV. (2011) Akt increases sox2 expression in adult hippocampal neural progenitor cells, but increased sox2 does not promote proliferation. *Stem Cells Dev* 20:1153-1161.
39. Zawadzki RJ, Jones SM, Olivier SS, Zhao M, Bower BA, Izatt JA, Choi S, Laut S, Werner JS. (2005) Adaptive-optics optical coherence tomography for high-resolution and high-speed 3D retinal in vivo imaging. *Opt Express* 13:8532-8546.
40. Tokunaga M, Imamoto N, Sakata-Sogawa K. (2008) Highly inclined thin illumination enables clear single-molecule imaging in cells. *Nat Methods* 5:159-161.
41. Betzig E, Patterson GH, Sougrat R, Lindwasser OW, Olenych S, Bonifacino JS, Davidson MW, Lippincott-Schwartz J, Hess HF. (2006) Imaging intracellular fluorescent proteins at nanometer resolution. *Science* 313:1642-1645.
42. Gurskaya NG, Verkhusha VV, Shcheglov AS, Staroverov DB, Chepurnykh TV, Fradkov AF, Lukyanov S, Lukyanov KA. (2006) Engineering of a monomeric green-to-red photoactivatable fluorescent protein induced by blue light. *Nature Biotechnology* 24:461-465.
43. van de Linde S, Loschberger A, Klein T, Heidbreder M, Wolter S, Heilemann M, Sauer M. (2011) Direct stochastic optical reconstruction microscopy with standard fluorescent probes. *Nat Protoc* 6:991-1009.
44. Peltier J, O'Neill A, Schaffer DV. (2007) PI3K/Akt and CREB regulate adult neural hippocampal progenitor proliferation and differentiation. *Dev Neurobiol* 67:1348-1361.

45. Yan Y, Yang D, Zarnowska ED, Du Z, Werbel B, Valliere C, Pearce RA, Thomson JA, Zhang SC. (2005) Directed differentiation of dopaminergic neuronal subtypes from human embryonic stem cells. *Stem Cells* 23:781-790.
46. Pollock JF, Ashton RS, Rode NA, Schaffer DV, Healy KE. (2012) Molecular characterization of multivalent bioconjugates by size-exclusion chromatography with multiangle laser light scattering. *Bioconjug Chem* 23:1794-1801.
47. Kuwabara T, Hsieh J, Muotri A, Yeo G, Warashina M, Lie DC, Moore L, Nakashima K, Asashima M, Gage FH. (2009) Wnt-mediated activation of NeuroD1 and retro-elements during adult neurogenesis. *Nat Neurosci* 12:1097-1105.
48. Lindvall O. (2012) Dopaminergic neurons for Parkinson's therapy. *Nat Biotechnol* 30:56-58.
49. Politis M, Wu K, Loane C, Quinn NP, Brooks DJ, Rehncrona S, Bjorklund A, Lindvall O, Piccini P. (2010) Serotonergic neurons mediate dyskinesia side effects in Parkinson's patients with neural transplants. *Sci Transl Med* 2:38ra46.
50. Pietila R, Natynki M, Tammela T, Kangas J, Pulkki KH, Limaye N, Vikkula M, Koh GY, Saharinen P, Alitalo K, Eklund L. (2012) Ligand oligomerization state controls Tie2 receptor trafficking and Angiopoietin-2 ligand-specific responses. *J Cell Sci*.
51. Dore JJ, Jr., Edens M, Garamszegi N, Leof EB. (1998) Heteromeric and homomeric transforming growth factor-beta receptors show distinct signaling and endocytic responses in epithelial cells. *J Biol Chem* 273:31770-31777.

CHAPTER 4

BIOMATERIAL MICROENVIRONMENTS TO SUPPORT THE GENERATION OF NEW NEURONS IN THE ADULT BRAIN

Abstract

Neural stem cells (NSC) in two regions of the adult mammalian brain – the subventricular zone (SVZ) and hippocampus – continuously generate new neurons, enabled by a complex repertoire of factors that precisely regulate the activation, proliferation, differentiation, and integration of the newborn cells. A growing number of studies also report low level neurogenesis in regions of the adult brain outside these established neurogenic niches – potentially via NSC recruitment or activation of local, quiescent NSCs – under perturbations such as ischemia, cell death, or viral gene delivery of proneural growth factors. We have explored whether implantation of engineered biomaterials can stimulate neurogenesis in normally quiescent regions of the brain. Specifically, recombinant versions of factors found within the NSC microenvironment, Sonic hedgehog and ephrin-B2, were conjugated to long polymers, thereby creating highly bioactive, multivalent ligands that begin to emulate components of the neurogenic niche. In this engineered biomaterial microenvironment, new neuron formation was observed in normally non-neurogenic regions of the brain, the striatum and cortex, and combining these multivalent biomaterials with SDF-1α increased neuronal commitment of newly divided cells 7- to 8-fold in these regions. Additionally, the decreased hippocampal neurogenesis of geriatric rodents was partially rescued toward levels of young animals. We thus demonstrate for the first time *de novo* neurogenesis in both the cortex and striatum of adult rodents stimulated solely by delivery of synthetic biomaterial forms of proteins naturally found within adult neurogenic niches, offering the potential to replace neurons lost in neurodegenerative disease or injury as an alternative to cell implantation.

Introduction

Two specific regions of the adult mammalian central nervous system (CNS) harbor active neural stem cells: the subgranular zone (SGZ) of the hippocampal dentate gyrus, a region that plays central roles in several forms of learning and memory [1], and the subventricular zone (SVZ) of the lateral ventricles, which gives rise to neurons that migrate to the olfactory bulb [2]. These neurogenic regions harbor unique cellular and biochemical microenvironments that both enable and control their neurogenic potential. For example, bone morphogenic protein [3] and Notch [4,5] signaling modulate the balance between quiescent and proliferative NSCs in the hippocampus, and Sonic hedgehog (Shh) [6], fibroblast growth factor-2 [7], vascular endothelial growth factor [8], and Wnt7a [9] regulate NSC proliferation. Additionally, ephrin-B2 [10], Wnt3a [11], and gamma aminobutyric acid (GABA) inputs from local neuronal circuitry [12] regulate neuronal differentiation. Furthermore, neurogenesis decreases with age [13], likely due to imbalances in biochemical factors and an accompanying decline in NSC function [14,15,16].

In addition to broadly accepted evidence for two neurogenic regions in adult mammals, some reports suggest neurogenesis in other CNS regions under various conditions. For example,

introducing a reactive chromophore to induce apoptosis of corticothalamic neurons led to low levels of apparent new neuron formation in associated regions [17]. Focal cerebral ischemia has also been reported to induce aberrant neurogenesis in several locations – including the cortex [18,19]; striatum [20]; and SVZ [21] – and the latter reportedly generate neuroblasts that migrate and subsequently differentiate into neurons appropriate to the infracted regions [21]. Furthermore, chemical ablation of dopaminergic neurons in the adult mammalian substantia nigra [22] and midbrain [23] is reportedly sufficient to induce modest proliferation and subsequent dopaminergic differentiation of endogenous quiescent neural progenitor cells, a small number of which survive beyond two weeks. Lastly, neurodegeneration in the hypothalamus due to mitochondrial dysfunction induced cell proliferation and generation of regionally-specific neuronal subtypes as a potential compensatory mechanism [24].

While these studies raise the promising possibility that endogenous NSCs could be activated or recruited for potential cell replacement therapies, such as in the striatum for Parkinson's or Huntington's diseases or cortex for Alzheimer's disease, considerable tissue damage or inflammation is often required. Furthermore, while these studies establish that *de novo* neurogenesis can occur, the levels, fates, and locations of the new neurons could be further controlled and enhanced. To address these needs, recent studies have used gene delivery of proneurogenic factors into the rodent neocortex [25] and neostriatum [26], with and without inducing ischemia, respectively. The resulting sustained overexpression of the factors led to moderate increases in *de novo* neurogenesis.

Biomaterials functionalized with ligands present in natural neurogenic microenvironments may offer a transient, biomedically advantageous microenvironment to stimulate neuronal regeneration within damaged or diseased regions of the brain. The finite half-life of wild type proteins may limit the efficacy of protein delivery for stimulating the generation and maturation of new neurons. However, we have recently engineered multivalent ligands, composed of proteins conjugated to a linear biopolymer, that cluster their cognate receptors and thereby substantially elevate signaling relative to corresponding, monovalent ligands [27,28]. This raises the possibility that ligands found within the stem cell niche could be integrated into highly bioactive materials and thereby begin to create a synthetic stem cell microenvironment for controlling cell fate decisions. For example, one recent study used a functionalized material coating on the surface of bone implants to promote osseointegration, potentially by manipulating osteoprecursors *in situ* [28]. Additionally, we have recently established that biomaterials presenting individual bioactive factors have the ability to significantly increase the neuronal differentiation of NSCs in the adult hippocampus (Conway *et al*., manuscript submitted). However, these two studies utilized single factors, and no studies have explored the potential for bioactive microenvironments to present combinations of signals to stimulate endogenous stem or progenitor cells and induce their ectopic differentiation, particularly in delicate tissues such as the central nervous system.

Accordingly, we have engineered soluble, multivalent biomaterial conjugates harboring factors present within the naturally neurogenic hippocampus, specifically ephrin-B2 [10] and Shh [6], and these materials were injected into the interstitial space of both the striatum and cortex of the adult brain to create a synthetic, engineered stem cell microenvironment that stimulates the proliferation and neuronal differentiation of normally quiescent progenitor cells. Additionally, by including the chemokine stromal cell-derived factor-1α (SDF-1α), a more than four-fold increase in the basal level of neurogenesis compared to controls was observed, suggesting potential recruitment of endogenous NSCs from the neurogenic SGZ and SVZ to the

normally non-neurogenic regions. Synthetic stem cell microenvironments therefore represent a new strategy to induce *de novo* neurogenesis and thereby potentially replace neurons lost to neurodegenerative disease or traumatic brain injury.

Materials and Methods

Recombinant Protein Production, Purification, and Multivalent Biomaterial Conjugation

Murine ephrin-B2 ectodomain sequence (amino acids 31-227) was amplified from the plasmid pcDNA3.1-ephrin-B2-hFc, and rat Shh N-terminal signaling domain (amino acids 25-198) was produced as previously described [6]. A C-terminal hexahistidine tag and cysteine were added during PCR, followed by insertion into the bacterial expression plasmid pBAD. Protein was expressed and purified as previously described [27]. Protein purity was assessed by confirmation of a single band following SDS-PAGE. Purified ephrin-B2 was conjugated to 800 kDa hyaluronic acid (HA) (Genzyme) through a two-step reaction using carbodiimide chemistry at the HA carboxylate group and a maleimide reaction at the protein C-terminal cysteine [27]. In the first step, 3,3´-*N*-(ε-Maleimidocaproic acid) hydrazide (EMCH, Pierce, 1.2 mg/mL), *N*-hydroxysulfosuccinimide (Sulfo-NHS, Pierce, 2.8 mg/mL), and 1-ethyl-3-(3-dimethylaminopropyl) carbodiimide hydrochloride (EDC, Pierce, 10 mg/mL) were added to a 3 mg/mL solution of HA in 0.1 M 2-(*N*-morpholino)ethanesulfonic acid (MES) (Sigma) buffer pH 6.5 and allowed to react at 4 °C for 4 hours. The solution was then dialyzed into pH 7.0 PBS containing 10% glycerol and 2 mM EDTA. Recombinant ephrin-B2 was reduced using 200-fold molar excess Tris(2-carboxyethyl)phosphine hydrochloride (TCEP) (Pierce) at 4 °C for 5 minutes. Activated HA-EMCH was then added at desired molar ratios with reduced ephrin-B2 and allowed to react at 4 °C overnight. To remove unreacted ephrin from ephrin-conjugated HA, the solution was then dialyzed with 100 kDa MWCO tubing (Spectrum Labs) in pH 7.0 PBS with 2 mM EDTA. Purified ephrin and HA-conjugated ephrin protein concentrations were measured using a BCA assay, and valencies were verified using SEC-MALS as previously described [27].

Antibody-Clustered Ephrin-B Formation

To create clustered ephrin-B2 complexes (Fc-ephrin-B2), recombinant mouse ephrin-B2/Fc chimera (R&D Systems) was incubated with goat anti-human IgG, Fc-fragment specific, (Jackson ImmunoResearch) antibody at a 1:9 ratio (w/w), which led to maximal activity of the resulting clusters (data not shown). After 90 min at 4 °C, complexes were immediately used.

Stereotactic Injections

All animal protocols were approved by the University of California, Berkeley Animal Care and Use Committee and conducted in accordance with National Institutes of Health guidelines. 8-week-old adult female and 19-month-old adult male Fisher 344 rats were intraperitoneally injected with halogenated thymidine analog (163 µmol/kg) for three days prior to surgery. On the fourth day, each animal was anesthetized with a ketamine/xylazine cocktail and underwent bilateral intrahippocampal stereotactic injections with 3 µL of either HA (4.7 nM) or multivalent protein (4.7 nM HA, 282 nM protein). The hippocampal injection coordinates with respect to bregma were 3.5 mm anteriorposterior (AP), -3.3 mm dorsoventral (DV) (from dura), and ±1.8 mm mediolateral (ML). Striatal coordinates used were 0.3 mm AP, -5.0 mm DV,

and ±3.5 mm ML. Cortical coordinates used were 0.3 mm AP, -0.7 mm DV, and ±3.5 mm ML. For the study involving SDF-1α, striatal coordinates were -1.0 mm AP, -4.0 mm DV, and ±3.0 mm ML, and cortical coordinates were -1.0 mm AP, -1.0 mm DV, and ±3.0 mm ML. To assess neuronal maturation, two subsequent stereotactic injections were performed 30 days apart. For cortical and striatal injections, an Alexa 488-dextran conjugate (Molecular Probes, cat. #D-22910) was included in the injection solution (20 mg/mL final concentration in PBS) to label the injection region for quantification purposes. Before injections, animals received a buprenorphine/meloxicam cocktail in saline as an analgesic and to avoid dehydration. Directly after the surgery a 1 mL intraperitoneal injection of yohimbine in saline was administered to counteract the effects of xylazine. Another injection of buprenorphine/meloxicam in saline was provided 6-8 hours and 24 hours post-surgery as additional analgesic. On the sixth day after surgery, the rats were perfused with 4% PFA, and brains were extracted, stored in fixative for 24 hours, and allowed to settle in a 30% sucrose solution prior to processing for immunostaining.

Immunostaining

Coronal brain sections (40 μm) were processed, stored, and stained as previously described [29]. Primary antibodies used were mouse antibody to BrdU (1:100, Roche, cat. #11170376001), mouse antibody to NeuN (1:100, Millipore, cat. #MAB377), mouse antibody to nestin (1:1,000, BD Pharmingen, cat. #556309), guinea pig antibody to doublecortin (1:1,000, Millipore, cat. #AB2253), goat antibody to ephrin-B2 (1:10, R&D Systems, cat. #AF496), rabbit antibody to Sox2 (1:250, Millipore, cat. #AB5603), goat antibody to EphB4 (1:50, Santa Cruz, cat. #sc-7285), rat antibody to CldU (1:500, Novus Biologicals, cat. #NB500-169), and mouse antibody to IdU (1:25, Becton Dickinson, cat. #347580). Appropriate Cy3-, Cy5- or Alexa Fluor 488–conjugated secondary antibodies (1:125, Jackson Immunoresearch; affinity-purified whole IgG with minimal cross-reactivity, 1:250, Life Technologies, Alexa Fluor-conjugated secondary antibodies) were used. For sections stained with rat antibody to CldU, biotin-conjugated antibody to rat IgG (1:250, Jackson Immunoresearch, cat. #712-065-150) was used as the secondary, which was then washed and incubated with Cy3-conjugated streptavidin (1:1,000, Jackson Immunoresearch, cat. #016-160-084) for 2 h to amplify the signal. DAPI (20 μg/mL, Invitrogen) was used as a nuclear counterstain. Sections were then mounted on glass slides, and either stereological analysis (Stereo Investigator, MBF Biosciences) or confocal microscopy (Zeiss LSM 710) was performed. In short, using an optical fractionator method, marker+ cells were counted in a Systematic Randomly Sampled (SRS) set of unbiased virtual volumes inside the subgranular zone and granular cell layer of both the left and right sides of the hippocampus. For striatal and cortical sections, marker+ cells were quantified inside bulk volumes positive for dextran-488. An estimate of the total number of marker+ cells in brain regions was then generated.

Statistical Analysis

Statistical significance of the results was determined using an ANOVA and multiple means comparison function (Tukey-Kramer method) in MATLAB with an alpha level of 0.05 unless otherwise noted. All error bars are reported in s.d. from the mean, with $n = 3$ unless otherwise noted.

Results

EphB4$^+$ Cells that also Express Neural Progenitor Markers Exist throughout the Brain

We recently discovered that the transmembrane protein ligand ephrin-B2 is a strong regulator of adult hippocampal neurogenesis. In particular, ephrin-B2 expressed from hippocampal astrocytes activates the EphB4 receptor on neighboring neural stem cells (NSCs) to induce neuronal fate commitment in the hippocampal subgranular zone (SGZ) [10]. To examine the broader expression of ephrin-B2 and its receptor EphB4, we performed immunostaining of the hippocampus (**Fig. 1a**) and various non-neurogenic regions of the brain, including the striatum (**Fig. 1b**) and cortex (**Fig. 1c**). Interestingly, cells positive for the receptor EphB4 were present throughout the brain, a subset of which co-expressed the NSC marker Sox2 in the SGZ, cortex, and striatum. The neurogenic ligand ephrin-B2, however, was markedly absent or spatially separate from EphB4$^+$ cells in the normally non-neurogenic striatum and cortex, respectively. Due to the juxtacrine nature of Eph-ephrin interactions, the absence of ligand-expressing cells in these regions indicates a lack of EphB4 signaling, which could potentially contribute to the absence of neurogenesis under normal physiological conditions. Furthermore, previous studies have reported a notable absence of Shh expression in both the striatum and the upper layers of the cortex, whereas its receptor Patched and associated protein Smoothened were often present [30].

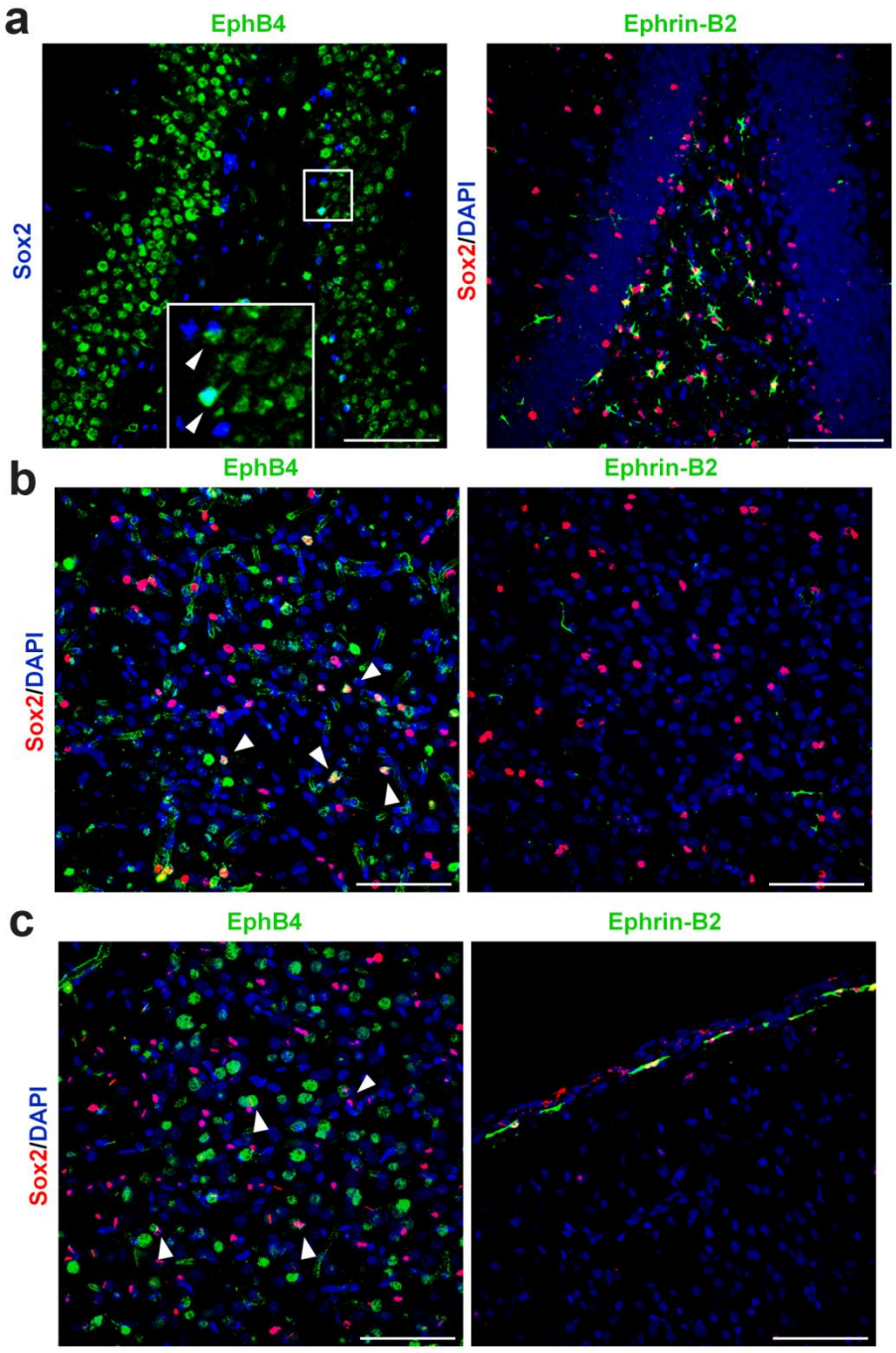

Figure 1: Expression of EphB4 and ephrin-B2 in the adult brain. (a) Representative image of the adult hippocampus containing EphB4^{+} cells, a subset of which are positive for the neural stem cell (NSC) marker Sox2 (high magnification inset), in close proximity to its neurogenic ligand ephrin-B2 (right panel). **(b,c)** Representative image of the adult striatum (b) and cortex (c), containing EphB4^{+} cells expressing the NSC marker Sox2 but devoid of the neurogenic ephrin-B2 signal. Scale bars represent 100 µm. Arrowheads point to relevant cells.

Highly Multivalent Ephrin-B2 Enhances Hippocampal Neurogenesis and Induces *De Novo* Striatal and Cortical Neurogenesis

Ectopic activation of Eph/ephrin signaling – which naturally requires the assembly or clustering of receptor complexes [31] – currently involves the addition antibody-clustered ephrin ectodomains, a method that requires high protein concentrations and involves poorly controlled clustering of Eph receptors. We have recently shown that creating multivalent biomaterials, composed of multiple ligands conjugated to a linear polymer, can dramatically increase the bioactivity of a given protein [27] (Conway *et al*., manuscript submitted). Combining several such multivalent ligands along with soluble chemokines may begin to reconstruct the bioactive NSC niche (**Fig. 2a**). Following 3 days of bromodeoxyuridine injection to mark mitotic cells, we injected a multivalent form of ephrin-B2 to determine the ability of exogenous ephrin-B2 administration to enhance neurogenesis in the hippocampus after 5 days (**Fig. 2b**). Antibody-clustered ephrin-B2 (Fc-ephrin-B2) administration significantly increased the fraction of mitotically labeled cells that acquired markers indicative of neuronal fate commitment (60.1 ± 2.14%) compared to hyaluronic acid (HA) controls (49.9 ± 3.61%) ($P < 0.05$), which in general were similar in counts to uninjected brains (Conway *et al*., manuscript submitted). Furthermore, consistent with our prior results (Conway *et al*., manuscript submitted), highly multivalent ephrin-B2 (1:22 HA:Ephrin-B2) substantially enhanced the extent of neuronal differentiation in this region, at a three-fold higher potency than Fc-ephrin-B2 (83.9 ± 4.92%) (**Fig. 2c**).

Since exogenous administration of highly multivalent ephrin-B2 was capable of enhancing neurogenesis in the naturally neurogenic hippocampus, we investigated whether this bioactive ligand could induce *de novo* neurogenesis in quiescent regions of the brain that harbor cells coexpressing its receptor EphB4 and the NSC marker Sox2. Following the same experimental paradigm (**Fig. 2b**), and additionally injecting fluorescently labeled dextran (Dextran-488) to mark the injection site, we found that multivalent ephrin-B2 induced a 6-fold increase in the fraction of newly divided cells expressing the early neuronal marker DCX in the adult rat striatum ($P < 0.01$) (**Fig. 2d,e**). Interestingly, similar results were seen in the cortex, with highly multivalent ephrin-B2 inducing an almost 3-fold increase in early markers of neurogenesis compared to the antibody-clustered form ($P < 0.05$) (**Fig. 2f,g**). These data represent the first example of *de novo* neurogenesis in the adult rodent brain resulting from solely recombinant protein or biomaterial administration under normal physiological conditions.

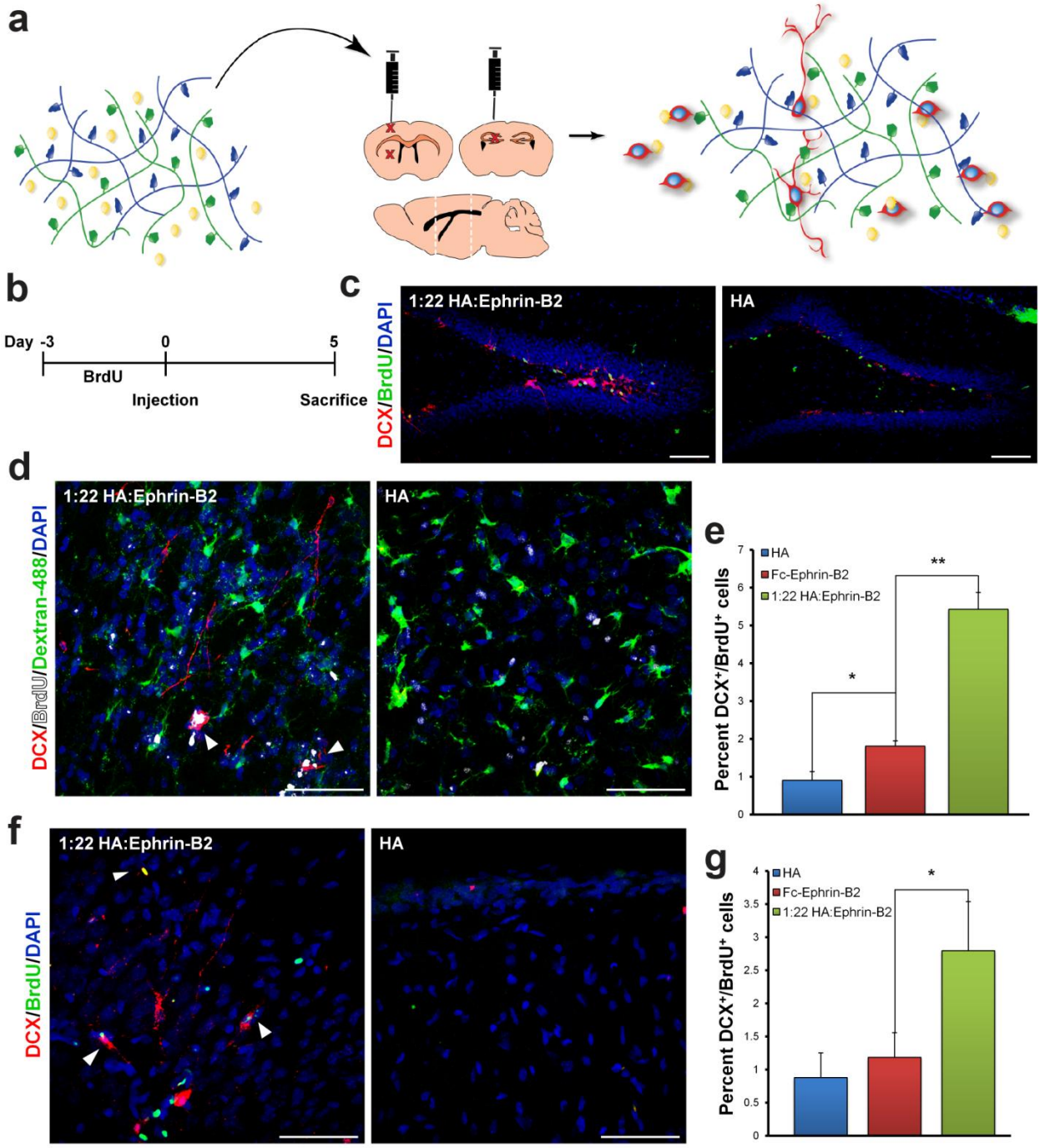

Figure 2: Highly multivalent ephrin-B2 enhances hippocampal neurogenesis and induces *de novo* striatal and cortical neurogenesis. (a) Schematic of combinatorial multivalent biomaterial (blue and green) and soluble chemokine (yellow) injection into the brain to attract neural stem cells (red) and subsequently differentiate them into neurons. **(b)** Schematic of experimental timeline. **(c)** Representative image of increased hippocampal neurogenesis resulting from highly multivalent ephrin-B2 administration versus HA control. **(d)** Representative image of *de novo* striatal neurogenesis and HA control. The cell marker dextran-488 labels the site of stereotactic injection. **(e)** Quantification of fraction of newly divided cells expressing the early neuronal marker DCX after striatal stereotactic injection. **(f)** Representative image of *de novo* cortical neurogenesis and HA control. **(g)** Quantification of fraction of newly divided cells expressing the early neuronal marker DCX after cortical injection. All scale bars represent 100 μm. Arrowheads point to relevant cells. * $P < 0.05$ and ** $P < 0.01$. Error bars represent ± s.d.

Dual Administration of Multivalent Conjugates Enhances Short- and Long-Term Hippocampal Neurogenesis and *De Novo* Striatal and Cortical Neurogenesis in Young Rats

Adult neurogenic niches present factors that regulate both proliferation and differentiation; therefore, to take an additional step towards an ectopic neurogenic environment, Sonic hedgehog (Shh) was utilized in addition to bioactive ephrin-B2. To track both long- and short-term neurogenesis the same animal, two separate systemic administrations of two distinct thymidine analogs – chlorodeoxyuridine (CldU) and iododeoxyuridine (IdU) – were performed 33 days apart, each followed by intracranial stereotactic injections of neurogenic factors (**Fig. 3a**). To test short-term bioactivity in the neurogenic SGZ, CldU was administered, and multivalent biomaterial forms of both ephrin-B2 (1:22 HA:Ephrin-B2) and Shh (1:16 HA:Shh) were injected into the hippocampus either separately or combined (Ephrin-B2/Shh) (**Fig. 3b**). Subsequently, the overall number of newly-divided $CldU^+$ cells (**Fig. 3c**) and the fraction of new neurons (**Fig. 3d**) were quantified. While multivalent Shh administration either singly or in combination with multivalent ephrin-B2 did not statistically increase the number of newly divided cells 5 days after injection, groups containing highly multivalent ephrin-B2 showed significantly higher levels of hippocampal neurogenesis compared to controls ($P < 0.05$). The differential specificity of the antibody used to detect IdU, as well as the difference in propensity of IdU to integrate into the host DNA of dividing NSCs [32] may explain the difference in the fraction of colabeled DCX^+ cells compared to previous experiments using BrdU.

We next assessed whether Shh and ephrin-B2 administration to a non-neurogenic region could modulate short-term proliferation or differentiation. Furthermore, several studies have used chemokines to attract stem cells surrounding an implanted material to promote tissue integration – primarily in the bone [33,34], muscle [35], and cartilage [36,37] – and stromal cell-derived factor-1α (SDF-1α) has been reported to modulate NSC migration *in vivo* [38,39]. We therefore also included this molecule as a soluble factor to potentially recruit nearby, active NSCs from the subventricular zone (SVZ) and thereby take steps towards a more complete synthetic stem cell microenvironment. In this case, highly multivalent Shh in conjunction with ephrin-B2 showed a significant proliferative effect compared to controls ($P < 0.05$) (**Fig. 3e,f**). Furthermore, the administration of the chemokine SDF-1α together with ephrin-B2 and Shh biomaterials (Ephrin-B2/Shh/SDF-1) induced a 7-fold increase in the basal level of neurogenesis in the region compared to vehicle control (**Fig. 3g**), suggesting that a combinatorial effect of *de novo* neurogenesis and possible recruitment of active NSCs followed by signaling from neurogenic factors potentially occurred. The combination of ephrin-B2 and Shh was also administered into the cortex (**Fig. 3h**) and yielded a significant increase in the number of newly-divided cells (**Fig. 3i**) and a nearly 8-fold increase fraction of neurons formed over a 5 day period post-intracranial injection relative to the vehicle control ($P < 0.05$) (**Fig. 3j**).

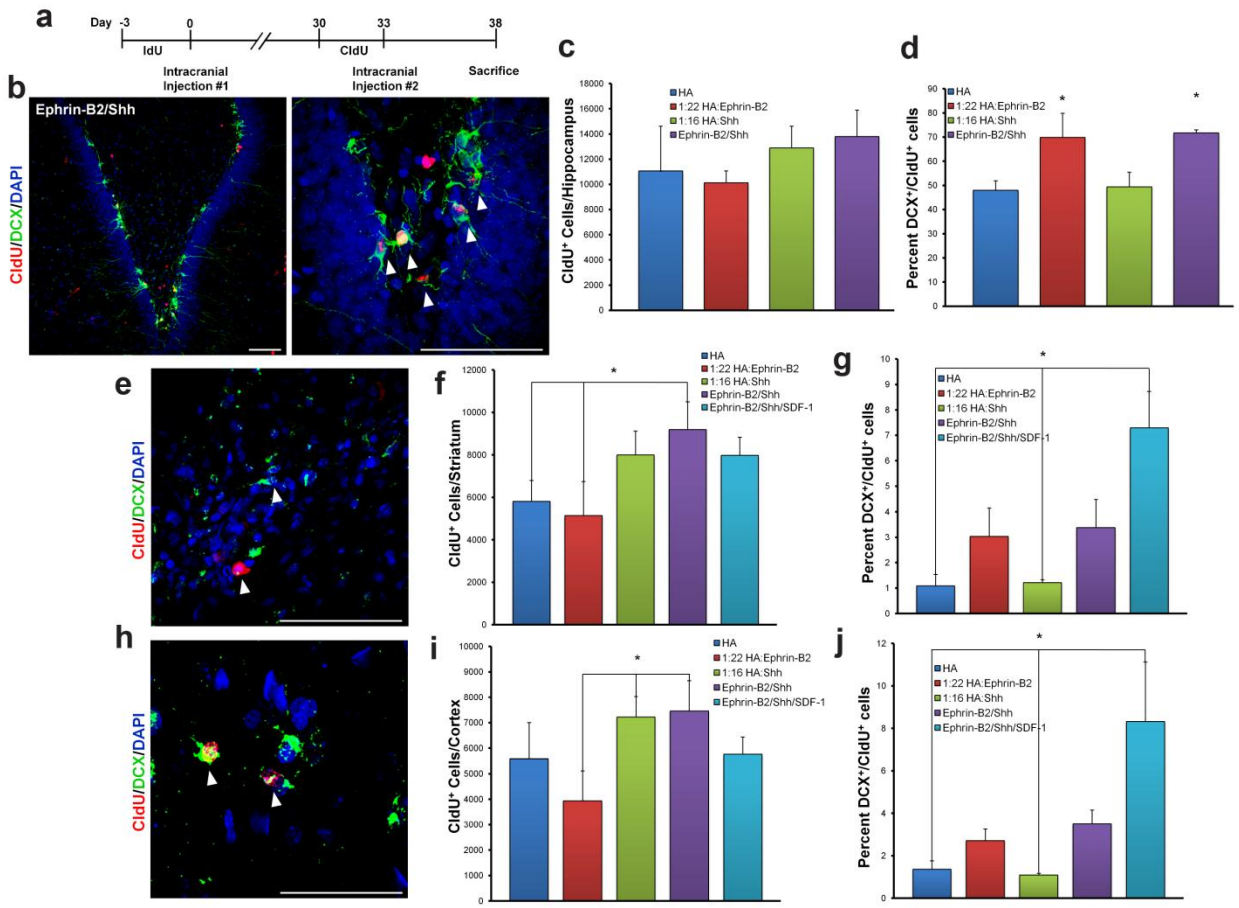

Figure 3: Dual administration of ephrin-B2 and Shh multivalent conjugates enhances short-term hippocampal neurogenesis and *de novo* striatal and cortical neurogenesis. (a) Schematic of experimental timeline. **(b)** Representative image of increased hippocampal neurogenesis resulting from co-administration of multivalent ephrin-B2 and Shh (Ephrin-B2/Shh). **(c)** Quantification of total number of newly divided cells x days after hippocampal stereotactic injection. **(d)** Quantification of fraction of newly divided cells expressing the early neuronal marker DCX 5 days after hippocampal stereotactic injection. **(e)** Representative image of *de novo* striatal neurogenesis. **(f)** Quantification of total number of newly divided cells after striatal stereotactic injection. **(g)** Fractions of newly divided cells expressing the early neuronal marker DCX after striatal stereotactic injection. **(h)** Representative image of *de novo* cortical neurogenesis. **(i)** Quantification of total number of newly divided cells after stereotactic cortical injection. **(j)** Fractions of newly divided cells expressing the early neuronal marker DCX after stereotactic cortical injection. All scale bars represent 100 μm. Arrowheads point to relevant cells. * $P < 0.05$. Error bars represent ± s.d.

The introduction of factors from an active neurogenic stem cell niche thus induced early stages of neurogenesis in normally quiescent regions of the brain, raising the question of whether these newborn neurons could undergo long-term survival. Therefore, the fate of cells that had divided and were therefore labeled by IdU between 38 and 41 days previously, and were exposed to neurogenic factors 38 previously, was analyzed. In the hippocampus (**Fig. 4a**), highly multivalent Shh significantly increased the number of IdU^+ cells ($P < 0.05$) (**Fig. 4b**). Furthermore, exposure to highly multivalent ephrin-B2 increased the fraction of such IdU^+ cells expressing the mature neuronal marker NeuN 38 days later (**Fig. 4c**).

Within the ordinarily non-neurogenic striatum (**Fig. 4d**), Shh did not increase the number of IdU-labeled cells observed after 38 days (**Fig. 4e**); however, the fraction of IdU+ cells that

differentiated into mature neurons was over 2-fold greater with ephrin-B2/Shh and SDF-1α administration ($P < 0.05$) (**Fig. 4f**). A similar trend was observed in the cortex (**Fig. 4g,h,i**), suggesting that a significant fraction of new neurons born in normally quiescent regions (~7-8% of dividing cells) survived for long periods of time (~2.5% of dividing cells) post-treatment with the addition of SDF-1α.

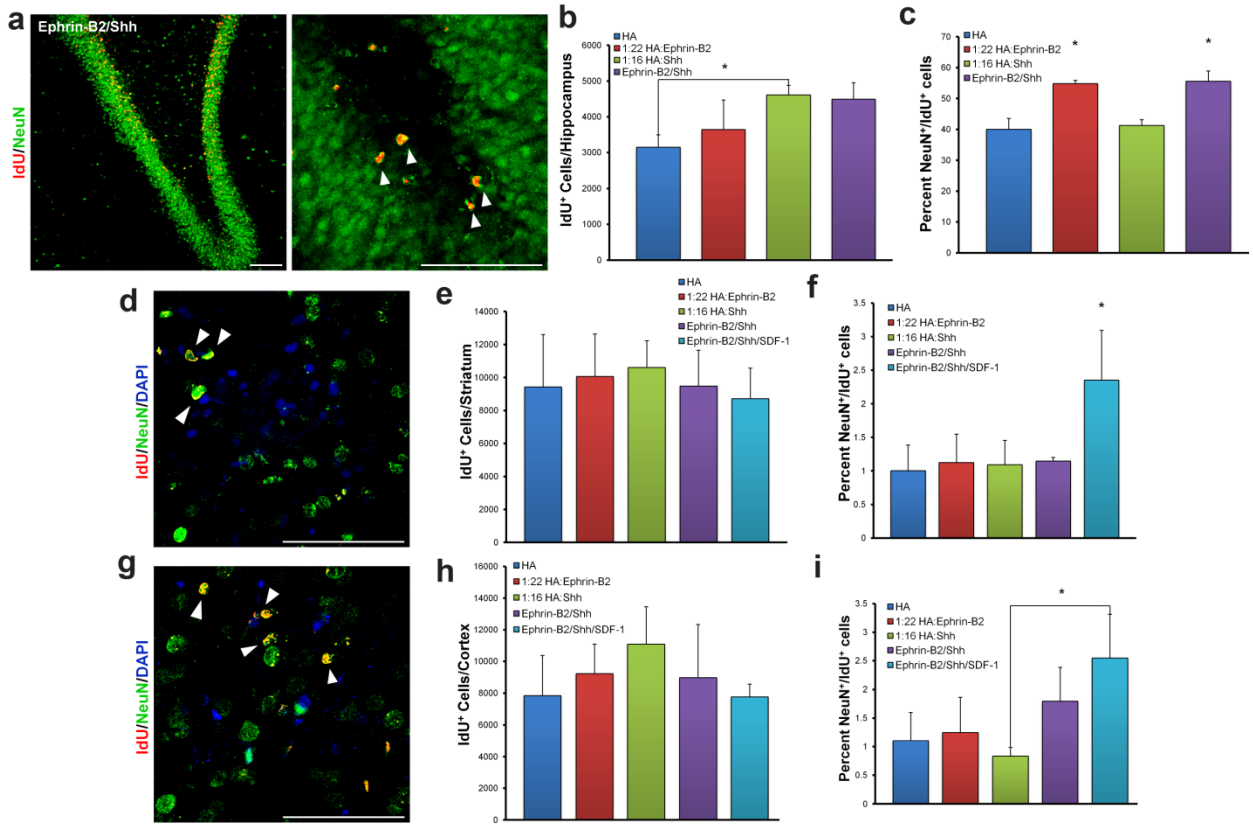

Figure 4: Dual administration of multivalent conjugates enhances long-term hippocampal neurogenesis and *de novo* striatal and cortical neurogenesis. (a) Representative image of increased hippocampal neurogenesis resulting from dual multivalent ephrin-B2 and Shh administration (Ephrin-B2/Shh). **(b)** Quantification of total number of newly divided cells after hippocampal stereotactic injection. **(c)** Fractions of newly divided cells expressing the mature neuronal marker NeuN 38 days after intracranial injection of biomaterials. **(d)** Representative image of *de novo* striatal neurogenesis. **(e)** Quantification of total number of newly divided cells after striatal stereotactic injection. **(f)** Fractions of newly divided cells expressing the mature neuronal marker NeuN after striatal injection. **(g)** Representative image of *de novo* cortical neurogenesis. **(h)** Quantification of total number of newly divided cells after cortical stereotactic injection. **(i)** Fractions of newly divided cells expressing the mature neuronal marker NeuN after cortical stereotactic injection. All scale bars represent 100 μm. Arrowheads point to relevant cells. * $P < 0.05$. Error bars represent ± s.d.

Multivalent Conjugates Partially Rescue Short-Term Hippocampal Neurogenesis in Geriatric Rats

Lastly, it has been well-documented [13,14,16] that there is a substantial decline in adult hippocampal neurogenesis with organismal aging; therefore, we explored whether administration of highly bioactive, synthetic forms of factors naturally present within the young neurogenic stem cell niche could partially restore this deficit. Initially, we confirmed that the overall number of immature neurons appeared to be dramatically lower in old animals (**Fig. 5a**). Both young

female and old male rats were kept unexposed to enriched environments as well as free of any spatial training to assure levels of neurogenesis were comparable between sexes [40]. Furthermore, compared to young animals (**Fig. 5b**), the total number of surviving newly-divided cells over both short and long timepoints was less in old brains (**Fig. 5c**). Next, using a similar experimental timeline as our previous studies (**Fig. 5d**), we injected highly multivalent Shh and ephrin-B2 separately or in combination. After 38 days post-injection, the combination showed no significant change ($P < 0.402$) in the number of newly divided cells or fraction of mature neurons remaining compared to controls (**Fig. 5e,f,g**). However, the combination of bioactive materials (**Fig. 5h**) was found to significantly increase the number of newly divided cells compared to controls ($P < 0.075$) (**Fig. 5i**), while highly multivalent ephrin-B2 was capable of increasing the fraction of labeled cells that underwent neuronal differentiation within 5 days (**Fig. 5j**) to levels comparable to that of young animals (Conway *et al*., manuscript submitted). Additional molecular engineering of the bioactive material, such as designing strategies for controlled release or chemical stabilization of the polymer backbone, may promote sustained signaling that may be able to fully rescue the level of neurogenesis in elderly individuals to that of young ones.

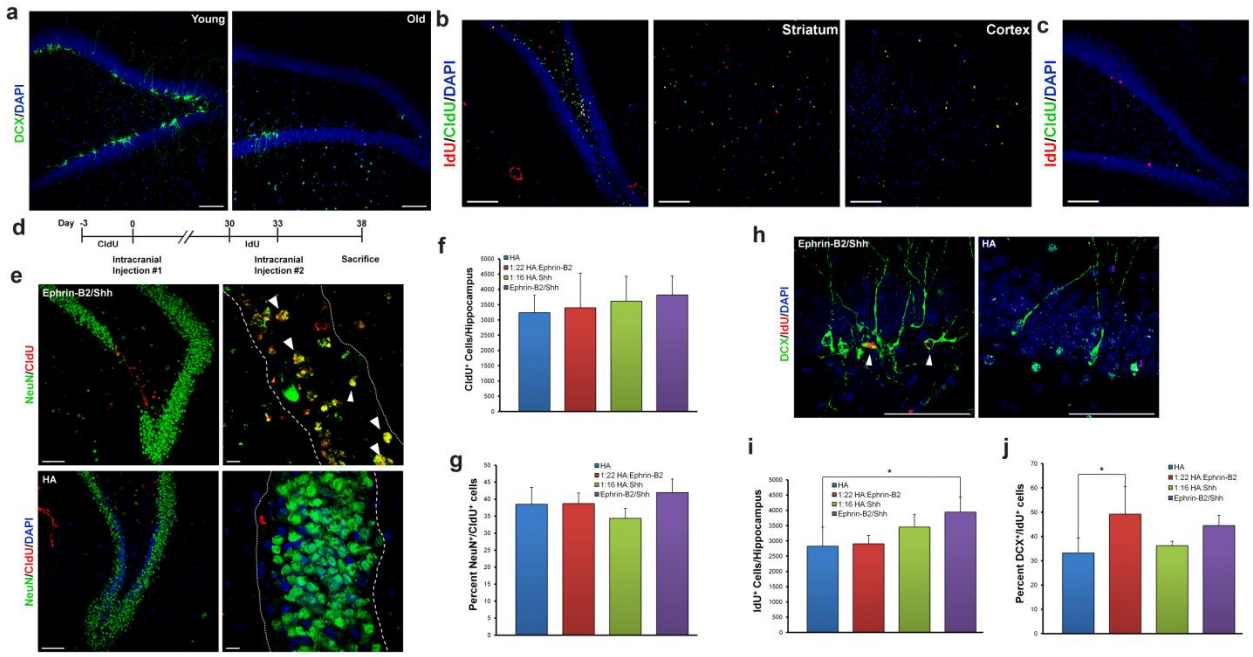

Figure 5: Multivalent conjugates partially rescue short-term hippocampal neurogenesis in geriatric rats. (a) Representative images of newly formed neurons in young versus old hippocampi. **(b)** Representative images of newly divided cells in the hippocampus, striatum, and cortex of a young rat 5 days (green) and 38 days (red) after intraperitoneal injection of distinct thymidine analogs. **(c)** Representative image of newly divided cells in the hippocampus of an old rat 5 days (red) and 38 days (green) after intraperitoneal injection of distinct thymidine analogs. **(d)** Schematic of experimental timeline. **(e)** Representative image of hippocampus after dual multivalent ephrin-B2 and Shh (Ephrin-B2/Shh) administration versus HA control. **(f)** Quantification of total number of newly divided cells 38 days after hippocampal injection of biomaterials. **(g)** Quantification of fraction of newly divided cells expressing the mature neuronal marker NeuN 38 days after hippocampal injection of biomaterials. **(h)** Representative image of increased hippocampal neurogenesis resulting from dual multivalent ephrin-B2 and Shh administration versus HA control. **(i)** Quantification of total number of newly divided cells 5 days after hippocampal injection. **(j)** Fractions of newly divided cells expressing the early neuronal marker DCX 5 days after hippocampal injection. All scale bars represent 100 μm. Arrowheads point to relevant cells. * $P < 0.08$. Error bars represent ± s.d.

Discussion

We have explored the concept of whether biomaterials can be engineered to create an ectopic stem cell microenvironment, and these results demonstrate for the first time *de novo* neurogenesis in the adult brain under physiologically normal conditions using only recombinant proteins, as components of highly bioactive materials. In addition, this work explored three signaling molecules found within the neurogenic stem cell niche – ephrin-B2, Shh, and SDF-1α – and the platform can be further engineered to modulate additional factors such as the Notch signaling pathway [5], Noggin and BMP receptors [3], Wnt3a [11], and the neurotransmitter GABA [41]. Interestingly, the cellular source in the adult brain of the factors used in this study varied from astrocytes within the hilus [10], neurons of the ventral forebrain which project axons into the dentate gyrus (DG) [42], to interneurons and endothelial cells within the DG [43]. Receptors for all these factors, however, are expressed by neural stem and progenitor cells of the SGZ as well as immature and mature neurons of the GCL [6,10,43]. A combinatorial approach to deliver these factors as well as additional factors from the neurogenic stem cell niche into damaged or degenerated regions of the brain may further override endogenous, non-neurogenic microenvironments to activate quiescent NSCs, or recruit nearby NSCs, and form new neurons. The marker EphB4 could also potentially serve as a marker to partially identify endogenous stem and progenitor cells. Furthermore, despite NSCs having been successfully cultured from non-neurogenic regions of the brain, it is still unclear whether these cells exist as quiescent endogenous progenitors or are reprogrammed due to cell culture conditions that often include serum. This work provides evidence supporting the existence of quiescent progenitors since, even in the absence of the NSC migration factor SDF-1α, local administration of pro-neurogenic factors immobilized to high molecular weight soluble biomaterials are capable of inducing a 3- to 5-fold increase in neuronal differentiation in normally inactive regions of the brain compared to controls (**Figs. 2e,g** and **3g,j**). Future work may explore the extent to which these cells arise from local quiescent cells or are recruited from active neurogenic niches.

Several hurdles must be overcome for this approach to represent a viable therapeutic strategy. First, it is not sufficient to produce new neurons, but those cells must also be of the appropriate neuronal subtype and in many cases must appropriately integrate into the existing neuronal circuitry [44]. For example, many of the neurons that would be therapeutically attractive to generate in the adult CNS were originally created long ago during organismal development, and it will thus be challenging to recapitulate the relevant neurodevelopmental niches to generate the appropriate neuronal subtype within adults. A more thorough, basic understanding of stem cell self-renewal and differentiation mechanisms will further enable cell replacement therapy efforts, potentially aided by synthetic microenvironments presenting additional cues. Secondly, a single administration of these bioactive factors may not be sufficient to yield the number of cells necessary to replace the ones lost due to disease, which often consists of progressive neuronal degeneration. Therefore, a long-term biomaterial delivery system, with appropriate release kinetics [45] and tuning of relative cell self-renewal and differentiation, may enable levels of neurogenesis and long-term neuronal survival necessary to repair affected regions. Finally, correct functional integration of newborn neurons must be achieved for neurological recovery. Functionalized biomaterials containing axonal migration factors could possibly be used to promote long-distance axonal projection of newly-differentiated neurons into their appropriate regional target in the brain [46].

In summary, we propose a novel approach for engineering synthetic materials to promote newborn neurons in regions of the brain that are predominantly quiescent. Our findings raise the possibility of utilizing a blend of biomaterials and bioactive factors to manipulate stem cell fate in other tissues. Future work to encompass additional factors from stem cell niches, as well characterize the fate and function of newborn neurons, will take steps closer to potential clinical applications.

Acknowledgements

We thank T. Miyamoto (Keio University) for mouse ephrin-B2 cDNA. This work was supported by NIH R21 EB007295 and California Institute for Regenerative Medicine (CIRM) grant RT2-02022. A.C. was partially supported by training grant fellowships from CIRM (T1-00007).

References

1. Clelland CD, Choi M, Romberg C, Clemenson GD, Jr., Fragniere A, Tyers P, Jessberger S, Saksida LM, Barker RA, Gage FH, Bussey TJ. (2009) A functional role for adult hippocampal neurogenesis in spatial pattern separation. *Science* 325:210-213.
2. Lois C, Alvarez-Buylla A. (1994) Long-distance neuronal migration in the adult mammalian brain. *Science* 264:1145-1148.
3. Mira H, Andreu Z, Suh H, Lie DC, Jessberger S, Consiglio A, San Emeterio J, Hortiguela R, Marques-Torrejon MA, Nakashima K, Colak D, Gotz M, Farinas I, Gage FH. (2010) Signaling through BMPR-IA regulates quiescence and long-term activity of neural stem cells in the adult hippocampus. *Cell Stem Cell* 7:78-89.
4. Ehm O, Goritz C, Covic M, Schaffner I, Schwarz TJ, Karaca E, Kempkes B, Kremmer E, Pfrieger FW, Espinosa L, Bigas A, Giachino C, Taylor V, Frisen J, Lie DC. (2010) RBPJkappa-dependent signaling is essential for long-term maintenance of neural stem cells in the adult hippocampus. *J Neurosci* 30:13794-13807.
5. Lugert S, Basak O, Knuckles P, Haussler U, Fabel K, Gotz M, Haas CA, Kempermann G, Taylor V, Giachino C. (2010) Quiescent and active hippocampal neural stem cells with distinct morphologies respond selectively to physiological and pathological stimuli and aging. *Cell Stem Cell* 6:445-456.
6. Lai K, Kaspar BK, Gage FH, Schaffer DV. (2003) Sonic hedgehog regulates adult neural progenitor proliferation in vitro and in vivo. *Nat Neurosci* 6:21-27.
7. Jin K, Sun Y, Xie L, Batteur S, Mao XO, Smelick C, Logvinova A, Greenberg DA. (2003) Neurogenesis and aging: FGF-2 and HB-EGF restore neurogenesis in hippocampus and subventricular zone of aged mice. *Aging Cell* 2:175-183.
8. Cao L, Jiao X, Zuzga DS, Liu Y, Fong DM, Young D, During MJ. (2004) VEGF links hippocampal activity with neurogenesis, learning and memory. *Nat Genet* 36:827-835.
9. Qu Q, Sun G, Li W, Yang S, Ye P, Zhao C, Yu RT, Gage FH, Evans RM, Shi Y. (2010) Orphan nuclear receptor TLX activates Wnt/beta-catenin signalling to stimulate neural stem cell proliferation and self-renewal. *Nat Cell Biol* 12:31-40; sup pp 31-39.
10. Ashton RS, Conway A, Pangarkar C, Bergen J, Lim KI, Shah P, Bissell M, Schaffer DV. (2012) Astrocytes regulate adult hippocampal neurogenesis through ephrin-B signaling. *Nat Neurosci* 15:1399-1406.

11. Lie DC, Colamarino SA, Song HJ, Desire L, Mira H, Consiglio A, Lein ES, Jessberger S, Lansford H, Dearie AR, Gage FH. (2005) Wnt signalling regulates adult hippocampal neurogenesis. *Nature* 437:1370-1375.
12. Tozuka Y, Fukuda S, Namba T, Seki T, Hisatsune T. (2005) GABAergic excitation promotes neuronal differentiation in adult hippocampal progenitor cells. *Neuron* 47:803-815.
13. Kuhn HG, Dickinson-Anson H, Gage FH. (1996) Neurogenesis in the dentate gyrus of the adult rat: age-related decrease of neuronal progenitor proliferation. *J Neurosci* 16:2027-2033.
14. Villeda SA, Luo J, Mosher KI, Zou B, Britschgi M, Bieri G, Stan TM, Fainberg N, Ding Z, Eggel A, Lucin KM, Czirr E, Park JS, Couillard-Despres S, Aigner L, Li G, Peskind ER, Kaye JA, Quinn JF, Galasko DR, Xie XS, Rando TA, Wyss-Coray T. (2011) The ageing systemic milieu negatively regulates neurogenesis and cognitive function. *Nature* 477:90-94.
15. Okamoto M, Inoue K, Iwamura H, Terashima K, Soya H, Asashima M, Kuwabara T. (2011) Reduction in paracrine Wnt3 factors during aging causes impaired adult neurogenesis. *FASEB J* 25:3570-3582.
16. Miranda CJ, Braun L, Jiang Y, Hester ME, Zhang L, Riolo M, Wang H, Rao M, Altura RA, Kaspar BK. (2012) Aging brain microenvironment decreases hippocampal neurogenesis through Wnt-mediated survivin signaling. *Aging Cell* 11:542-552.
17. Magavi SS, Leavitt BR, Macklis JD. (2000) Induction of neurogenesis in the neocortex of adult mice. *Nature* 405:951-955.
18. Jiang W, Gu W, Brannstrom T, Rosqvist R, Wester P. (2001) Cortical neurogenesis in adult rats after transient middle cerebral artery occlusion. *Stroke* 32:1201-1207.
19. Ohira K, Furuta T, Hioki H, Nakamura KC, Kuramoto E, Tanaka Y, Funatsu N, Shimizu K, Oishi T, Hayashi M, Miyakawa T, Kaneko T, Nakamura S. (2010) Ischemia-induced neurogenesis of neocortical layer 1 progenitor cells. *Nat Neurosci* 13:173-179.
20. Parent JM, Vexler ZS, Gong C, Derugin N, Ferriero DM. (2002) Rat forebrain neurogenesis and striatal neuron replacement after focal stroke. *Ann Neurol* 52:802-813.
21. Arvidsson A, Collin T, Kirik D, Kokaia Z, Lindvall O. (2002) Neuronal replacement from endogenous precursors in the adult brain after stroke. *Nat Med* 8:963-970.
22. Shan X, Chi L, Bishop M, Luo C, Lien L, Zhang Z, Liu R. (2006) Enhanced de novo neurogenesis and dopaminergic neurogenesis in the substantia nigra of 1-methyl-4-phenyl-1,2,3,6-tetrahydropyridine-induced Parkinson's disease-like mice. *Stem Cells* 24:1280-1287.
23. Berg DA, Kirkham M, Beljajeva A, Knapp D, Habermann B, Ryge J, Tanaka EM, Simon A. (2010) Efficient regeneration by activation of neurogenesis in homeostatically quiescent regions of the adult vertebrate brain. *Development* 137:4127-4134.
24. Pierce AA, Xu AW. (2010) De novo neurogenesis in adult hypothalamus as a compensatory mechanism to regulate energy balance. *J Neurosci* 30:723-730.
25. Iwai M, Abe K, Kitagawa H, Hayashi T. (2001) Gene therapy with adenovirus-mediated glial cell line-derived neurotrophic factor and neural stem cells activation after ischemic brain injury. *Hum Cell* 14:27-38.
26. Benraiss A, Bruel-Jungerman E, Lu G, Economides AN, Davidson B, Goldman SA. (2012) Sustained induction of neuronal addition to the adult rat neostriatum by AAV4-delivered noggin and BDNF. *Gene Ther* 19:582.

27. Wall ST, Saha K, Ashton RS, Kam KR, Schaffer DV, Healy KE. (2008) Multivalency of Sonic hedgehog conjugated to linear polymer chains modulates protein potency. *Bioconjug Chem* 19:806-812.
28. Petrie TA, Raynor JE, Dumbauld DW, Lee TT, Jagtap S, Templeman KL, Collard DM, Garcia AJ. (2010) Multivalent integrin-specific ligands enhance tissue healing and biomaterial integration. *Sci Transl Med* 2:45ra60.
29. Kempermann G, Kuhn HG, Gage FH. (1997) More hippocampal neurons in adult mice living in an enriched environment. *Nature* 386:493-495.
30. Traiffort E, Charytoniuk D, Watroba L, Faure H, Sales N, Ruat M. (1999) Discrete localizations of hedgehog signalling components in the developing and adult rat nervous system. *Eur J Neurosci* 11:3199-3214.
31. Davis S, Gale NW, Aldrich TH, Maisonpierre PC, Lhotak V, Pawson T, Goldfarb M, Yancopoulos GD. (1994) Ligands for EPH-related receptor tyrosine kinases that require membrane attachment or clustering for activity. *Science* 266:816-819.
32. Leuner B, Glasper ER, Gould E. (2009) Thymidine analog methods for studies of adult neurogenesis are not equally sensitive. *J Comp Neurol* 517:123-133.
33. Huang Q, Goh JC, Hutmacher DW, Lee EH. (2002) In vivo mesenchymal cell recruitment by a scaffold loaded with transforming growth factor beta1 and the potential for in situ chondrogenesis. *Tissue Eng* 8:469-482.
34. Thevenot PT, Nair AM, Shen J, Lotfi P, Ko CY, Tang L. (2010) The effect of incorporation of SDF-1alpha into PLGA scaffolds on stem cell recruitment and the inflammatory response. *Biomaterials* 31:3997-4008.
35. Fong EL, Chan CK, Goodman SB. (2011) Stem cell homing in musculoskeletal injury. *Biomaterials* 32:395-409.
36. Erggelet C, Neumann K, Endres M, Haberstroh K, Sittinger M, Kaps C. (2007) Regeneration of ovine articular cartilage defects by cell-free polymer-based implants. *Biomaterials* 28:5570-5580.
37. Lee CH, Cook JL, Mendelson A, Moioli EK, Yao H, Mao JJ. (2010) Regeneration of the articular surface of the rabbit synovial joint by cell homing: a proof of concept study. *Lancet* 376:440-448.
38. Itoh T, Satou T, Ishida H, Nishida S, Tsubaki M, Hashimoto S, Ito H. (2009) The relationship between SDF-1alpha/CXCR4 and neural stem cells appearing in damaged area after traumatic brain injury in rats. *Neurol Res* 31:90-102.
39. Carbajal KS, Schaumburg C, Strieter R, Kane J, Lane TE. (2010) Migration of engrafted neural stem cells is mediated by CXCL12 signaling through CXCR4 in a viral model of multiple sclerosis. *Proc Natl Acad Sci U S A* 107:11068-11073.
40. Chow C, Epp JR, Lieblich SE, Barha CK, Galea LA. (2012) Sex differences in neurogenesis and activation of new neurons in response to spatial learning and memory. *Psychoneuroendocrinology*.
41. Song J, Zhong C, Bonaguidi MA, Sun GJ, Hsu D, Gu Y, Meletis K, Huang ZJ, Ge S, Enikolopov G, Deisseroth K, Luscher B, Christian KM, Ming GL, Song H. (2012) Neuronal circuitry mechanism regulating adult quiescent neural stem-cell fate decision. *Nature* 489:150-154.
42. Ihrie RA, Shah JK, Harwell CC, Levine JH, Guinto CD, Lezameta M, Kriegstein AR, Alvarez-Buylla A. (2011) Persistent sonic hedgehog signaling in adult brain determines neural stem cell positional identity. *Neuron* 71:250-262.

43. Bhattacharyya BJ, Banisadr G, Jung H, Ren D, Cronshaw DG, Zou Y, Miller RJ. (2008) The chemokine stromal cell-derived factor-1 regulates GABAergic inputs to neural progenitors in the postnatal dentate gyrus. *J Neurosci* 28:6720-6730.
44. Politis M, Wu K, Loane C, Quinn NP, Brooks DJ, Rehncrona S, Bjorklund A, Lindvall O, Piccini P. (2010) Serotonergic neurons mediate dyskinesia side effects in Parkinson's patients with neural transplants. *Sci Transl Med* 2:38ra46.
45. Pritchard CD, O'Shea TM, Siegwart DJ, Calo E, Anderson DG, Reynolds FM, Thomas JA, Slotkin JR, Woodard EJ, Langer R. (2011) An injectable thiol-acrylate poly(ethylene glycol) hydrogel for sustained release of methylprednisolone sodium succinate. *Biomaterials* 32:587-597.
46. Gros T, Sakamoto JS, Blesch A, Havton LA, Tuszynski MH. (2010) Regeneration of long-tract axons through sites of spinal cord injury using templated agarose scaffolds. *Biomaterials* 31:6719-6729.